SAND2016-0931PE

Exceptional service in the national interest

Sandia National Laboratories

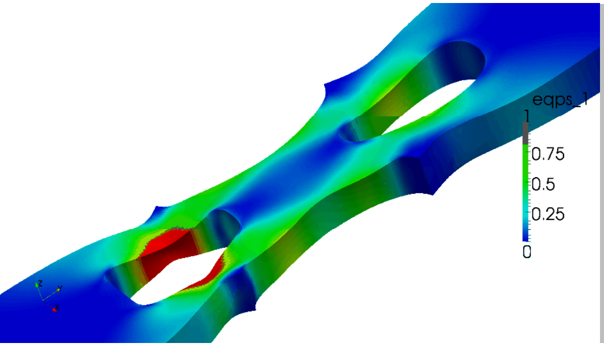

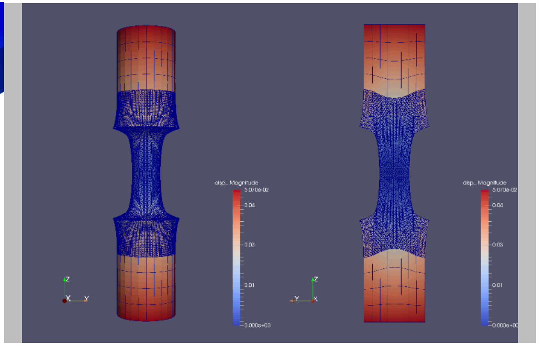

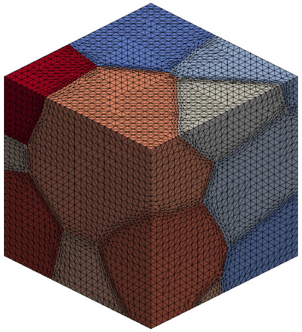

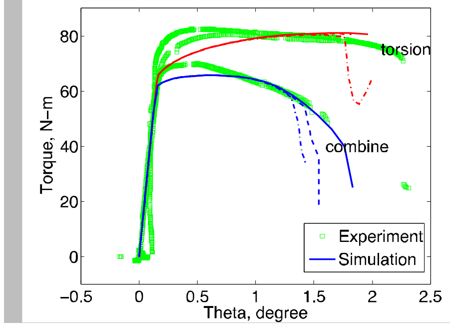

Mechanics of Materials Department

Computational Solid Mechanics

U.S. DEPARTMENT OF ENERGY
NNSA National Nuclear Security Administration

Sandia National Laboratories is a multi-program laboratory managed and operated by Sandia Corporation, a wholly owned subsidiary of Lockheed Martin Corporation, for the U.S. Department of Energy's National Nuclear Security Administration under contract DE-AC04-94AL85000. SAND NO. 2011-XXXXP

Who we are

Alejandro Mota
PhD Structural Engineering
Cornell University

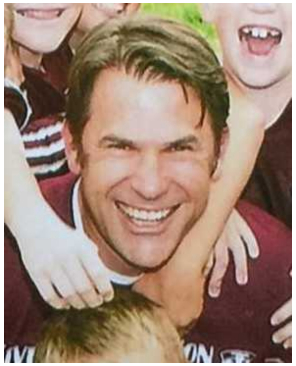

Jay Foulk
PhD Mechanical Engineering
University of California Berkeley

Jake Ostien
PhD Mechanical Engineering
University of Michigan Ann Arbor

Coleman Alleman
PhD Civil Engineering
Johns Hopkins University

The problems we address

- Transient or steady state behavior of solids and structures.
- Materials and structures subjected to very large deformations.
- Damage and failure of materials and structures.
- Crack initiation and propagation.
- Fracture and fragmentation.

Our approach

- Use mathematics, solid mechanics and computer science to understand and predict the behavior of solids and structures.
- Start from fundamental physical principles.
- Maintain mathematical rigor.
- Acknowledge that experiment is the ultimate arbiter.

www.trilinos.org

github.com/gahansen/Albany

Research, Open Source

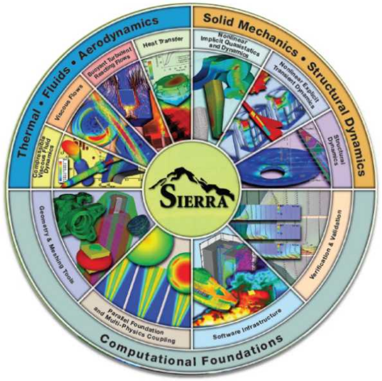

Production, Sandia Proprietary

Research

- Finite-Deformation Solid Mechanics
- Constitutive Behavior of Materials
- Finite Element Methods
- Coupled Physics
- Multiscale Modeling and Coupling
- Remeshing and Mesh Adaptation
- Damage, Failure and Fracture Mechanics

Element Technology, Fracture

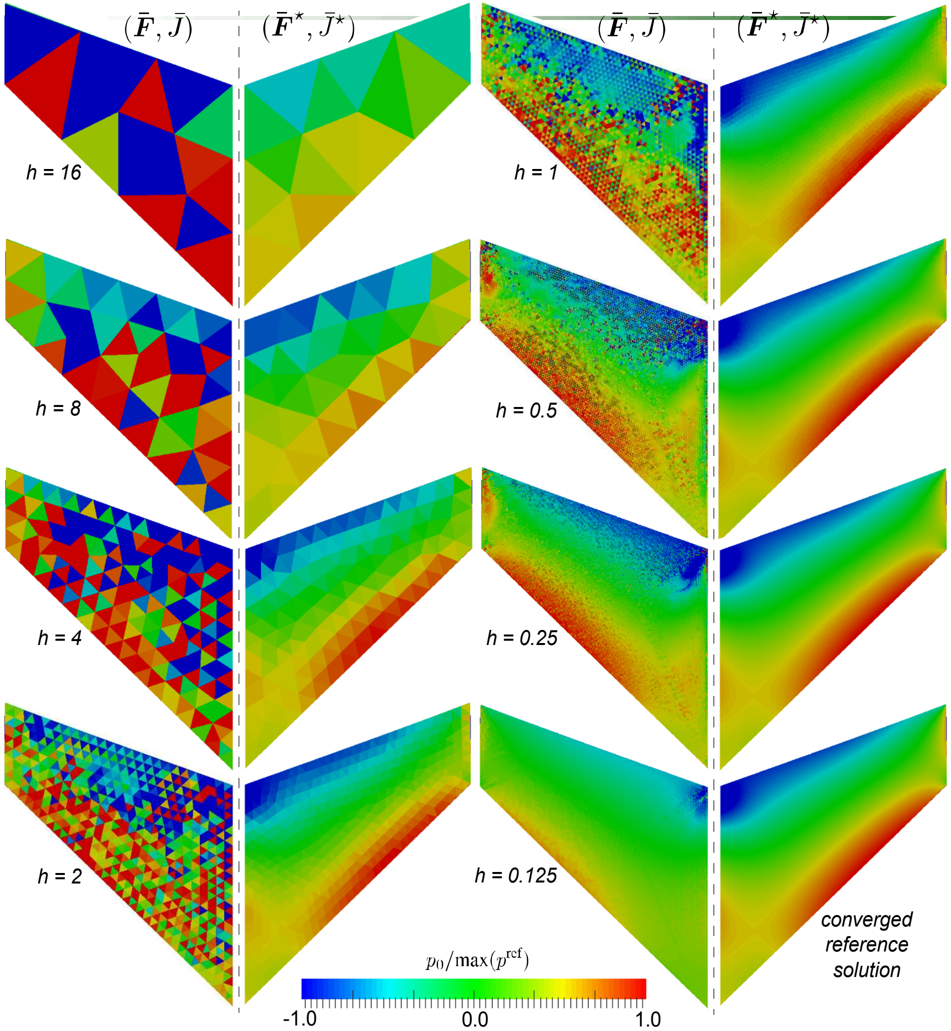

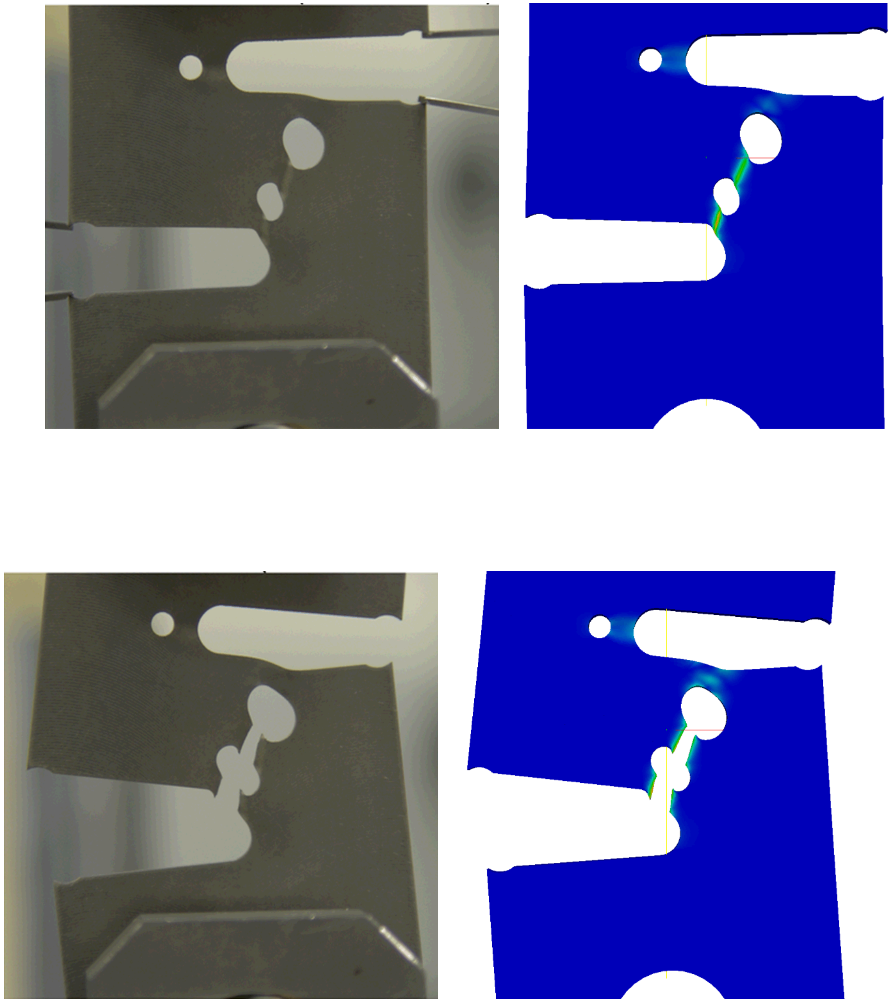

Accurate Pressure

Finite Deformation, Regularization, Schwarz Coupling

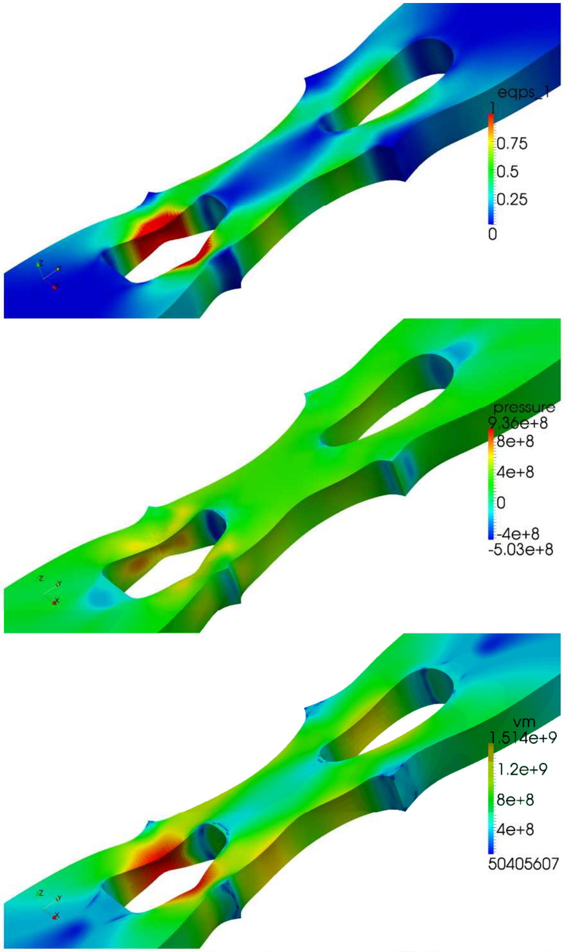

Figure 11: Zoomed view of deformed geometry and fields, equivalent plastic strain (eqps), pressure [Pa], and von Mises stress (vm) [Pa]

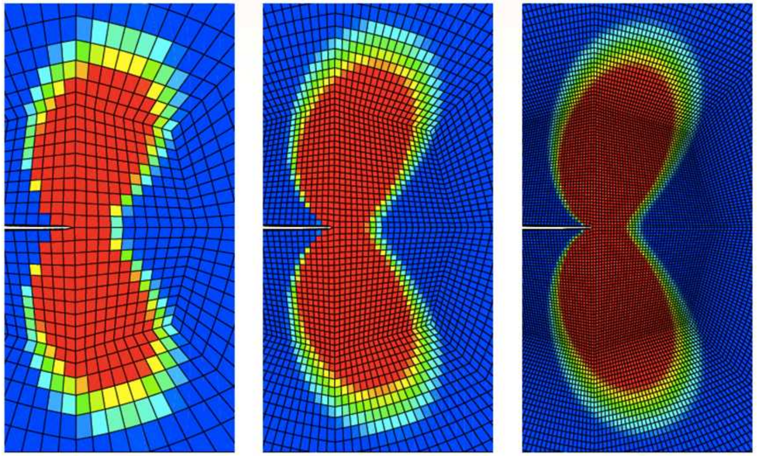

Contours of equivalent plastic strain, (0,.001), mesh sizes 60μm, 30μm, 15μm

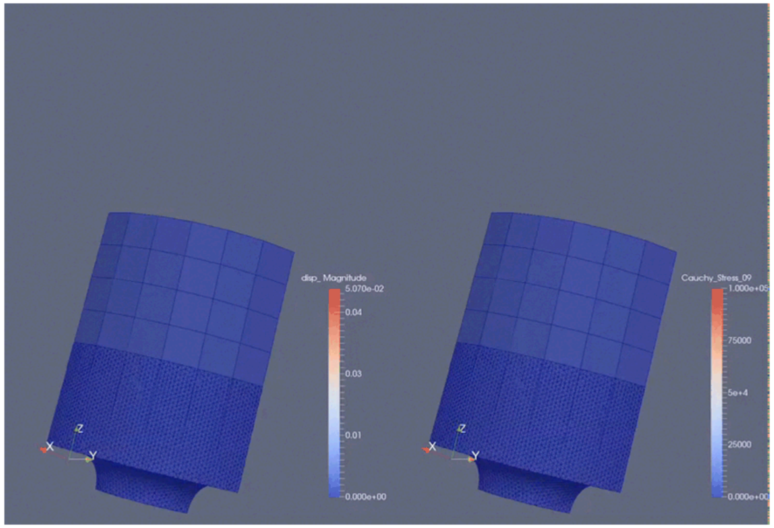

Schwarz Coupling

Strong Chemo-Mechanical Coupling

Block solve for displacement, concentration, and pressure at a crack tip

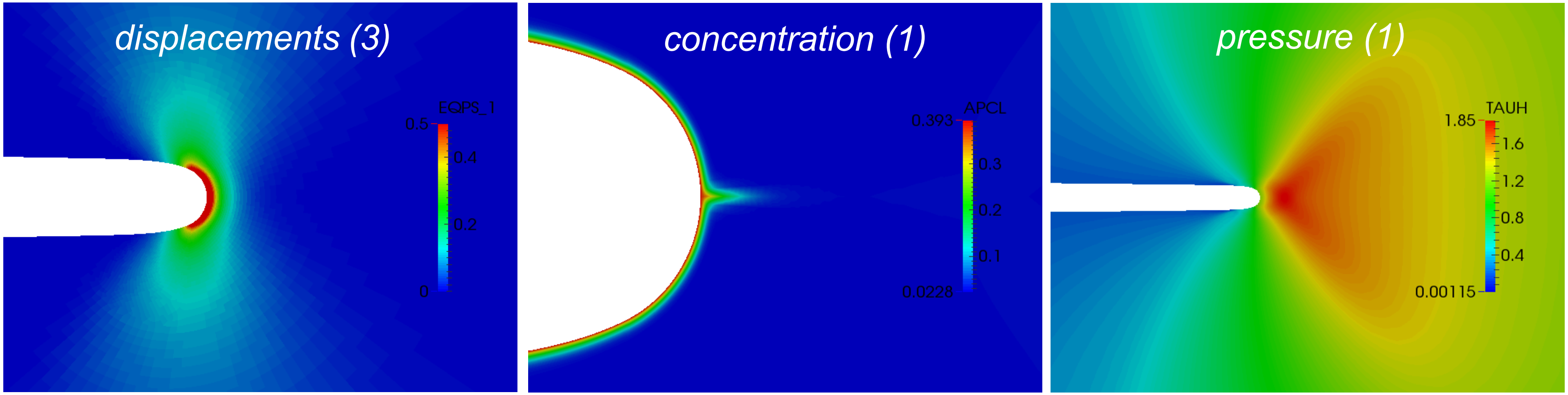

Exploring fast pathways through the inclusion of surface elements on grain boundaries

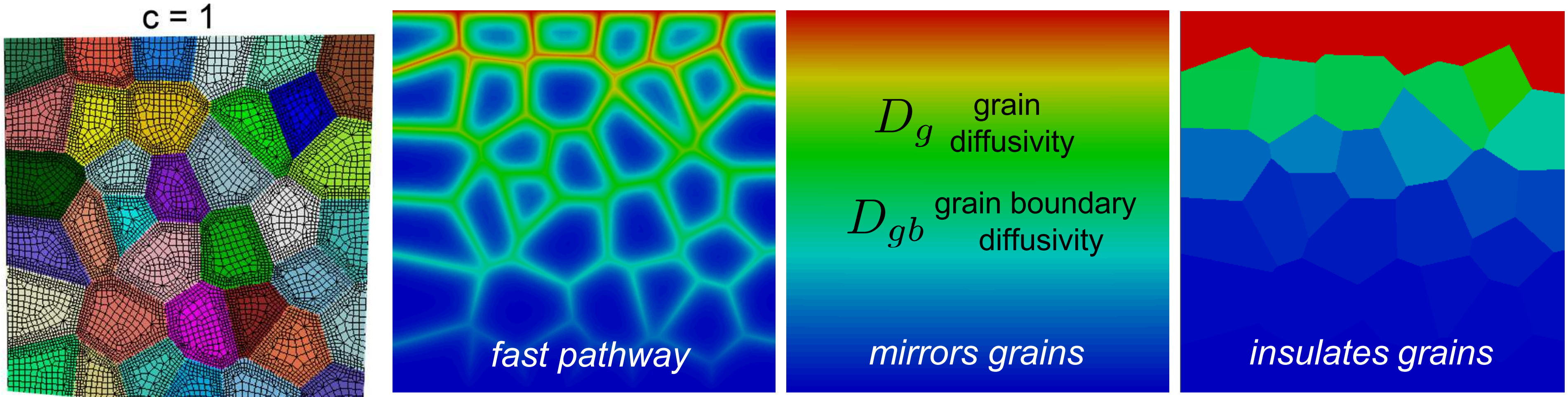

$D_{gb} = 1 \times 10^5 D_g$

$D_{gb} = D_g$

$D_{gb} = 1 \times 10^{-5} D_g$

Mesh Adaptation

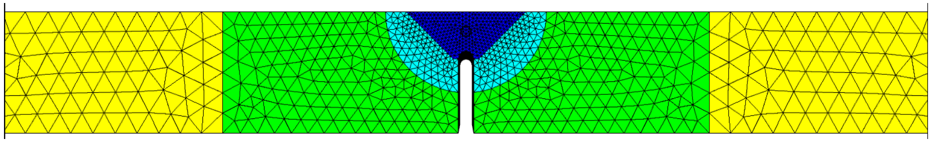

undeformed mesh
with notch

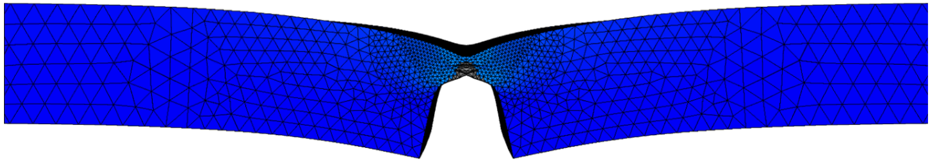

necking at
mid-plane

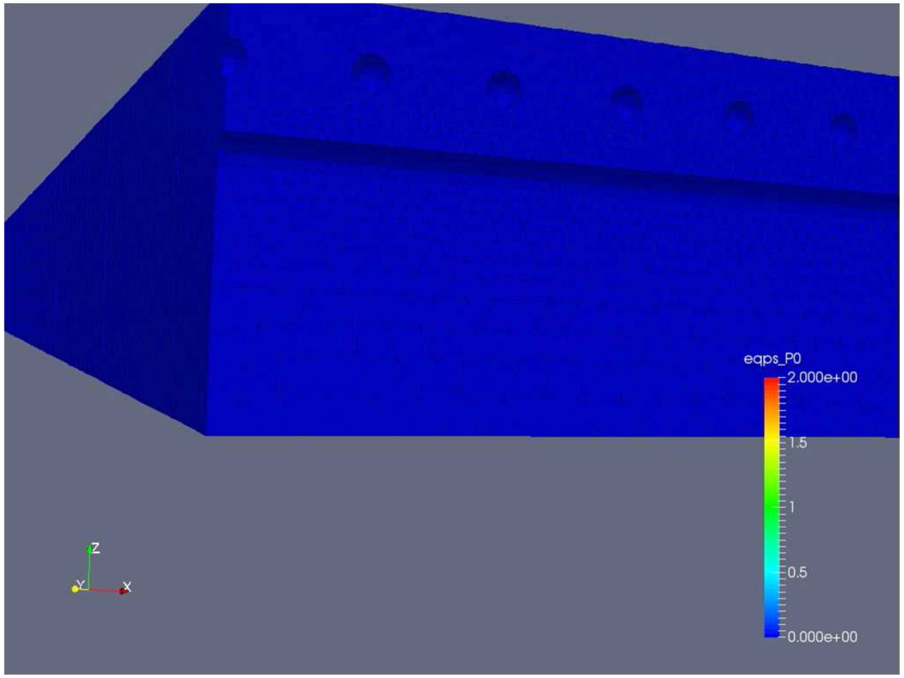

Resolving the evolution of pores in laser welds

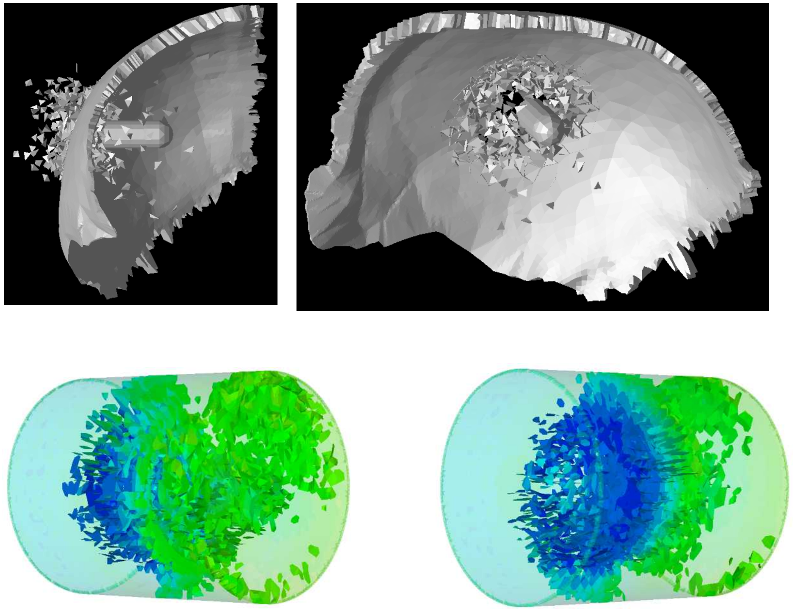

Multiple crack paths and fragmentation

Constitutive Model Development, Verification, and Validation

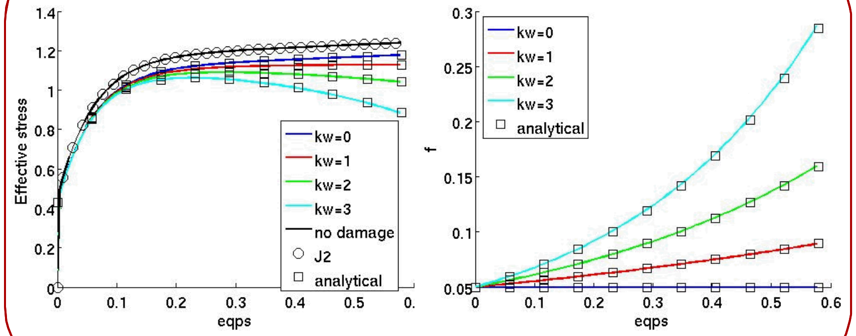

Verification in simple shear

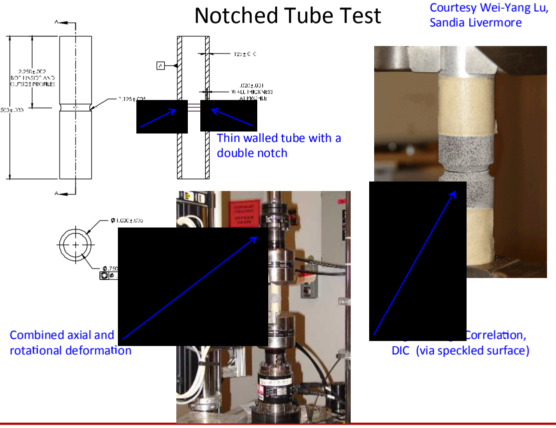

Courtesy Wei-Yang Lu, Sandia Livermore

Thin walled tube with a double notch

Combined axial and rotational deformation

Correlation, DIC (via speckled surface)

Validation experiments (courtesy W. Lu)

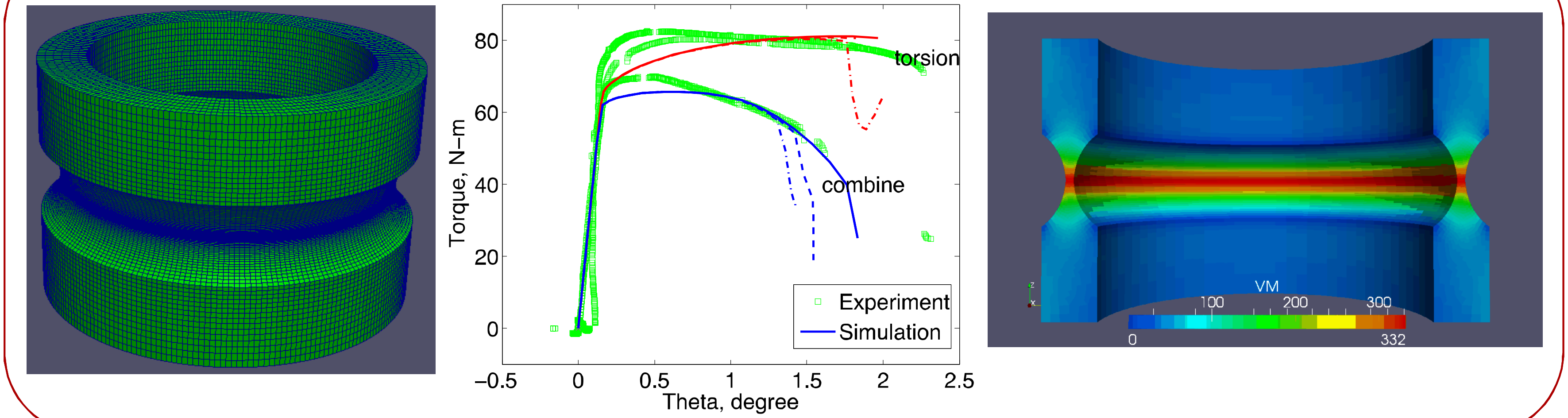

Preliminary simulation results and validation comparisons

Exceptional service in the national interest

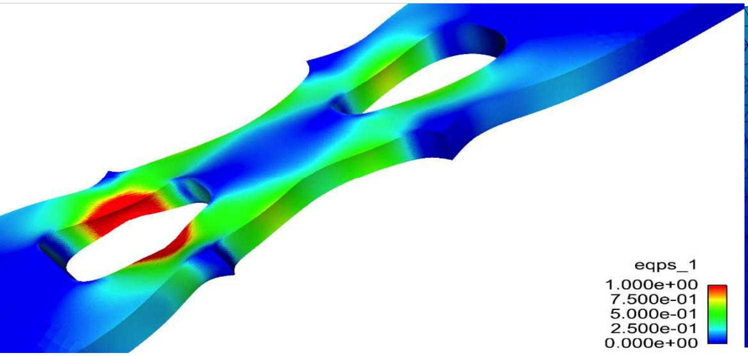

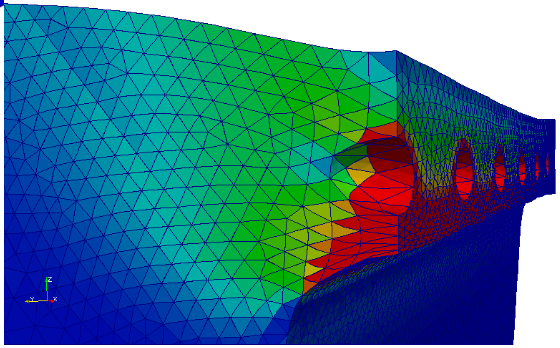

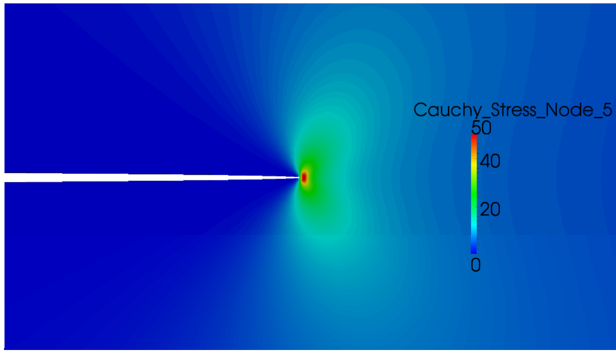

The Laboratory for Computational Mechanics

Jakob T. Ostien, James W. Foulk III, Alejandro Mota, Glen Hansen, Andy Salinger, Mike Veilleux, John Emery, Coleman Alleman

Sandia National Laboratories is a multi-program laboratory managed and operated by Sandia Corporation, a wholly owned subsidiary of Lockheed Martin Corporation, for the U.S. Department of Energy's National Nuclear Security Administration under contract DE-AC04-94AL85000. SAND NO. 2011-XXXXP

LCM research environment

The Laboratory for Computational Mechanics (LCM) is a research environment that leverages Albany which employs a host of reusable components in Trilinos

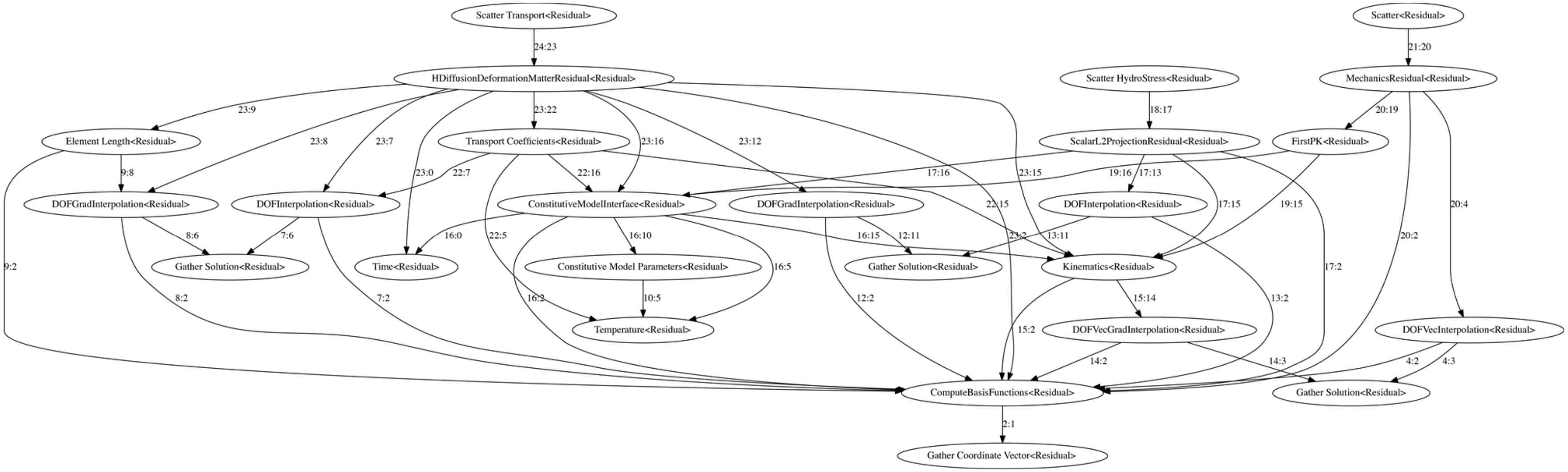

- *Phalanx* helps manage multiphysics dependencies
- *Intrepid* provides an extensive element library
- *Sacado* yields an exact Jacobian via automatic differentiation
- *NOX* provides nonlinear solution methods
- *Kokkos* provides support for manycore architectures

https://software.sandia.gov/albany/

http://trilinos.sandia.gov/

Trilinos and Albany

- The Trilinos Project http://trilinos.sandia.gov
  - Run out of the Computational Mathematics Center at Sandia NM
  - Consists of a collection of “packages” that address many problems of discretizing and solving PDEs
    - Finite element and topology libraries
    - Nonlinear solvers
    - Linear solvers
  - Additional utilities pertain to advanced and specialized features
    - Template based generic programming → Automatic Differentiation!
    - Multi-physics dependency management
  - And more…
- Albany
  - Originally established to test installations of Trilinos
  - Transitioned to be the testbed and first friendly user for advanced Trilinos packages
  - Was adopted by multiple LDRD projects (as well as the LCM project) as a code base
  - Stable and growing *developer* community
  - Creature comforts for *users* still in early stages

Anatomy of a Component-Based Application

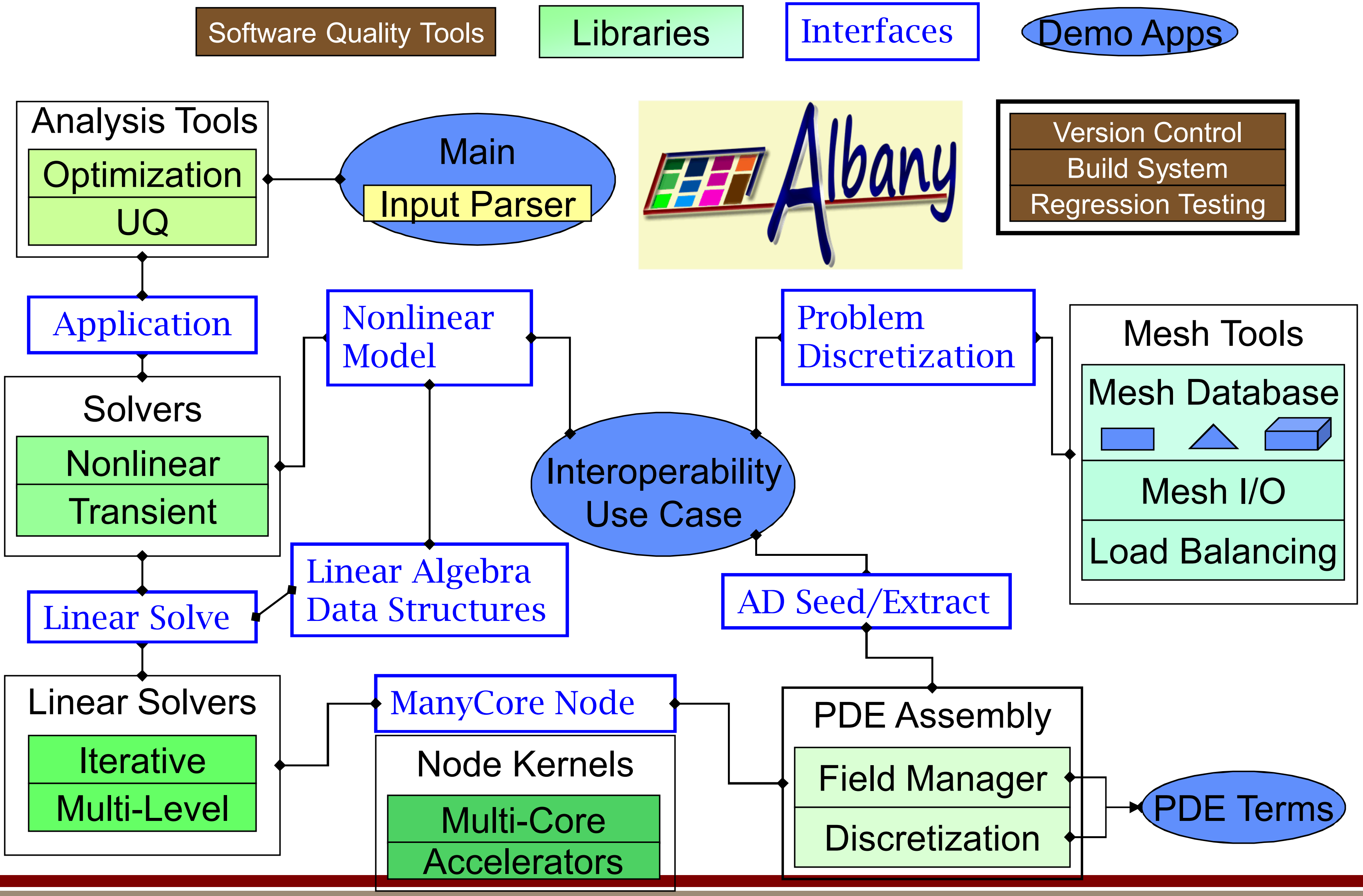

Reusable Math Libraries and Software Components

Analysis Tools (*black-box*)
- Optimization
- UQ (sampling)
- Parameter Studies
- V&V, Calibration
- OUU, Reliability

Analysis Tools (*embedded*)
- Nonlinear Solver
- Time Integration
- Continuation
- Sensitivity Analysis
- Stability Analysis
- Constrained Solves
- Optimization
- UQ Solver

Linear Algebra
- Data Structures
- Iterative Solvers
- Direct Solvers
- Eigen Solver
- Preconditioners
- Matrix Partitioning

Architecture-Dependent Kernels
- Multi-Core
- Accelerators

Composite Physics
- MultiPhysics Coupling
- System Models
- System UQ

Mesh Tools
- Mesh I/O
- Inline Meshing
- Partitioning
- Load Balancing
- Adaptivity
- Remeshing
- Grid Transfers
- Quality Improvement
- DOF map

Utilities
- Input File Parser
- Parameter List
- Memory Management
- I/O Management
- Communicators

PostProcessing
- Visualization
- Verification
- Model Reduction

Mesh Database
- Mesh Database
- Geometry Database
- Solution Database

Local Fill

Discretizations
- Discretization Library
- Field Manager

Derivative Tools
- Sensitivities
- Derivatives
- Adjoints
- UQ / PCE Propagation

Physics Fill
- Element Level Fill
- Material Models
- Objective Function
- Constraints
- Error Estimates
- MMS Source Terms

Data-Centric Algs
- Graph Algorithms
- SVDs
- Map-Reduce
- Linear Programming
- Network Models

Software Quality
- Version Control
- Regression Testing
- Build System
- Backups
- Verification Tests
- Mailing Lists
- Unit Testing
- Bug Tracking
- Performance Testing
- Code Coverage
- Porting
- Web Pages
- Release Process

The LCM project

- Project Objectives
  - Provide an open, collaborative computational mechanics research environment
  - Accelerate research transition into the production analysis environment
- Adopted Albany as a code base
  - Creates ties with the 'Math Guys'
  - Leverages existing repository, version control, testing infrastructure
- Infrastructure allows for spatially dependent boundary conditions (e.g. torsion) and parameters (e.g. shear modulus), consistent coupled physics dependence (e.g. temperature dependent flow rule), and some embedded uncertainty algorithms (e.g. stochastic Galerkin)
- Support for linear/nonlinear elasticity, inelasticity
- Current work is focusing on adaptivity and coupled physics
  - Projects in these areas use Albany to test out ideas, provide some funding to enable Albany to do what is necessary for the research
- Current limitations
  - No robust explicit time integration
  - No contact
  - Usability has not been a focus (i.e. XML input files)

Getting Started

- Abstraction #1 ModelEvaluator
  - Abstraction for a discretized PDE
  - In principle communicates with the solver, time integrator
  - In practice, time integration for LCM in computed in Albany
  - Keeps as data an ‘Application’, and a key evalModel() method
- Abstraction #2 Application
  - An Application owns a ‘Discretization’ (finite element mesh, fields)
  - Also owns a ‘Problem’
  - General methods to compute system Residual, Jacobian, Tangent
- Abstraction #3 Discretization
  - Interface to allows for multiple mesh representations
  - Currently the primary mesh representation is from the Sierra ToolKit (STK) available from Trilinos
- Abstraction #4 Problem
  - Here be physics, degrees of freedom, implementation of equations
  - Composed of a series of ‘Evaluators’ that compute intermediate quantities in the Residual
- Abstraction #5 Evaluators
  - Atomic computations with managed dependencies
  - Examples, basis functions, strain, conductivity, permeability, residual forces

Code Details

- Generic Internal Force Algorithm
  - Primary solution variable is the displacement vector
  - finite element basis used to compute the displacement and deformation gradient

$$\boldsymbol{H} = \frac{\partial \boldsymbol{u}}{\partial \boldsymbol{X}}; \quad \boldsymbol{F} = \mathbf{1} + \boldsymbol{H}$$

  - For Hyperelastic constitutive laws, compute Cauchy stress as a function of deformation gradient

$$\boldsymbol{\sigma} = J^{-1} \frac{\partial \Psi}{\partial \boldsymbol{F}} \boldsymbol{F}^T$$

  - For Hypoelastic constitutive laws, the rate of deformation and stress are computed from the logarithmic mapping of the incremental deformation gradient

$$\boldsymbol{l} = \dot{\boldsymbol{F}} \boldsymbol{F}^{-1} = \frac{\log \boldsymbol{f}}{\Delta t}; \quad \boldsymbol{f} = \boldsymbol{F}_{n+1} \boldsymbol{F}_n^{-1}; \quad \boldsymbol{\sigma} = \mathcal{F}(\operatorname{sym} \boldsymbol{l})$$

  - Internal force is computed as an integral over the reference configuration

$$\boldsymbol{f}^{int} = \int_{\Omega_0} \boldsymbol{\nabla}_X \cdot \boldsymbol{P} \, dV; \quad \boldsymbol{P} = J \boldsymbol{\sigma} \boldsymbol{F}^{-T}$$

Code Details

- Generic Tensor Library
    - Tensor (rank 1, 2, 3, 4) manipulation is handled via a Tensor class
    - Construction is dynamic and arbitrary
    - Scalar, Vector, Tensor arithmetic operations defined
    - A number invariants, decompositions (SVD, Polar), logarithmic and exponential mappings, and other goodies
    - Sample Code

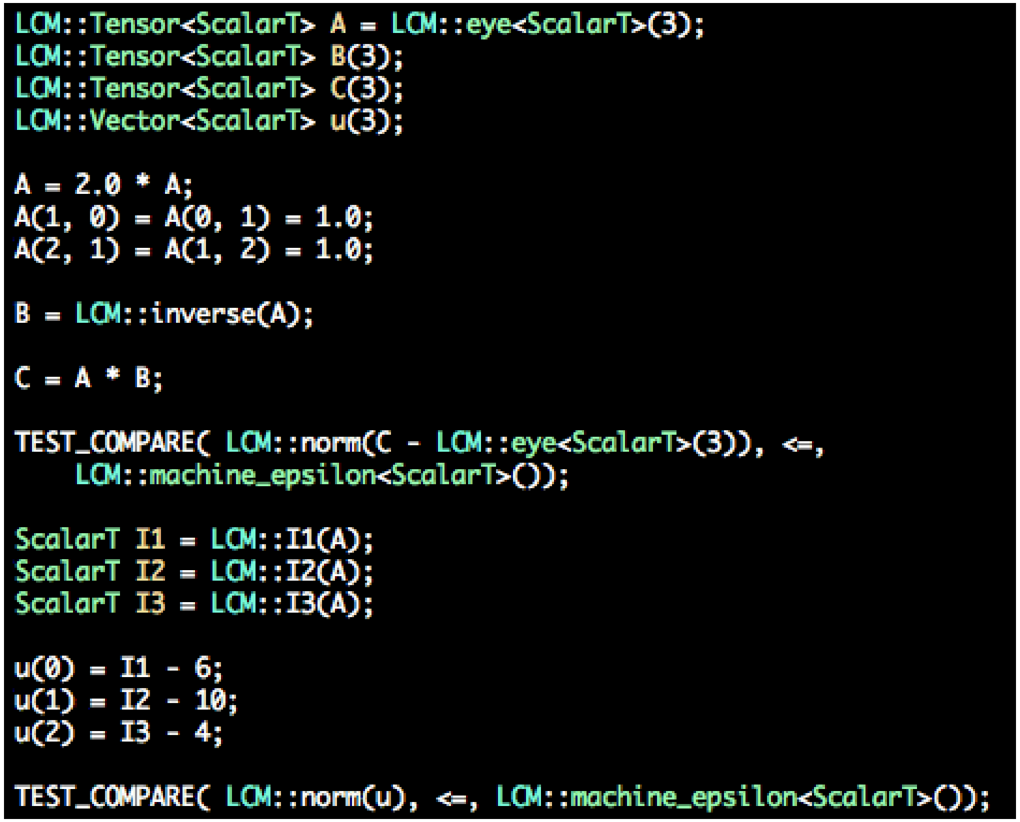

```
LCM::Tensor<ScalarT> A = LCM::eye<ScalarT>(3);
LCM::Tensor<ScalarT> B(3);
LCM::Tensor<ScalarT> C(3);
LCM::Vector<ScalarT> u(3);

A = 2.0 * A;
A(1, 0) = A(0, 1) = 1.0;
A(2, 1) = A(1, 2) = 1.0;

B = LCM::inverse(A);

C = A * B;

TEST_COMPARE( LCM::norm(C - LCM::eye<ScalarT>(3)), <=,
    LCM::machine_epsilon<ScalarT>());

ScalarT I1 = LCM::I1(A);
ScalarT I2 = LCM::I2(A);
ScalarT I3 = LCM::I3(A);

u(0) = I1 - 6;
u(1) = I2 - 10;
u(2) = I3 - 4;

TEST_COMPARE( LCM::norm(u), <=, LCM::machine_epsilon<ScalarT>());
```

Code Details

- Local Systems of Equations
  - Target is constitutive models that have internal state variables with evolution equations that produce a nonlinear system at each material point
  - Automatic Differentiation is exploited to compute the Jacobian of the nonlinear system in some cases
  - Matrix and vector are packaged up and shipped to LAPACK
  - Global system sensitivities are preserved by the LocalNonlinearSolver class
  - For usage example reference the utLocalNonlinearSolver unit test, GursonFD, CapImplicit
  - Example code

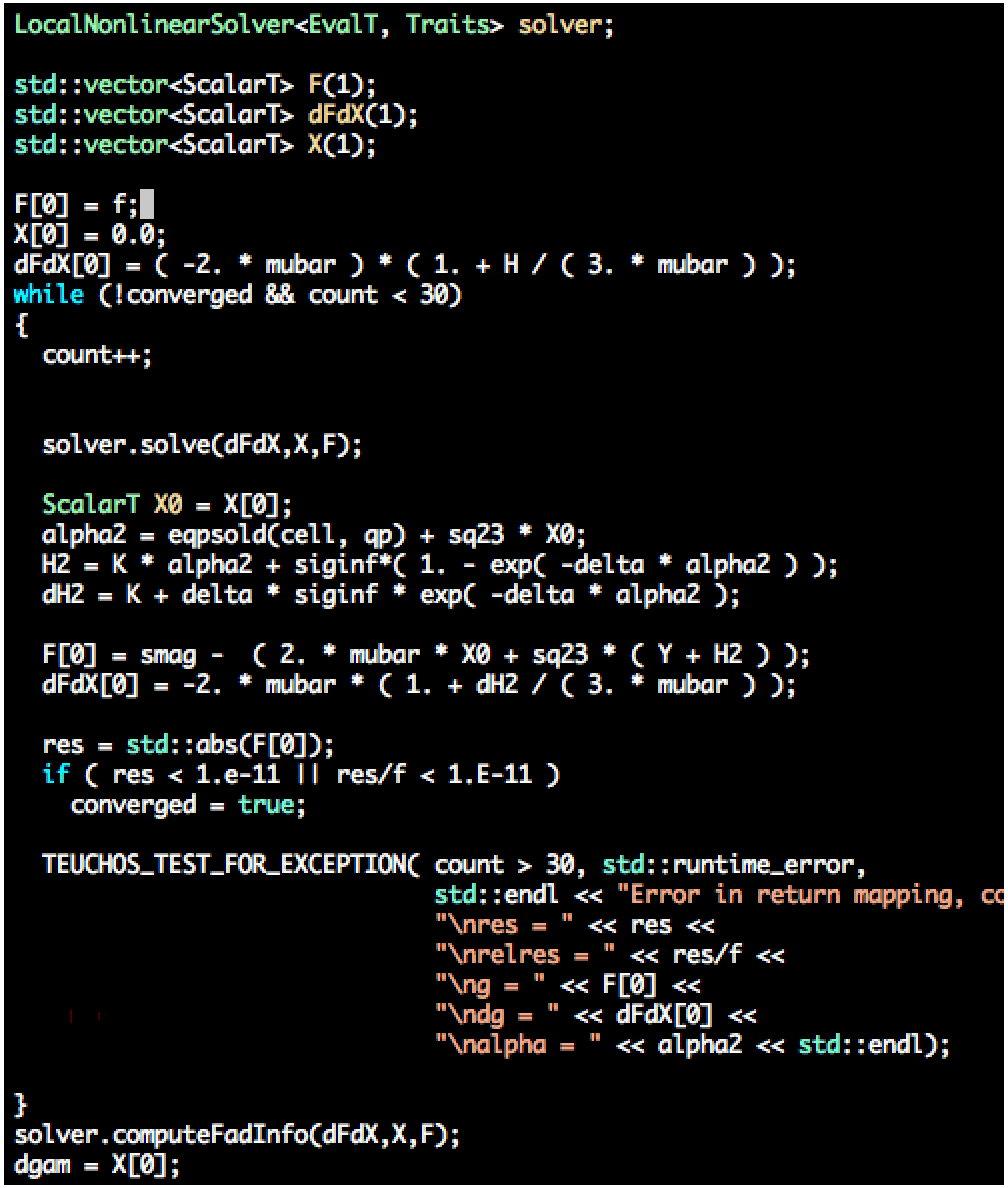

```
LocalNonlinearSolver<EvalT, Traits> solver;

std::vector<ScalarT> F(1);
std::vector<ScalarT> dFdX(1);
std::vector<ScalarT> X(1);

F[0] = f;
X[0] = 0.0;
dFdX[0] = ( -2. * mubar ) * ( 1. + H / ( 3. * mubar ) );
while (!converged && count < 30)
{
  count++;


  solver.solve(dFdX,X,F);

  ScalarT X0 = X[0];
  alpha2 = eqpsold(cell, qp) + sq23 * X0;
  H2 = K * alpha2 + siginf*( 1. - exp( -delta * alpha2 ) );
  dH2 = K + delta * siginf * exp( -delta * alpha2 );

  F[0] = smag -  ( 2. * mubar * X0 + sq23 * ( Y + H2 ) );
  dFdX[0] = -2. * mubar * ( 1. + dH2 / ( 3. * mubar ) );

  res = std::abs(F[0]);
  if ( res < 1.e-11 || res/f < 1.E-11 )
    converged = true;

  TEUCHOS_TEST_FOR_EXCEPTION( count > 30, std::runtime_error,
                              std::endl << "Error in return mapping, co
                              "\nres = " << res <<
                              "\nrelres = " << res/f <<
                              "\ng = " << F[0] <<
                              "\ndg = " << dFdX[0] <<
                              "\nalpha = " << alpha2 << std::endl);

}
solver.computeFadInfo(dFdX,X,F);
dgam = X[0];
```

Motivation for Coupled Physics

Thermomechanical behavior

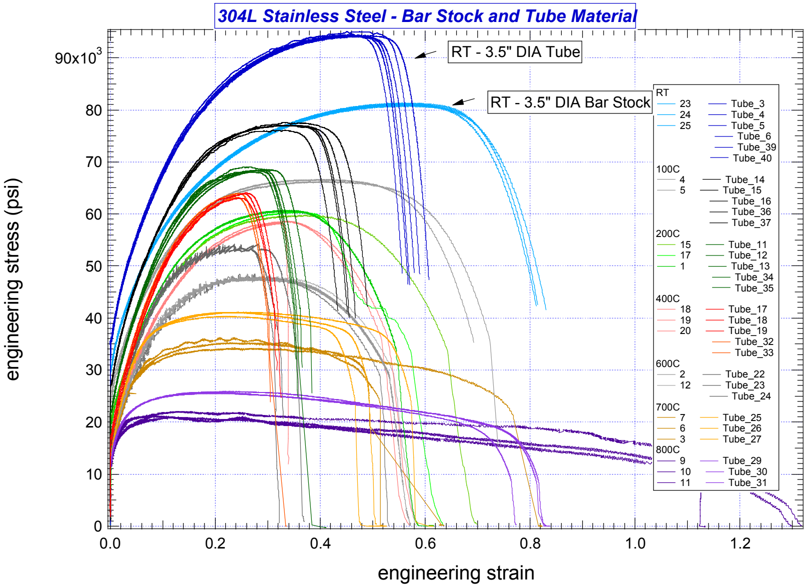

Mechanical response varies strongly with temperature

- Commonly assumptions are made
    - Isothermal at slow rates
    - Adiabatic at high rates
- Strong coupling is required as physics become richer, environment rates may span slow to fast

Hydrogen embrittlement

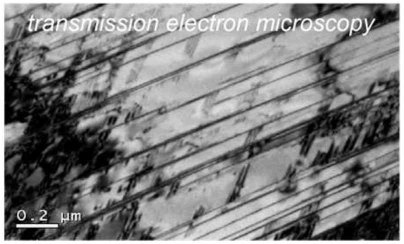

deformation twins

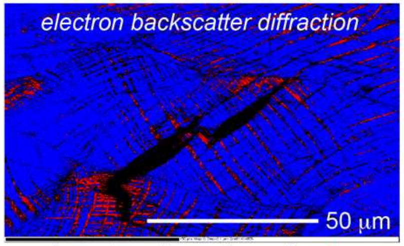

phase transformations, fcc, bcc

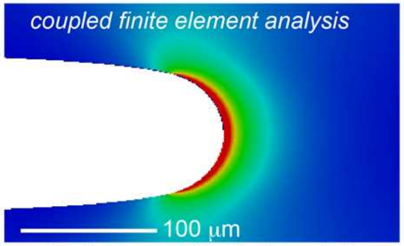

plastic zone at blunted crack tip

Hydrogen *activates* microstructure and *localizes* deformation processes

- Aids deformation bands/twinning (*nm*)
- Activates phase transformations (*nm* – μ*m*)
- Accentuates grain boundary interactions (*nm*)

Coupled Physics Computational Environment – Albany

- Some useful features for rapid development
  - Graph based multiphysics dependency management
  - Analytic Jacobians via Automatic Differentiation (AD), even for the cross coupling terms
  - Access to the whole suite of linear solvers (direct, iterative), nonlinear solver strategies, preconditioners (algebraic multigrid, physics based)
  - Fully parallel, with automatic mesh decomposition capabilities

Salinger, et al, Albany: A Component-Based Partial Differential Equation Code Built on Trilinos, ACM Transactions of Mathematical Software, 2013.

Kinematics of THM Problem at Finite Strain

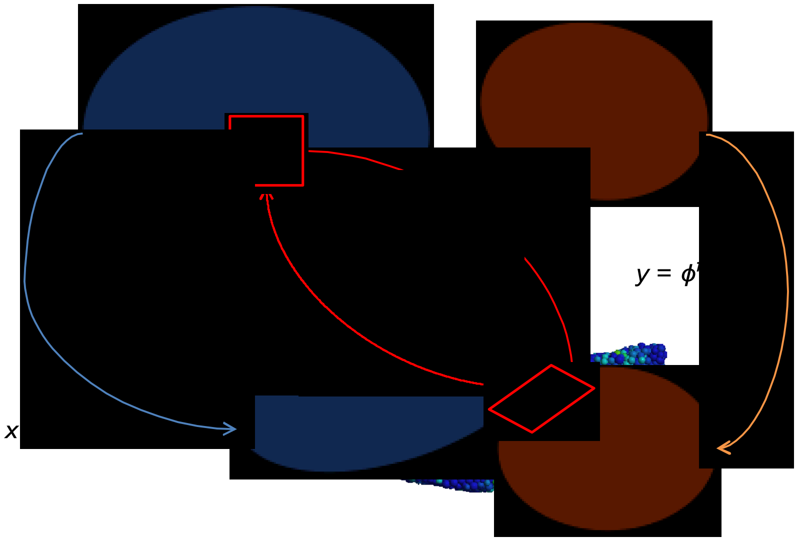

Trajectories of the solid and fluid constituent.

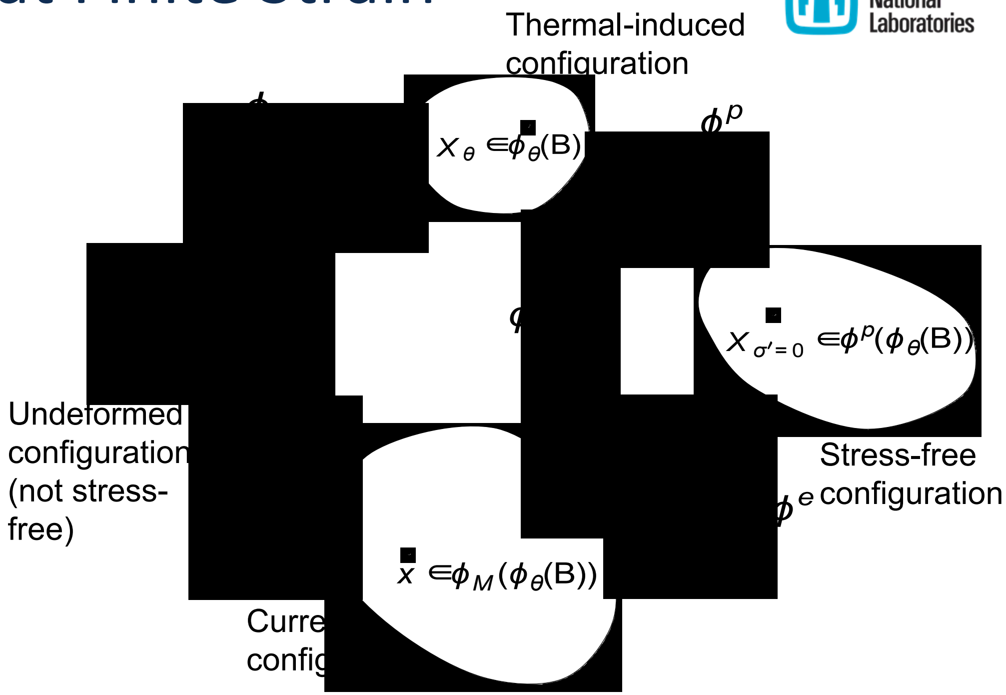

Multiplicative decomposition of the thermo-hydro-mechanics problem

Multiplicative decomposition of skeleton deformation gradient

$$\boldsymbol{F} = \frac{\partial \boldsymbol{\varphi}(\boldsymbol{X}, t)}{\partial \boldsymbol{X}} = \boldsymbol{F}_M \cdot \boldsymbol{F}_\theta \;\; ; \;\; \boldsymbol{F}_\theta = \frac{\partial \boldsymbol{\varphi}_\theta(\boldsymbol{X}, t)}{\partial \boldsymbol{X}} \;\; ; \boldsymbol{F}_M = \frac{\partial \boldsymbol{\varphi}_M(\boldsymbol{X}_\theta, t)}{\partial \boldsymbol{X}_\theta}$$

Isotropic tensor

Concept of Effective Stress

$$\boldsymbol{\sigma} = \boldsymbol{\sigma}' - B p^{\mathrm{f}} \boldsymbol{I},$$

$$B = 1 - \frac{K}{K_{\mathrm{s}}}$$

$$\boldsymbol{P}(\boldsymbol{F}, \boldsymbol{z}, p^f, \theta) = \boldsymbol{P}'(\boldsymbol{F}, \boldsymbol{z}, \theta) - J B p^f \boldsymbol{F}^{-T}$$

$$P(F_M, z, p^f) = P'(F_M, z) - J B p^f F^{-T},$$

Strong Form of THM Problem at Finite Strain

❑ Balance of Linear Momentum

$$\boxed{\nabla^{\boldsymbol{X}}\cdot\boldsymbol{P} + J(\rho^s + \rho^f)\boldsymbol{G} = \boldsymbol{0}}$$

where $P(F_M, z, p^f) = P'(F_M, z) - JBp^f F^{-T},$

Total Stress Effective Stress 1st PK pore pressure

❑ Balance of Mass

$$\boxed{\left(\frac{B}{J} - 3\alpha_{\mathrm{s}}(\theta - \theta_o)\right)\dot{J} + \frac{1}{M}\dot{p}^{\mathrm{f}} - 3\alpha^{\mathrm{m}}\dot{\theta} + \frac{1}{\rho_f}\nabla^{\boldsymbol{X}}\cdot\boldsymbol{W} = 0.}$$

where

$$\boldsymbol{W} = J\boldsymbol{F}^{-1}\cdot\boldsymbol{w}.$$

Piola's Transform

and

$$\boldsymbol{w} = \rho_{\mathrm{f}}\boldsymbol{k}\cdot\left[-\nabla^{\boldsymbol{x}}p^{\mathrm{f}} + \rho_{\mathrm{f}}(\boldsymbol{G} - \boldsymbol{a}^{\mathrm{f}})\right] - \rho_{\mathrm{f}}s_T\,\nabla^{\boldsymbol{x}}\theta,$$

Darcian Flow

Soret Effect
(neglected here)

❑ Balance of Energy

$$\boxed{c_{\boldsymbol{F}}\dot{\theta} = [D_{\mathrm{mech}} - H_\theta] + [-\nabla^{\boldsymbol{X}}\cdot\boldsymbol{Q}_\theta - \frac{\Phi^{\mathrm{f}}c_{\boldsymbol{F}\mathrm{f}}}{\rho_{\mathrm{f}}}\boldsymbol{W}\cdot\boldsymbol{F}^{-T}\nabla^{\boldsymbol{X}}\theta + R_\theta],}$$

Dissipation Heat Flux Convection Heat source

where

$$H_\theta = H_\theta^{\mathrm{s}} + H_\theta^{\mathrm{f}},$$

Total
Structural
Heating

and

$$H_\theta^{\mathrm{s}} = -\theta\frac{\partial}{\partial\theta}\boldsymbol{P}' : \dot{\boldsymbol{F}} = -3K\alpha_{sk}\theta\frac{\dot{J}}{J}$$

Solid Structural Heating (depending on which constitutive law being used)

$$H_\theta^{\mathrm{f}} = -\theta\frac{\partial}{\partial\theta}3\alpha^{\mathrm{m}}(\theta - \theta_o)\dot{p}^{\mathrm{f}} = -3\alpha^{\mathrm{m}}\theta\dot{p}^{\mathrm{f}}.$$

Fluid contribution

Remarks on Estimating Effective Thermal Conductivity from Microstructures

☐ Volume averaging effective thermal conductivity

$$\boldsymbol{k}_\theta = \phi^{\mathrm{f}} \boldsymbol{k}_\theta^{\mathrm{f}} + (1 - \phi^{\mathrm{f}}) \boldsymbol{k}_\theta^{\mathrm{s}}$$

(cf. Preisig & Prevost, IJGGC 2011)

☐ Homogenized effective conductivity via Eshelby equivalent inclusion method (for spherical inclusions)

$$\boldsymbol{k}_\theta = \left(k_\theta^f + \frac{\phi^{\mathrm{f}} (k_\theta^{\mathrm{s}} - k_\theta^{\mathrm{f}}) k_\theta^{\mathrm{f}}}{(k_\theta^{\mathrm{s}} - k_\theta^{\mathrm{f}}) \phi^{\mathrm{f}} + k_\theta^{\mathrm{f}}} \right) \boldsymbol{I}$$

(cf. Zhou & Meschke, IJNAMG 2013)

Important Note: In general, the temperature of the pore-fluid and solid skeleton are not the same in the RVE, until after sufficient diffusion takes place. This difference is neglected in current formulation.

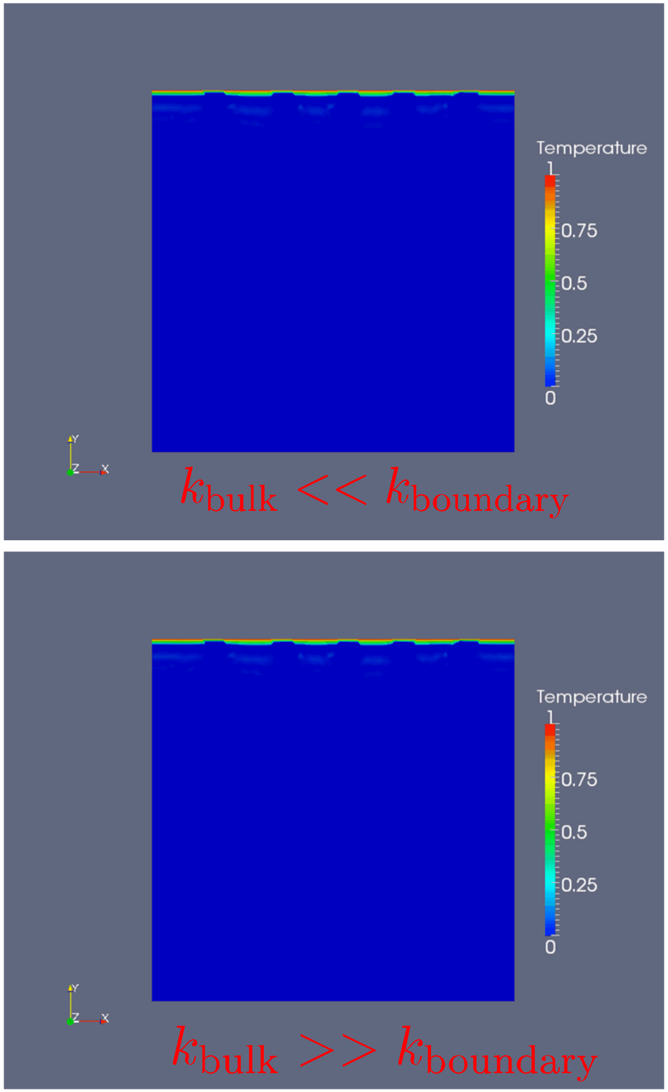

Solution of transient heat equation of two-phase materials

Exceptional service in the national interest

Sandia
National
Laboratories

Laser Weld

U.S. DEPARTMENT OF
ENERGY

NNSA
National Nuclear Security Administration

Large Deformation – Laser Welds

304L (stainless steel) is one of the most damage tolerant materials on the planet

The failure of 304L is a necking problem. Free surface creation is a 2nd order effect.

Pore size and distribution can aid the necking process

1. *Modeling pore growth requires remeshing and mapping*
2. *Component and system models must model failure through necking*

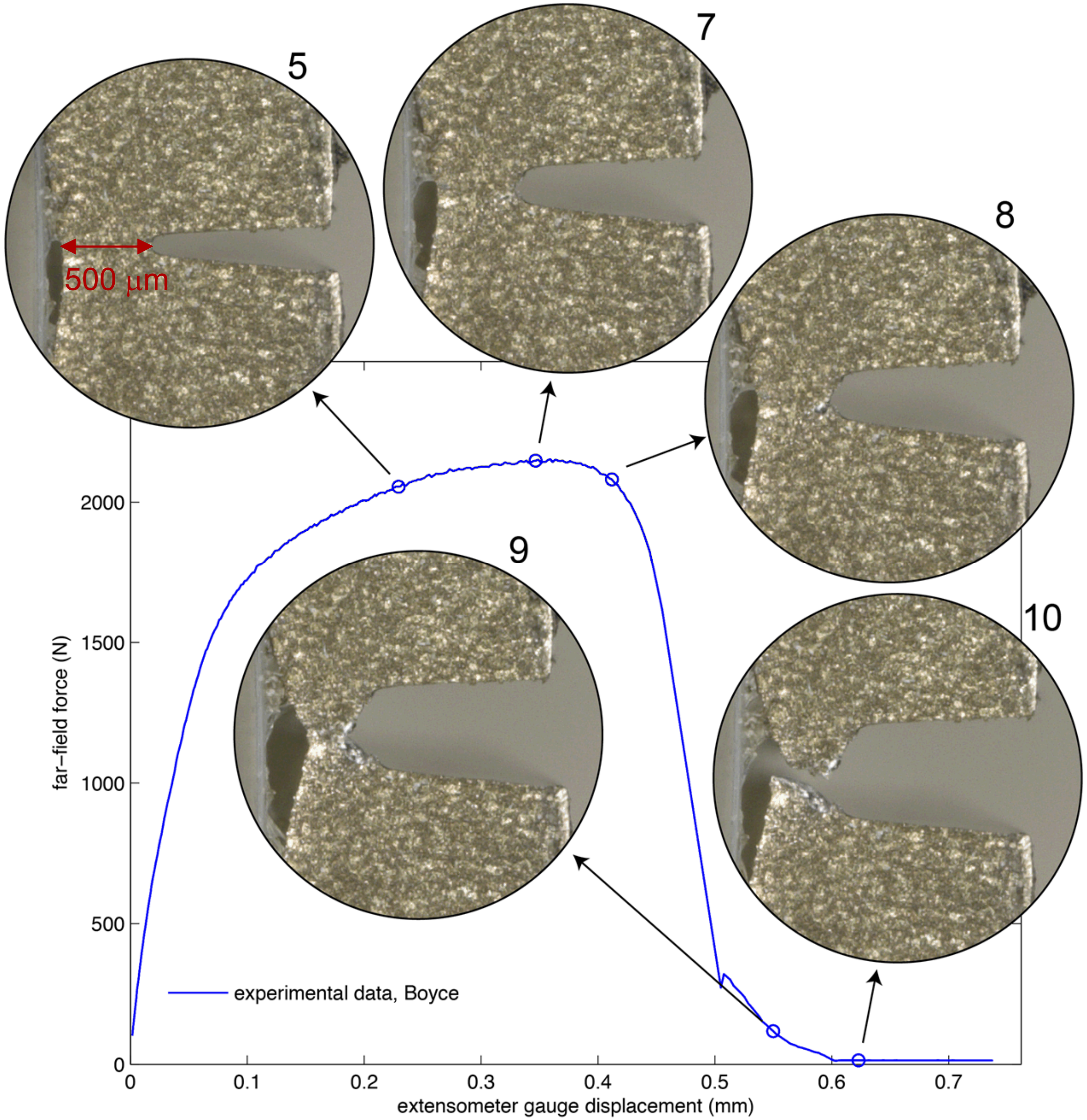

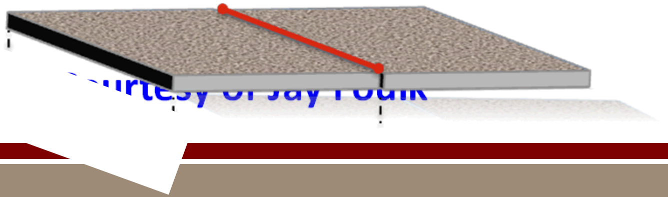

Large Deformation – Laser Welds

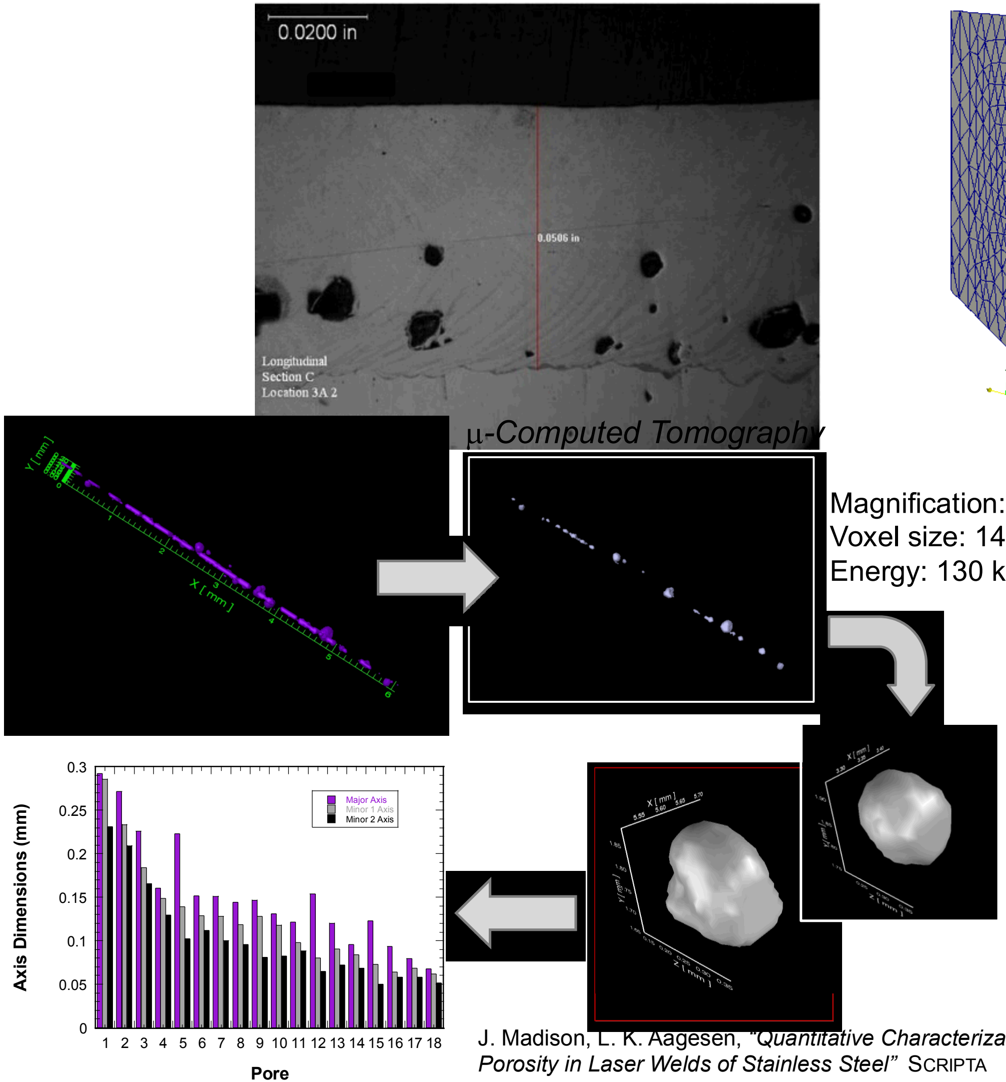

μ-Computed Tomography

Magnification: 9X
Voxel size: 14 μm
Energy: 130 keV

J. Madison, L. K. Aagesen, *"Quantitative Characterization of Porosity in Laser Welds of Stainless Steel"* SCRIPTA MATERIALIA (2012)

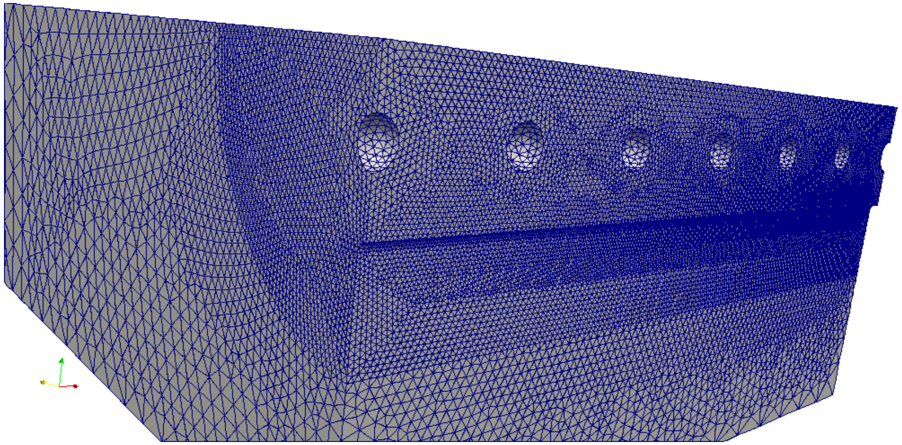

Sheet thickness: 1.6 mm
Ligament length: 508 μm
Number of voids: 6
Void diameter: 150 μm
Area fraction: 0.066 (~target)
Location: centerline of ligament
Coarse element size: 24 μm
Finer element size: 12 μm
Element type: composite-tet (10 nodes)

Courtesy of Jon Madison and Jay Foulk

Remeshing/mapping discrete pores

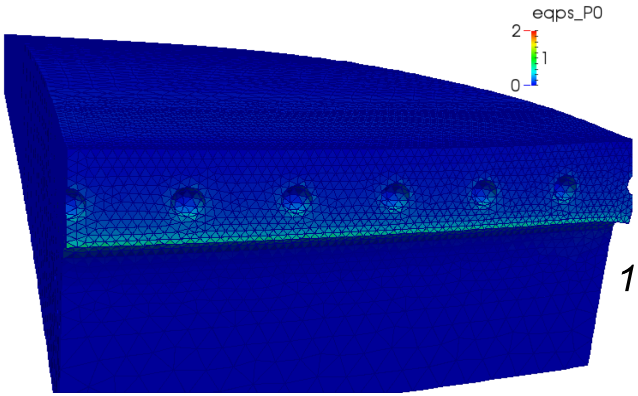

1st map

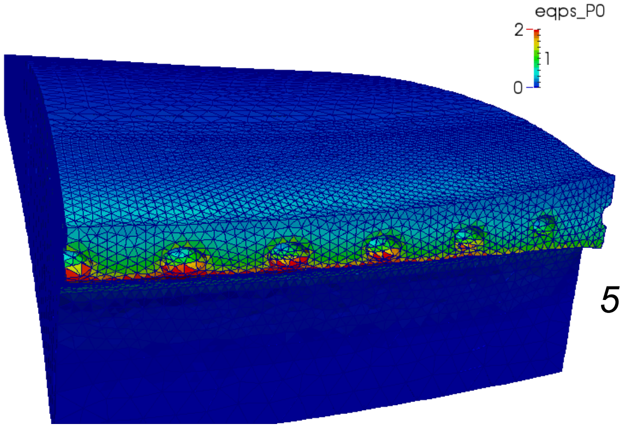

5th map

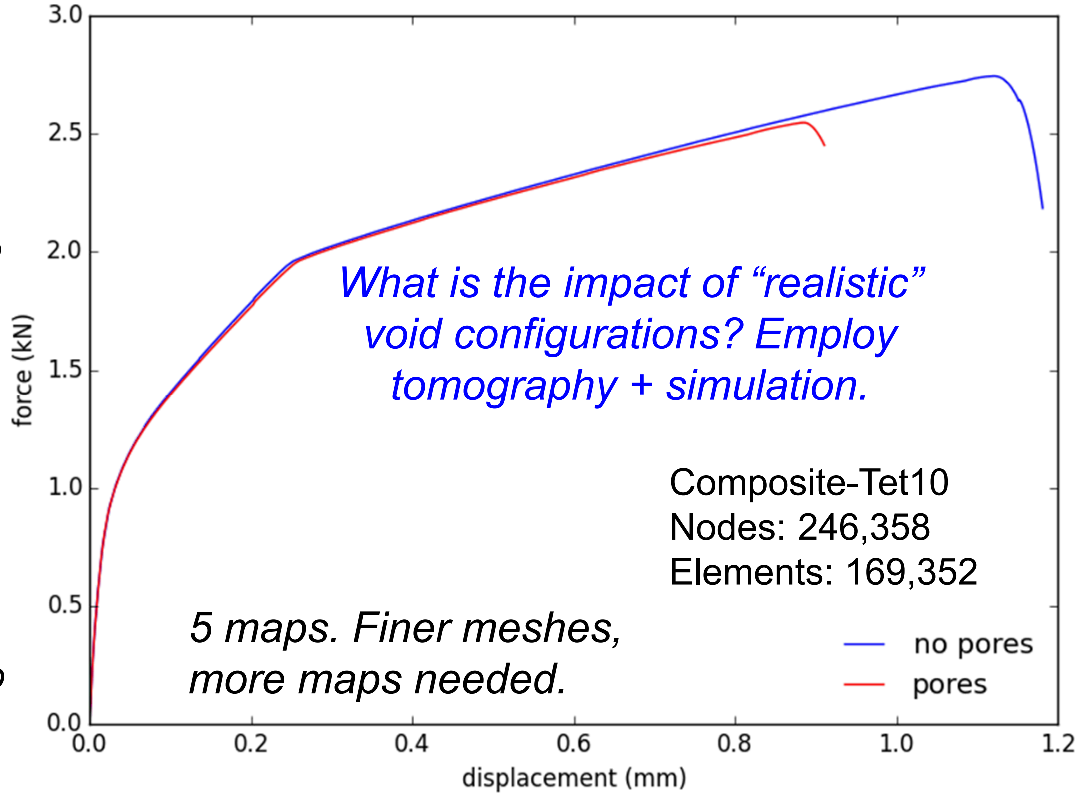

What is the impact of “realistic” void configurations? Employ tomography + simulation.

Composite-Tet10
Nodes: 246,358
Elements: 169,352

5 maps. Finer meshes, more maps needed.

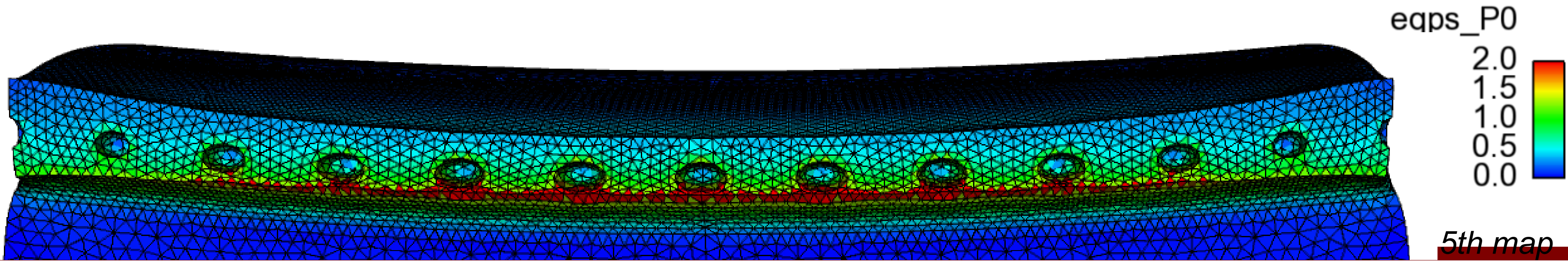

5th map

Additional views of necking process

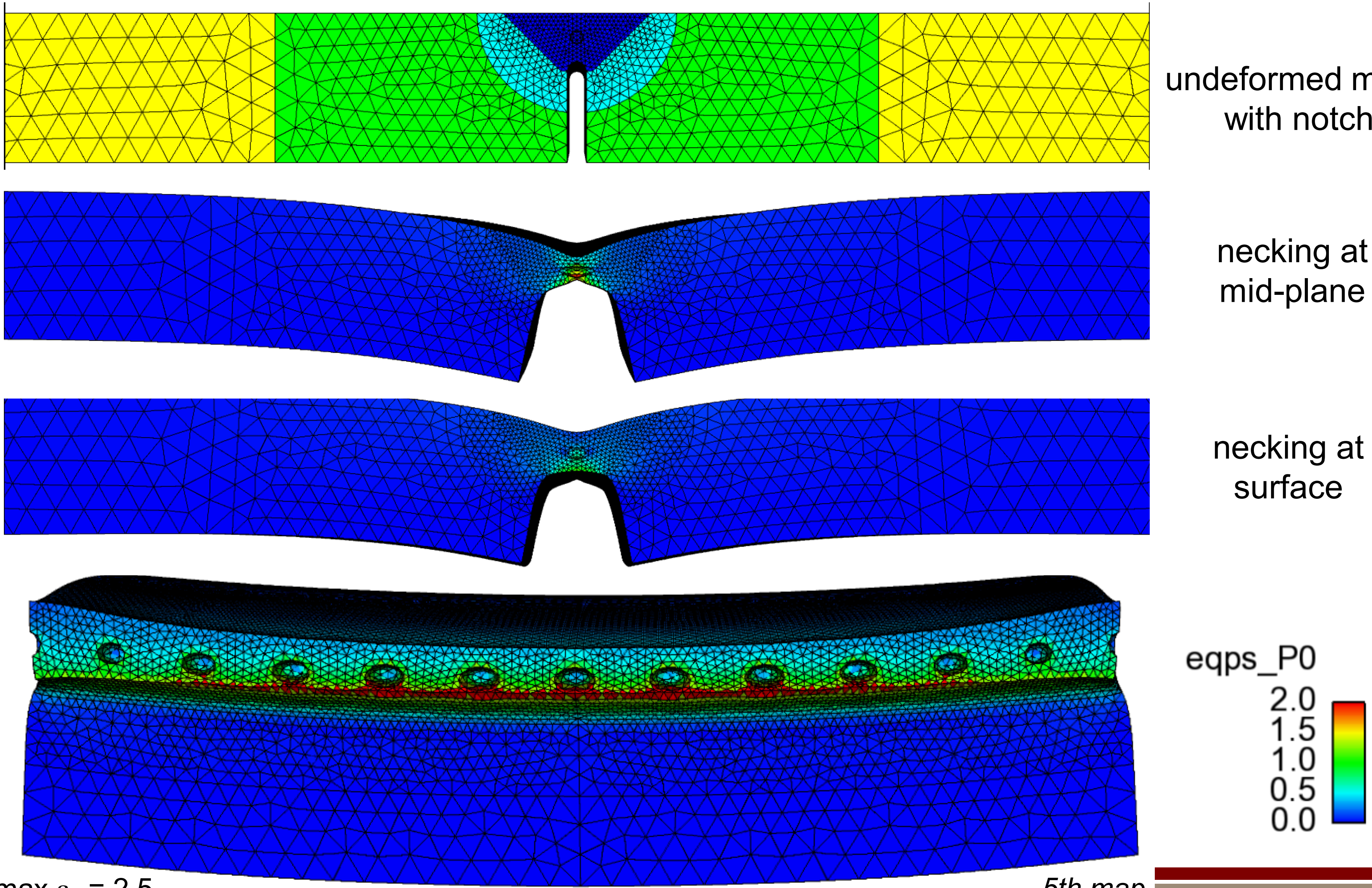

undeformed mesh
with notch

necking at
mid-plane

necking at
surface

max $\varepsilon_p = 2.5$

5th map

Increasing the number of mappings

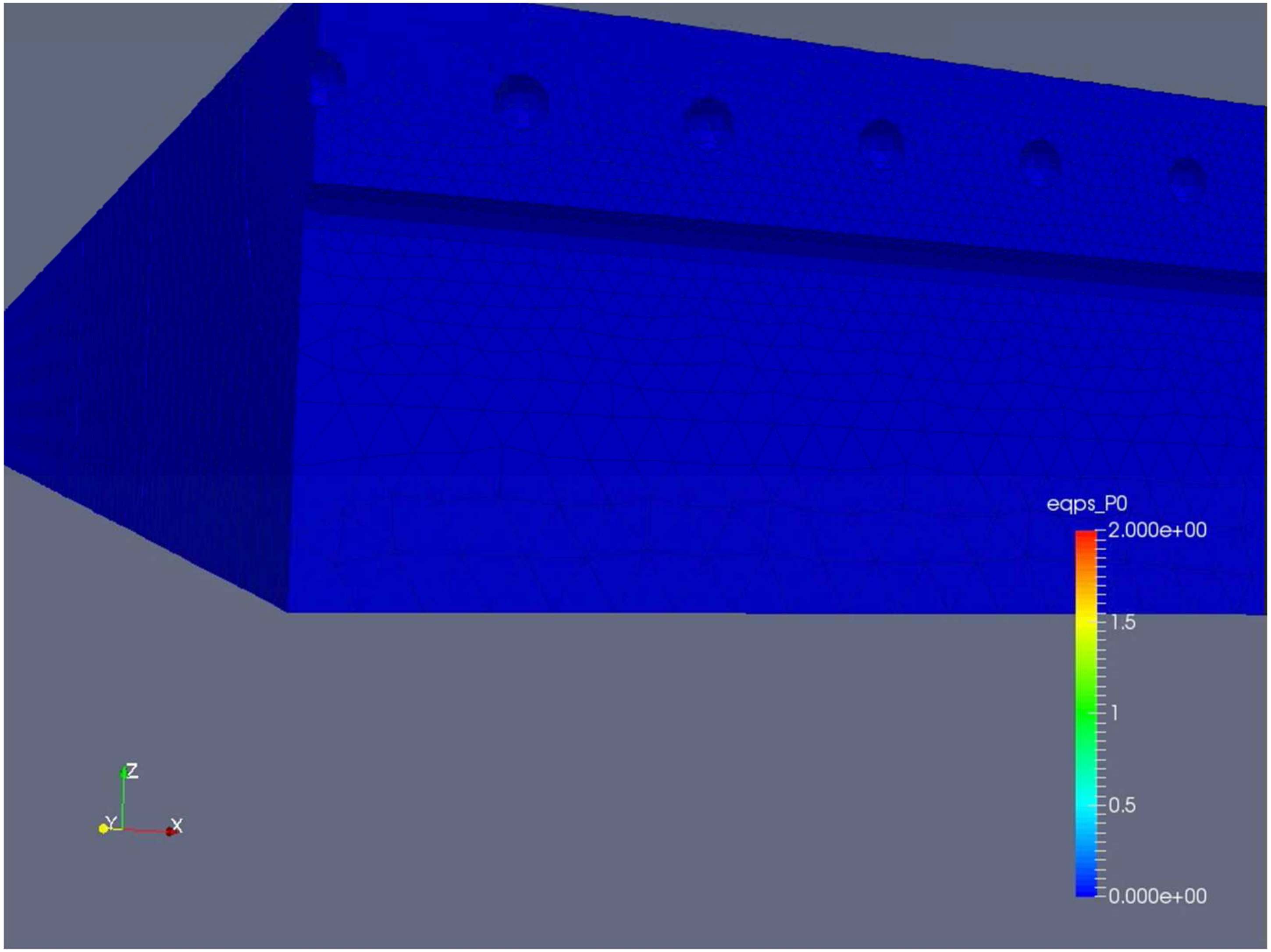

Deeper welds galvanize efforts

Weld schedule impacts porosity. Porosity impacts performance.

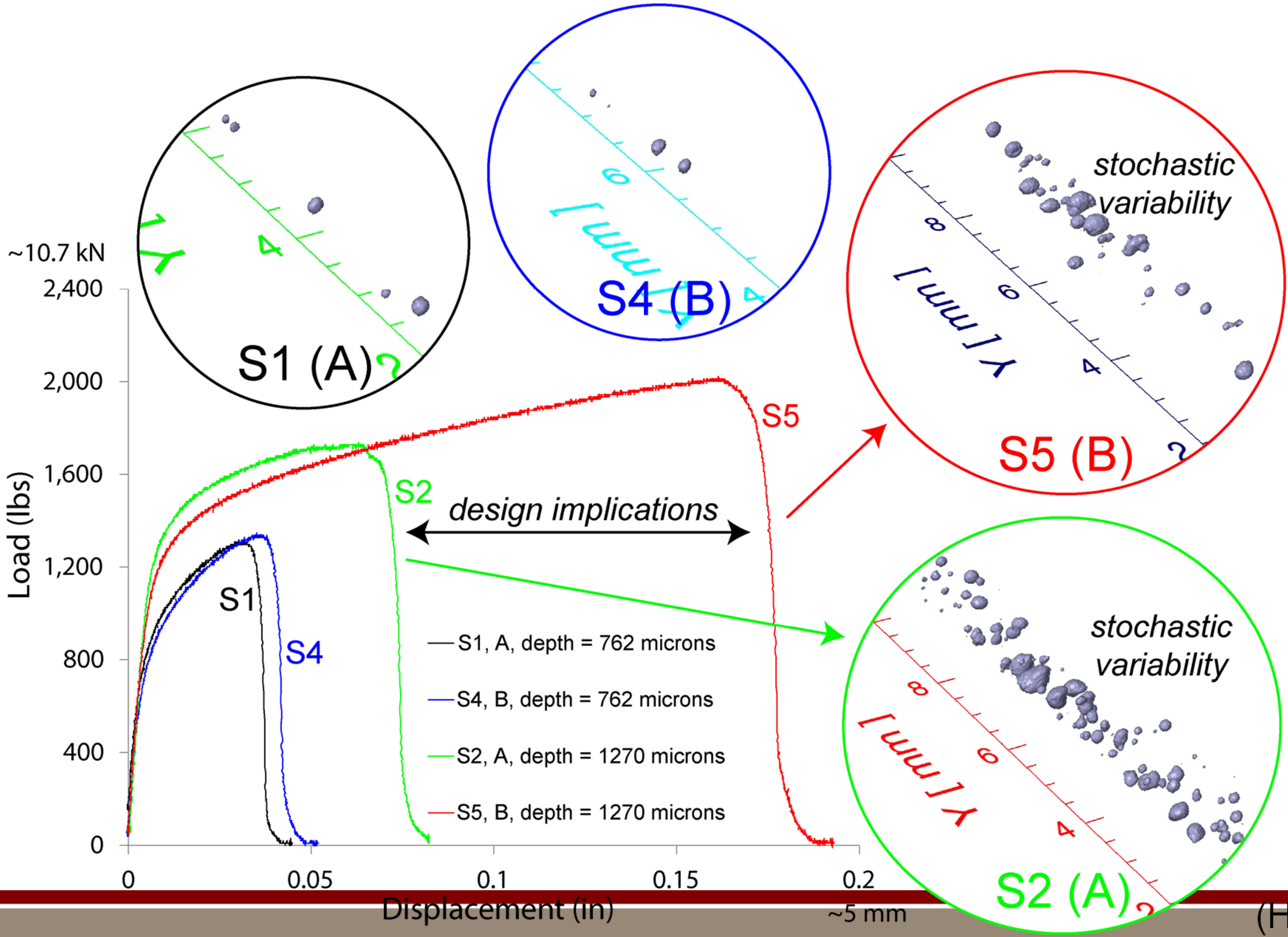

(H. Jin, J. Madison)

Hydrogen activates microstructure (stainless steel)

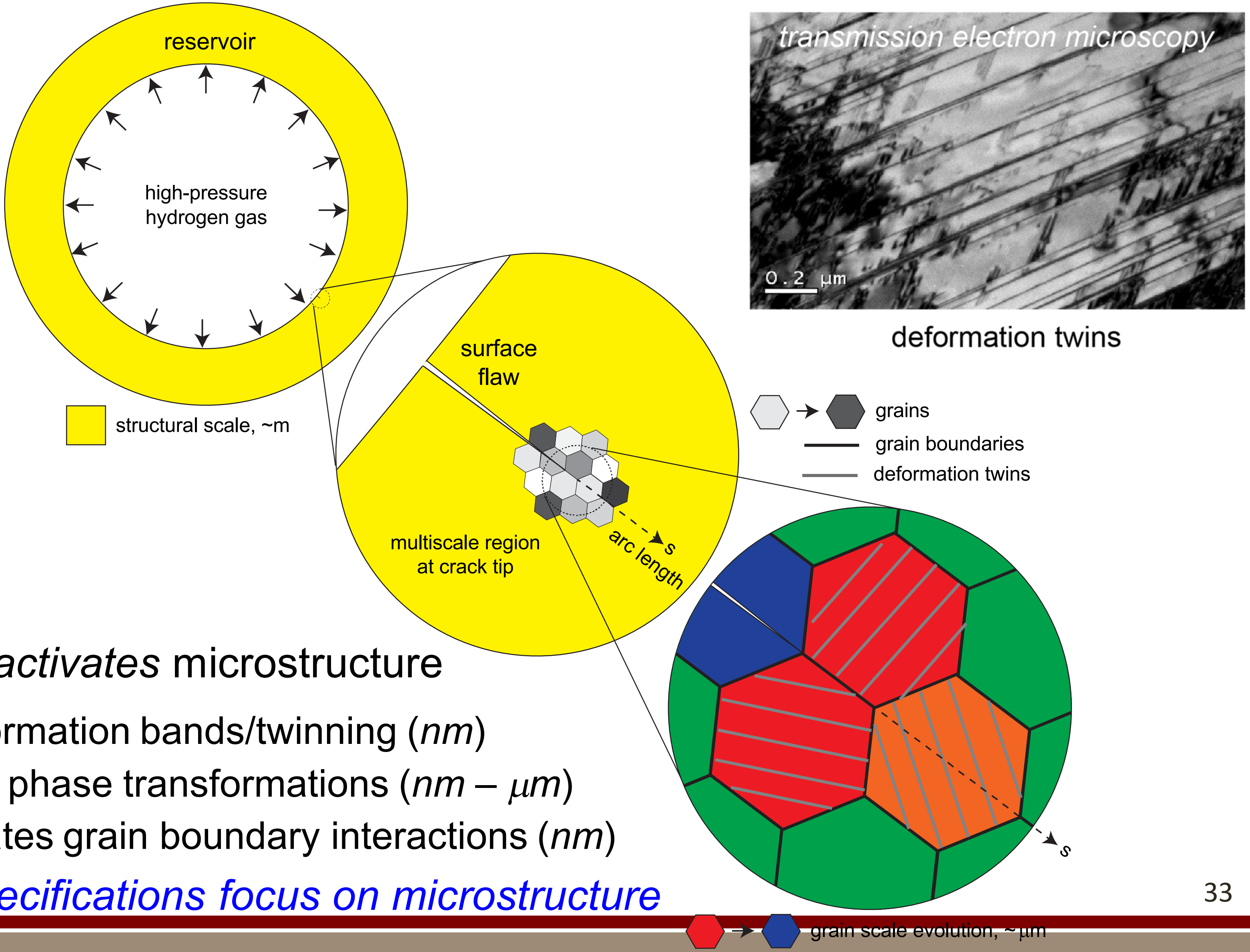

Hydrogen *activates* microstructure

- Aids deformation bands/twinning (*nm*)
- Activates phase transformations (*nm – µm*)
- Accentuates grain boundary interactions (*nm*)

Material specifications focus on microstructure

Demonstrate strong chemo-mechanical coupling

Block solve for displacement, concentration, and pressure at a crack tip

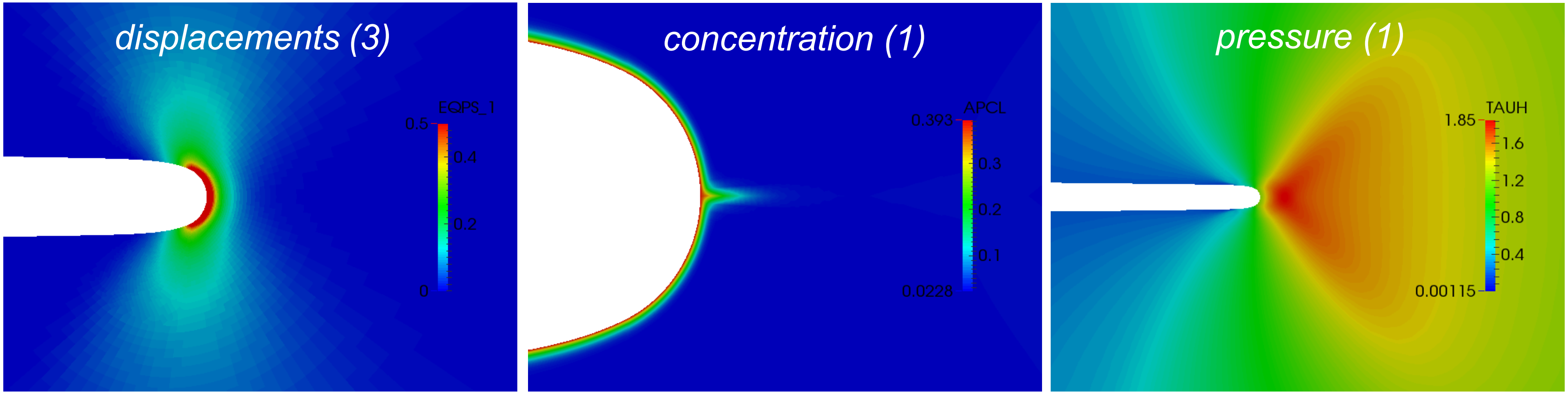

Exploring fast pathways through the inclusion of surface elements on grain boundaries

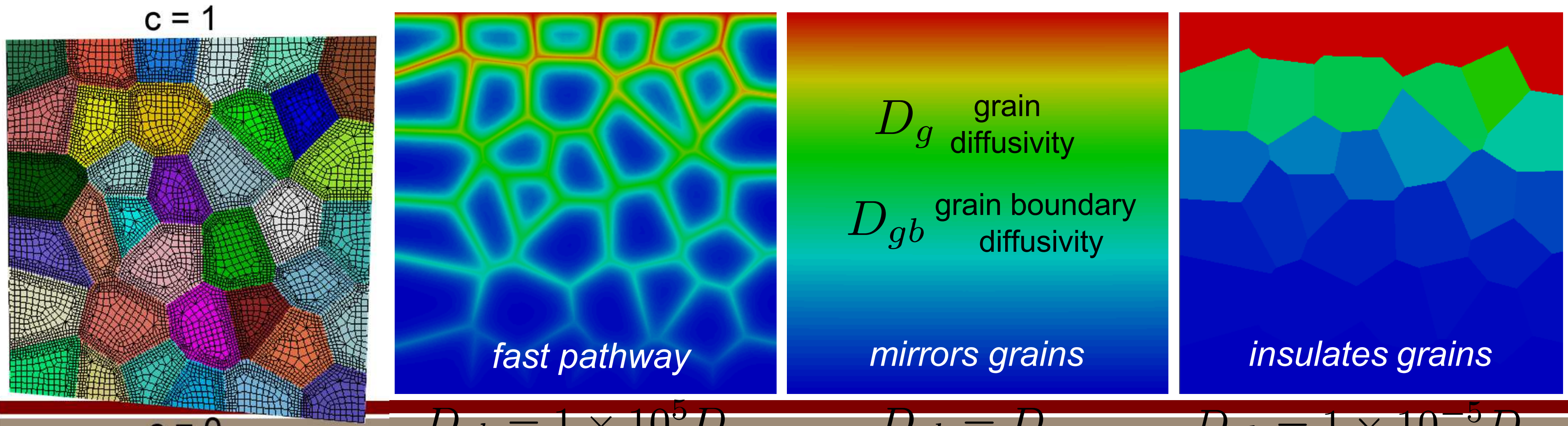

$D_{gb} = 1 \times 10^5 D_g$ $D_{gb} = D_g$ $D_{gb} = 1 \times 10^{-5} D_g$

Exceptional service in the national interest

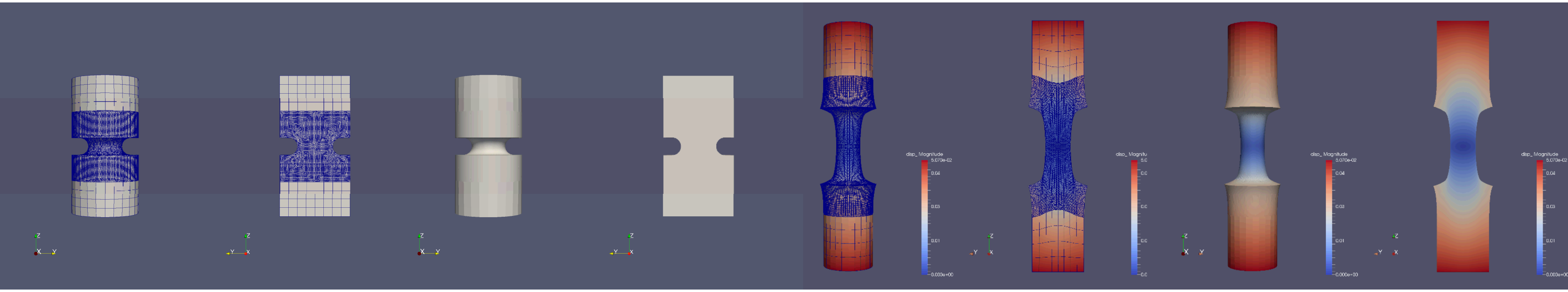

The Alternating Schwarz Method for Concurrent Multiscale in Finite Deformation Solid Mechanics

Alejandro Mota, Irina Tezaur, Coleman Alleman

Sandia National Laboratories, Livermore, CA

A Case for Concurrent Coupling

Q: Is a one-way transfer accurate? Conservative?

A: For failure processes involving localization, no.

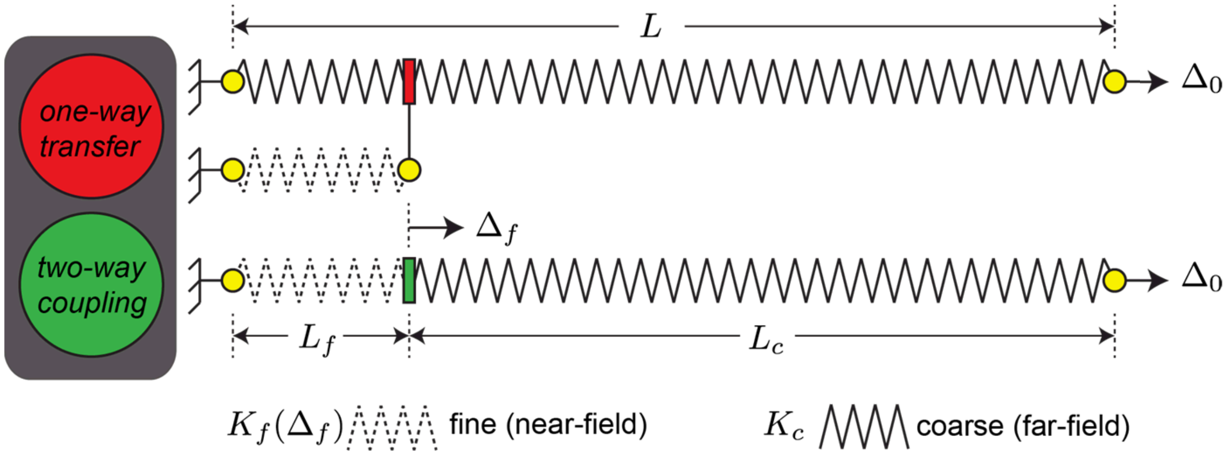

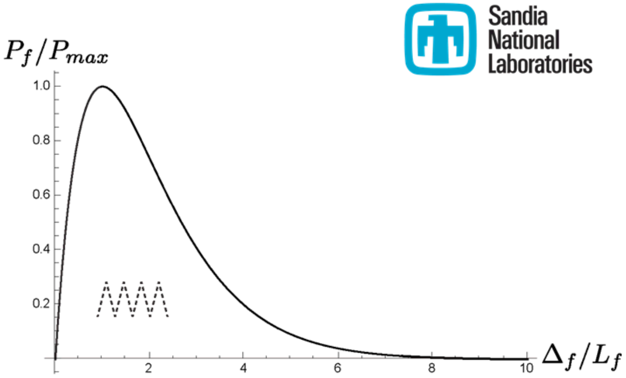

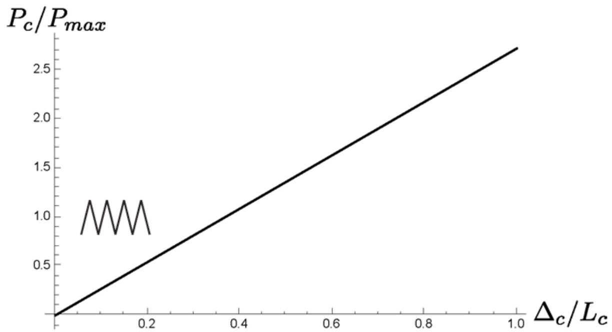

violates equilibrium

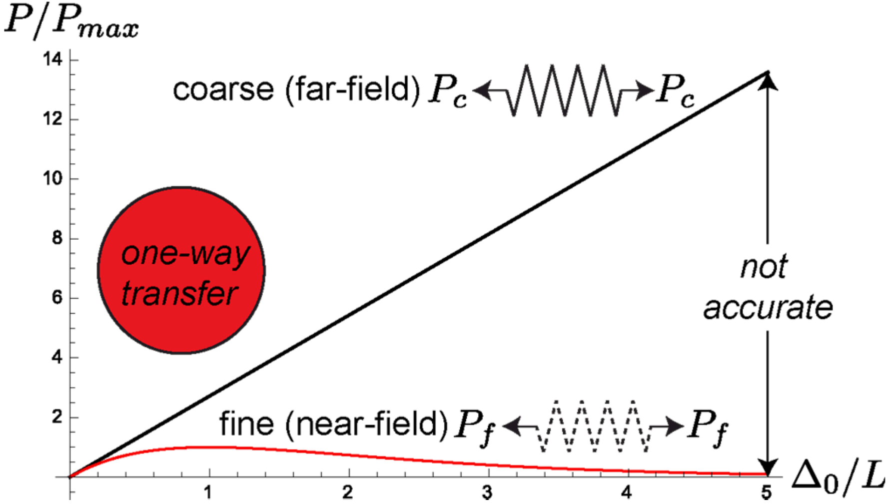

postpones failure

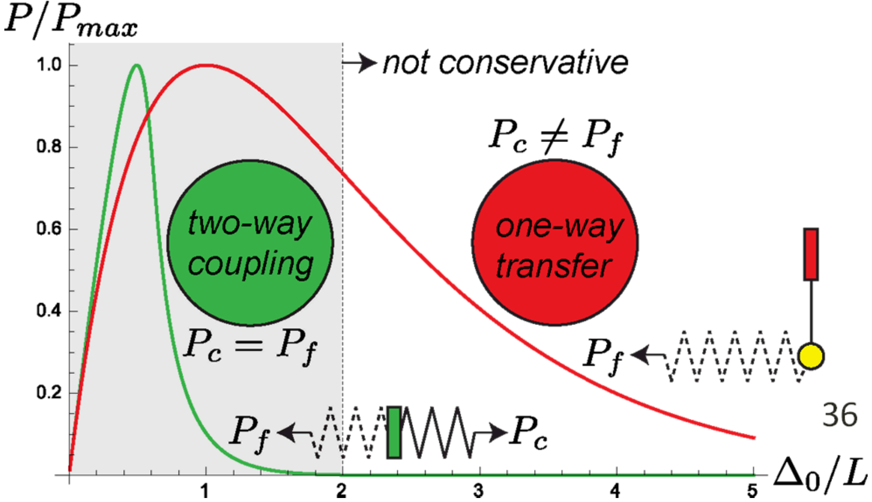

Alternating Schwarz for Domain Decomposition

- First developed in 1870 for solving Laplace's equation in irregularly shaped domains.
- Simple idea: if the solution is known in regularly shaped domains, use those as puzzle pieces to iteratively build a solution for the more complex domain.

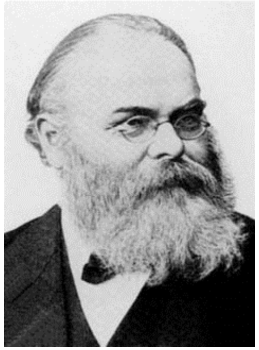

Karl Hermann Amandus Schwarz (1843 – 1921). Source: *bibmath.net*

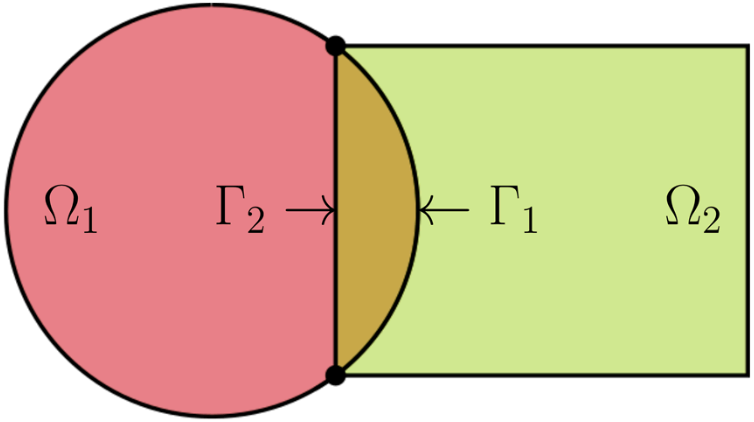

- Initialize:
  - Solve PDE by any method on Ω_1 using an initial guess for Dirichlet BCs on Γ_1.
- Iterate until convergence:
  - Solve PDE by any method (can be different than for Ω_1) on Ω_2 using Dirichlet BCs on Γ_2 that are the values just obtained for Ω_1.
  - Solve PDE by any method (can be different than for Ω_2) on Ω_1 using Dirichlet BCs on Γ_1 that are the values just obtained for Ω_2.

Alternating Schwarz after Schwarz

- S. L. Sobolev posed the Schwarz method for linear elasticity in variational form.
- He also proved convergence of the method for linear elasticity in 1936 by proposing a convergent sequence of energy functionals.
- Convergence for general linear elliptic partial differential equations was not proved until much later in 1951 by S. G. Mikhlin.
- We have derived a proof of convergence of the alternating Schwarz for the finite deformation, fully nonlinear PDE.
- We have also determined that the alternating Schwarz method converges geometrically for the finite deformation problem.

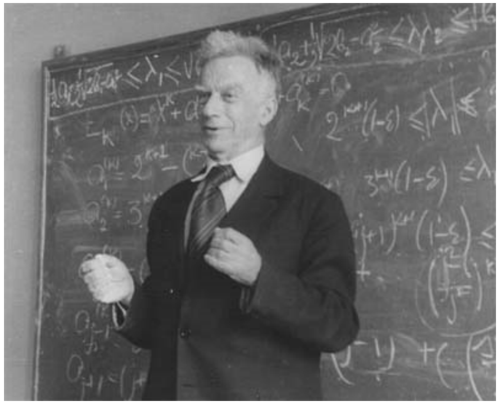

Sergei Lvovich Sobolev (1908 – 1989).

Source: *www.math.nsc.ru*

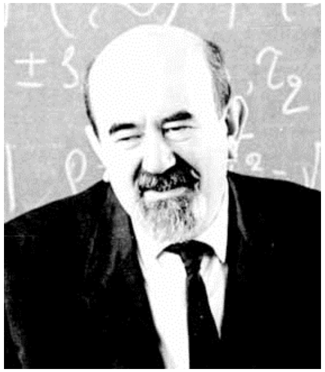

Solomon Grigoryevich Mikhlin (1908 – 1990).
Source: *www-history.mcs.st-andrews.ac.uk*

$$\Phi[\varphi] = \int_B W(\boldsymbol{F}, \boldsymbol{Z}, T)\, dV - \int_B \boldsymbol{B} \cdot \varphi\, dV - \int_{\partial_T B} \bar{\boldsymbol{T}} \cdot \varphi\, dS$$

$$\text{Div}\, \boldsymbol{P} + \boldsymbol{B} = \boldsymbol{0}$$

Alternating Schwarz in Albany

- Aternating Schwarz can be posed in the linear case as a block system.
- The block system can have different structures (see Smith et al., Domain Decomposition, 2004).
- In a nonlinear setting, the linear system results from the consistent linearization of the fully nonlinear system.
- The coupling terms appear in the RHS, resulting in a block diagonal system with a simpler structure that we exploit.
- Efficient solution is achieved with iterative linear solver using a block preconditioner.

$$\begin{pmatrix} \boldsymbol{K}^1_{AB} & \mathbf{0} \\ \mathbf{0} & \boldsymbol{K}^2_{AB} \end{pmatrix} \begin{Bmatrix} \triangle \boldsymbol{x}^1_B \\ \triangle \boldsymbol{x}^2_B \end{Bmatrix} = \begin{Bmatrix} -\boldsymbol{R}^1_A - \boldsymbol{K}^1_{Ab}\left(\boldsymbol{\chi}^1_b - \boldsymbol{x}^1_b\right) - \boldsymbol{K}^1_{A\beta}\left(P_{\Omega_2\to\Gamma_1}[\boldsymbol{x}^2] - \boldsymbol{x}^1_\beta\right) \\ -\boldsymbol{R}^2_A - \boldsymbol{K}^2_{Ab}\left(\boldsymbol{\chi}^2_b - \boldsymbol{x}^2_b\right) - \boldsymbol{K}^2_{A\beta}\left(P_{\Omega_1\to\Gamma_2}[\boldsymbol{x}^1] - \boldsymbol{x}^2_\beta\right) \end{Bmatrix}$$

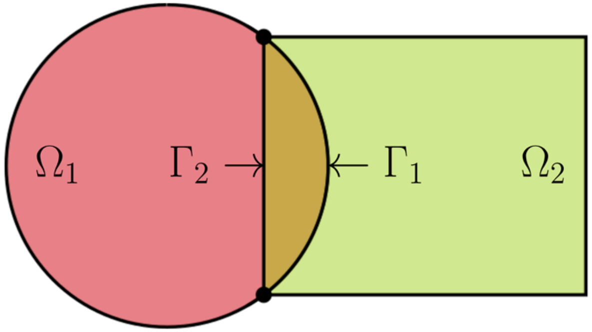

$$\begin{pmatrix} \boldsymbol{K}^1_{AB} & \boldsymbol{K}^1_{Ab} & \boldsymbol{K}^1_{A\beta} & & & \\ & \boldsymbol{I} & & & \mathbf{0} & \\ & & \boldsymbol{I} & & & \\ & & & \boldsymbol{K}^2_{AB} & \boldsymbol{K}^2_{Ab} & \boldsymbol{K}^2_{A\beta} \\ & \mathbf{0} & & & \boldsymbol{I} & \\ & & & & & \boldsymbol{I} \end{pmatrix} \begin{Bmatrix} \triangle \boldsymbol{x}^1_B \\ \triangle \boldsymbol{x}^1_b \\ \triangle \boldsymbol{x}^1_\beta \\ \triangle \boldsymbol{x}^2_B \\ \triangle \boldsymbol{x}^2_b \\ \triangle \boldsymbol{x}^2_\beta \end{Bmatrix} = \begin{Bmatrix} -\boldsymbol{R}^1_A \\ \boldsymbol{\chi}^1_b - \boldsymbol{x}^1_b \\ P_{\Omega_2\to\Gamma_1}[\boldsymbol{x}^2] - \boldsymbol{x}^1_\beta \\ -\boldsymbol{R}^2_A \\ \boldsymbol{\chi}^2_b - \boldsymbol{x}^2_b \\ P_{\Omega_1\to\Gamma_2}[\boldsymbol{x}^1] - \boldsymbol{x}^2_\beta \end{Bmatrix}$$

Example: Foulk's Singular Bar

- 1D Proof of concept problem.
- Test convergence and compare with literature (Evans, 1986).
- Expect faster convergence in fewer iterations with increased overlap.
- Strong singularity on left end of bar – area proportional to square root of length
- Simple hyperelestic model with damage

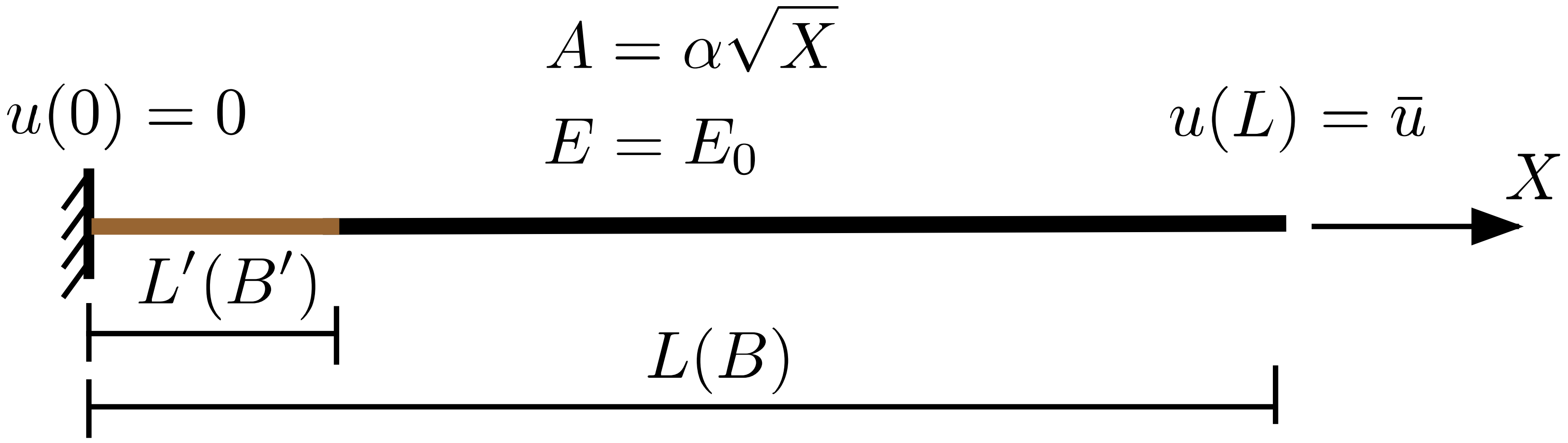

Schwarz Convergence: Symmetric Overlap

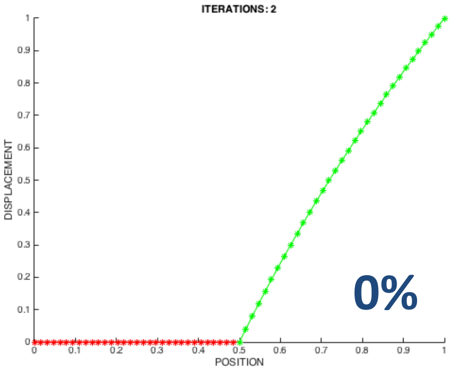

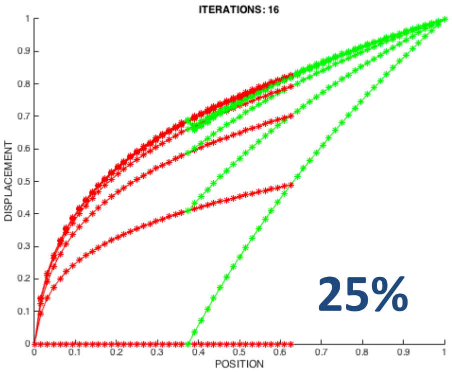

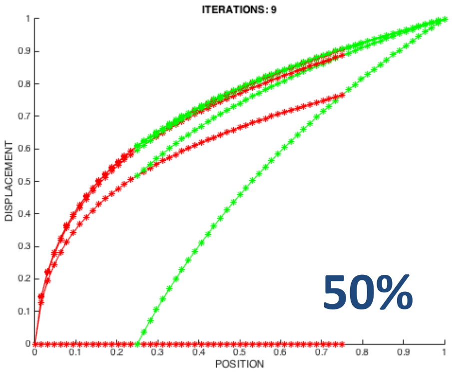

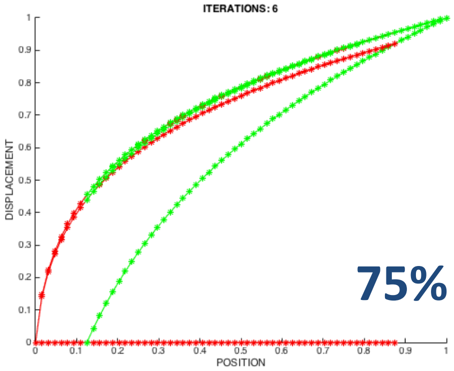

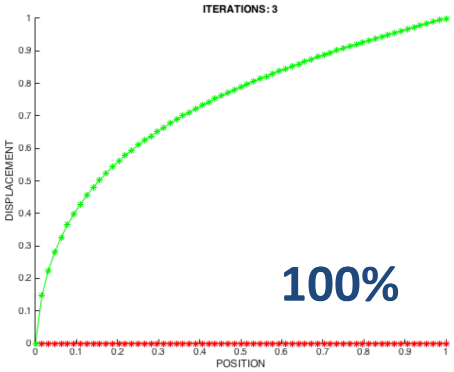

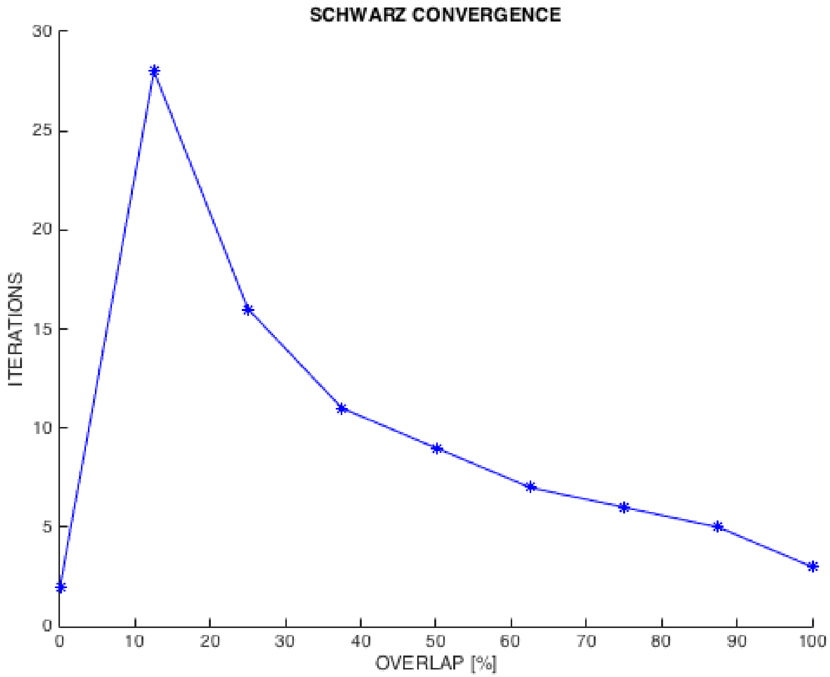

Hyperelastic Notched Cylinder

- Notched cylinder stretched to twice its original height.
- Stress concentrations and strain localization in the notch require a higher level of mesh refinement.
- The fine and coarse region overlap but the solutions are computed separately.

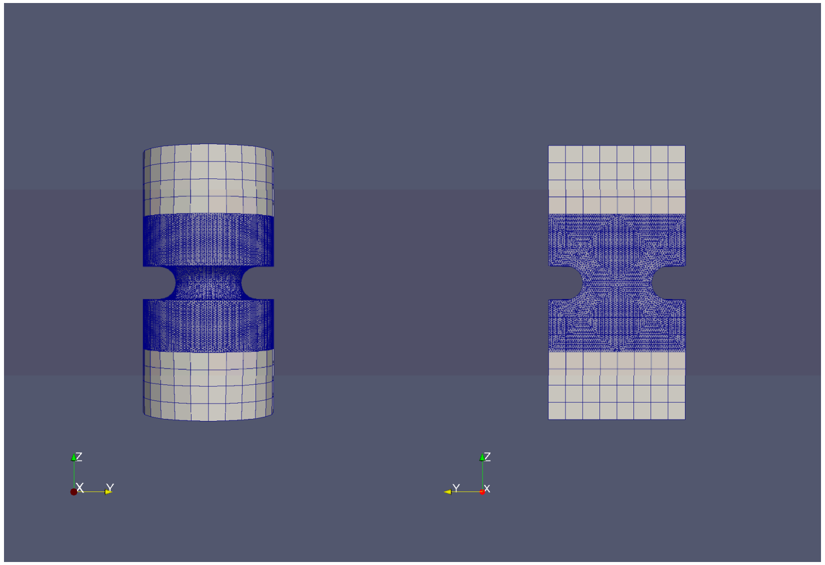

- The notched region, where stress concentrations are expected, is finely meshed with tetrahedral elements.
- The top and bottom regions, presumably of less interest, are meshed with coarser hexahedral elements.

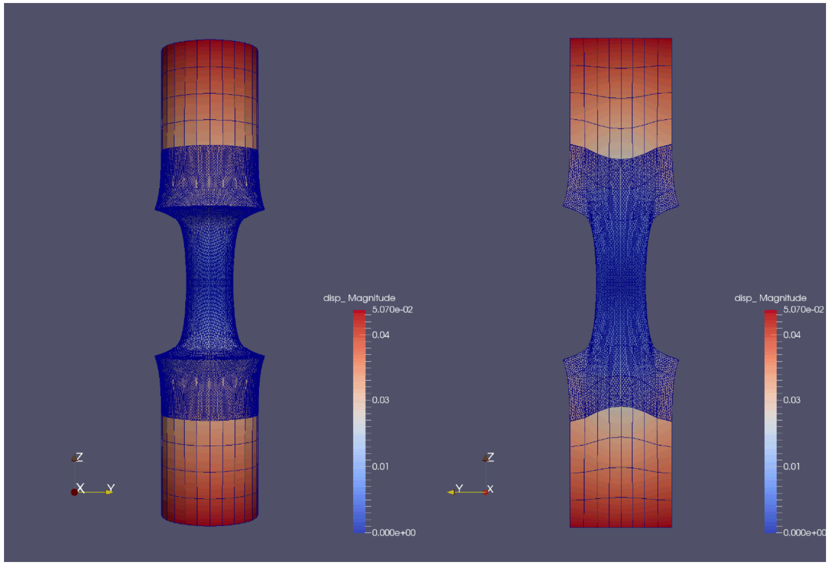

Deformed configuration colored with displacement magnitude. Smooth field transition even when the meshes do not match.

Coupling of Different Material Models

- The Schwarz method is capable of coupling regions with different material models.
  - Notched cylinder subjected to tensile load with an elastic and J2 elasto-plastic regions.
- When the overlap region is far from the notch, no plastic deformation exists in it: the coarse and fine regions predict the same behavior there.
- When the overlap region is near the notch, plastic deformation spills onto it and the two models predict different behavior, affecting convergence adversely. Independent of any method, this kind of solution is questionable.

Overlap far from notch　Overlap near notch

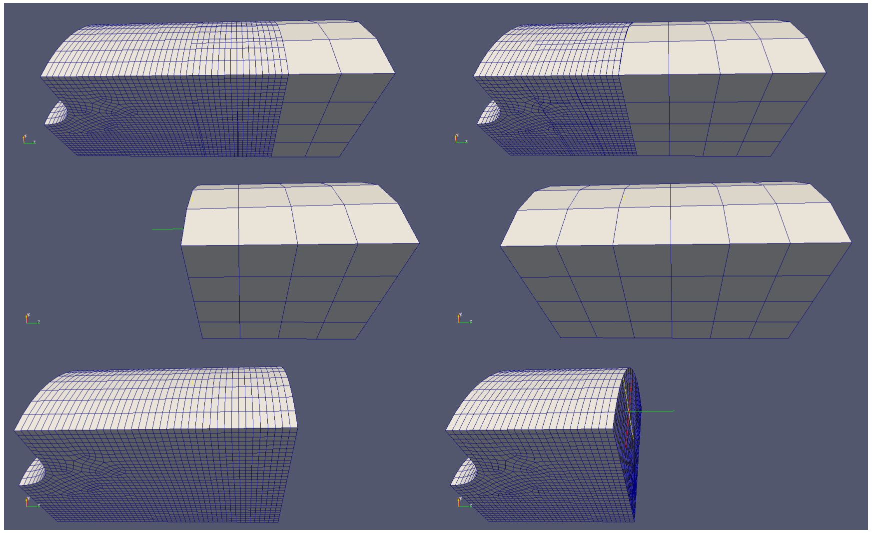

Overlap far from notch　Overlap near notch

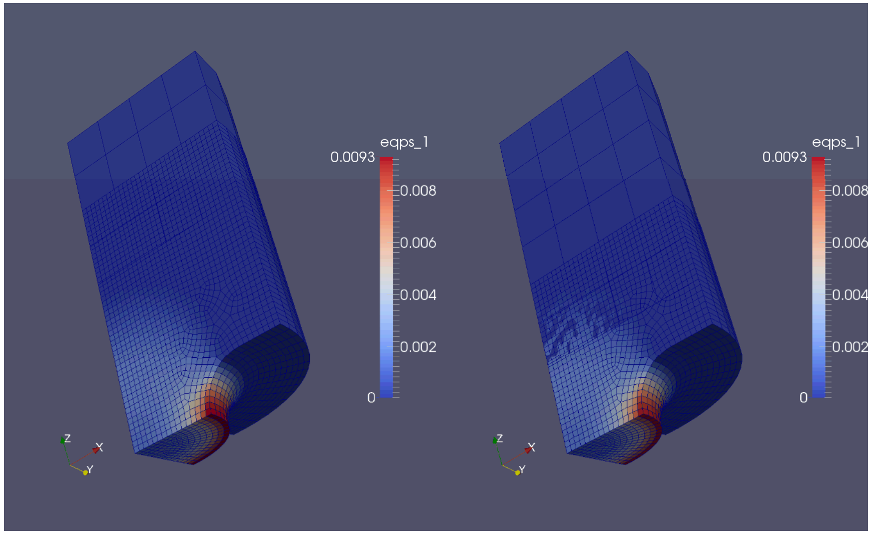

Coupled Isotropic and Crystal Hyperelasticity

Two distinct bodies, the component scale and the microstructural scale, are coupled iteratively with alternating Schwarz

Work by J. Foulk, D. Littlewood, C. Battaile, H. Lim

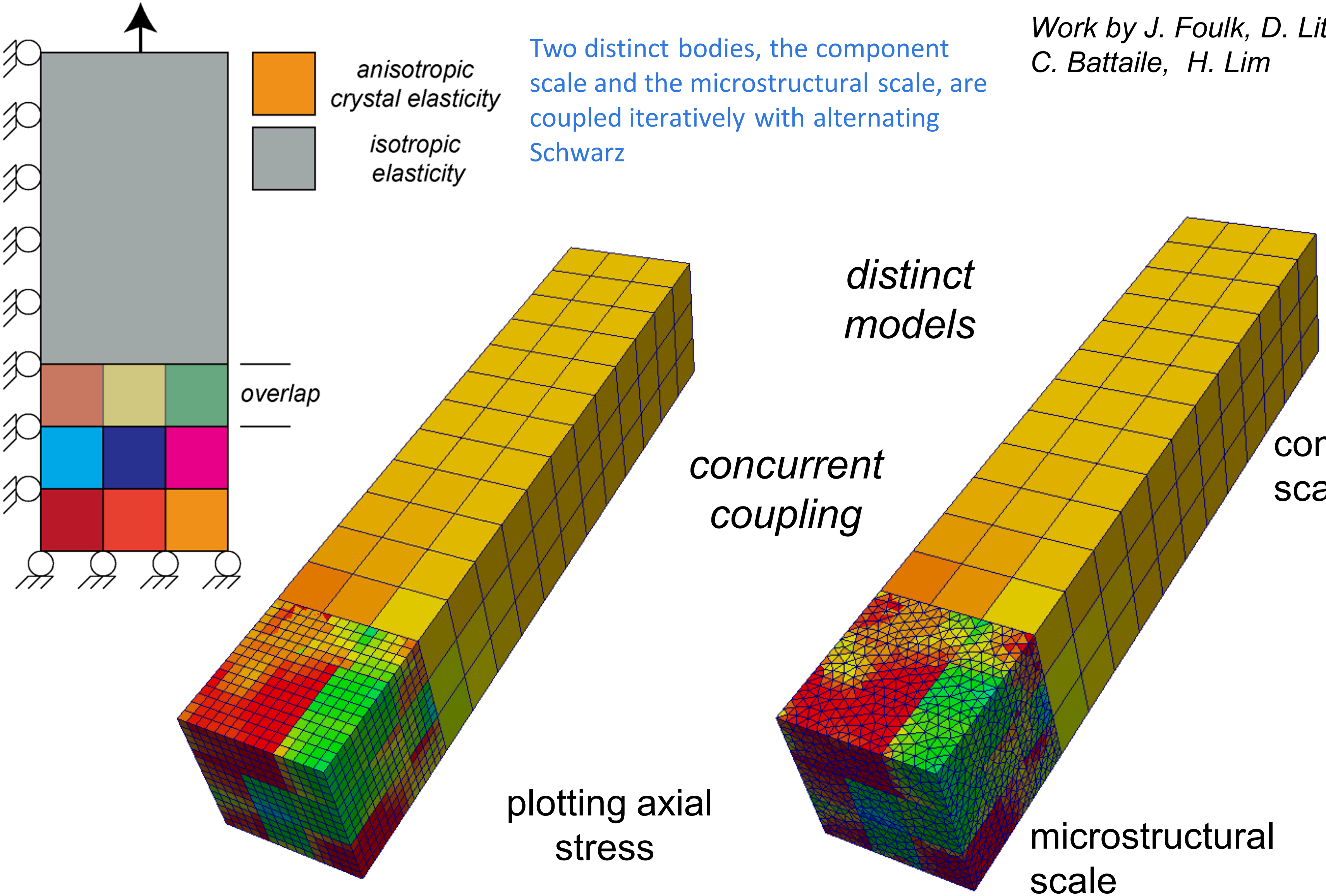

distinct models

concurrent coupling

component scale

plotting axial stress

microstructural scale

Dynamics with Schwarz

- Extend Schwarz coupling to dynamics using a governing time stepping algorithm to control time integrators in each domain.
- Can use different integrators and time steps in each domain.
- 1D results show smooth coupling; no numerical artifacts such as spurious wave reflections at boundaries of coupled domains.

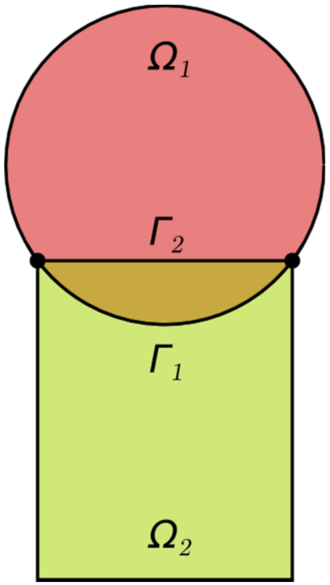

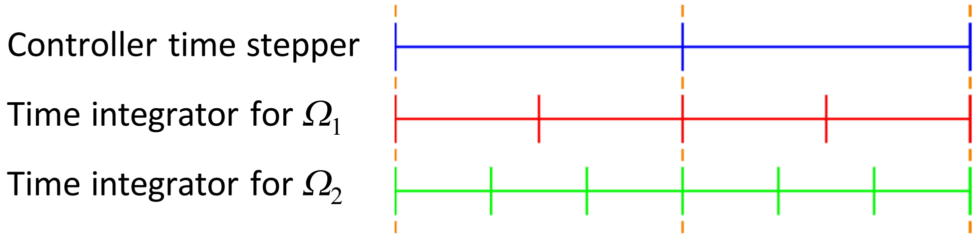
Controller time stepper

Time integrator for Ω_1

Time integrator for Ω_2

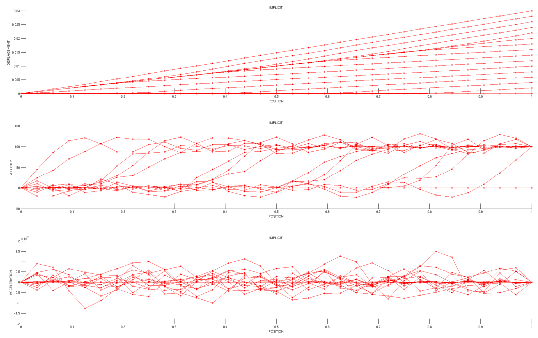
(a) Reference single-domain solution

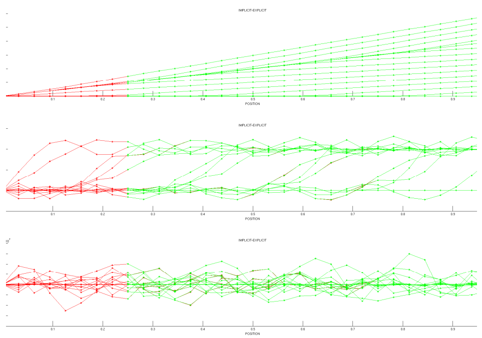
(b) Two-domain implicit-explicit solution equal to (a). No dynamic artifacts.


(c) Fine-coarse implicit-explicit coupling

Microstructure

Microstructural localization requires much more

Q: How does *microstructure influence* conditions for *necking instability*?

Q: *When does microstructure matter, and when can it be ignored in continuum models?*

O: Local deformations at the microstructural level vastly exceed component-scale predictions.

A. Ghahremaninezhad, K. Ravi-Chandar (IJF, 2013)

S. Haltom, S. Kyriakides, K. Ravi-Chan

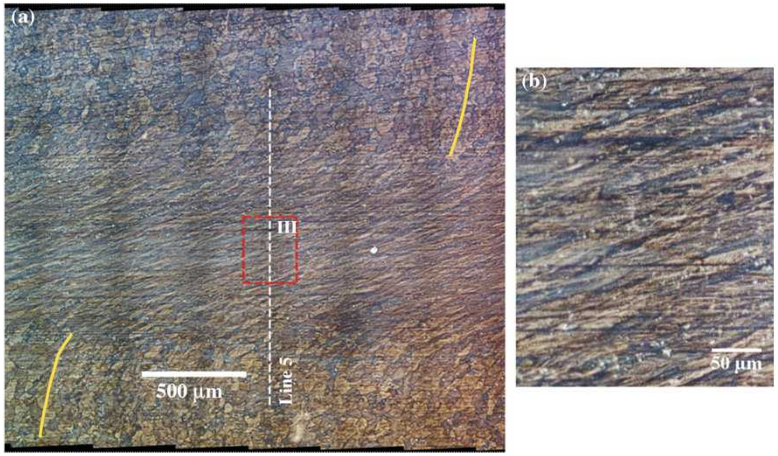

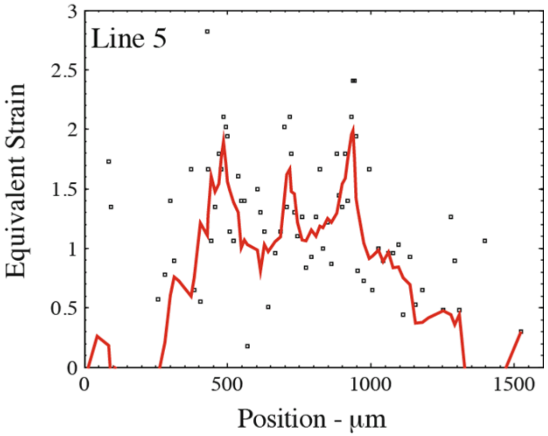

“strain values measured at the grain level are significantly larger”

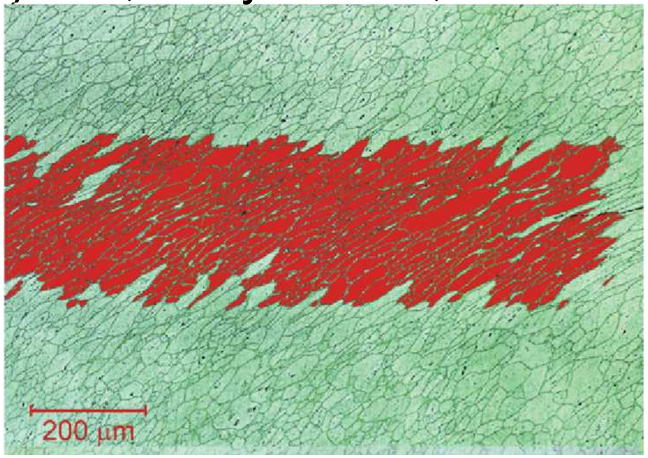

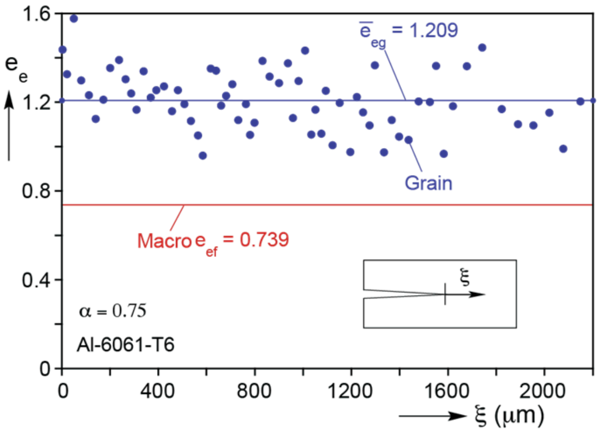

“void formation and coalescence is delayed until the very end of the life of the deforming material”

Revisiting CP with a focus on agility

- Consolidating crystal physics
- *Implicit implementation with automatic differentiation*
- Agility through plug-n-play interfaces
  - Multiple residuals
    - Solve for slip, slip + hardening (12, 24 unknowns)
    - Solve for **F**$_p$, **F**$_p$ + hardening (9, 21 unknowns)
  - Multiple solution schemes (Newton, CG, Trust Region)
  - Evolving physics
    - Models for elasticity, flow rule, and hardening
- Adopting modern software practices with rigorous testing

Rubik's cube case

- 512 elements/grain
- 27 grains w/random texture
- 100% engineering strain
- Vary step size
- Vary solution methods

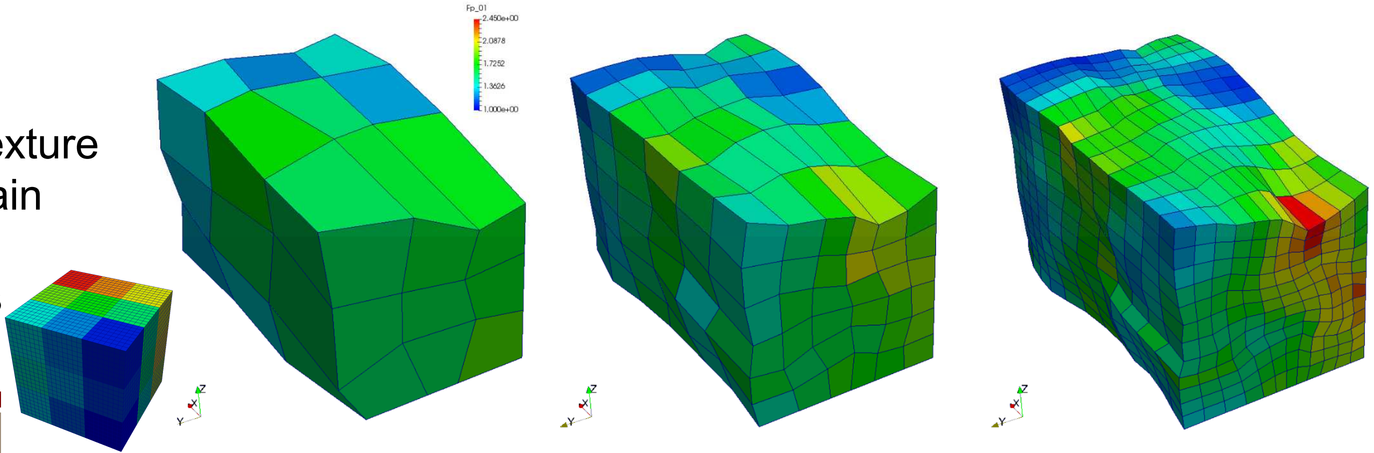

Focus on verification, robustness and microstructure

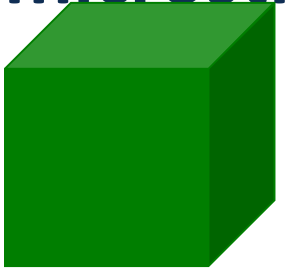

☑

single slip (analytical)

multiple slip systems (FCC)

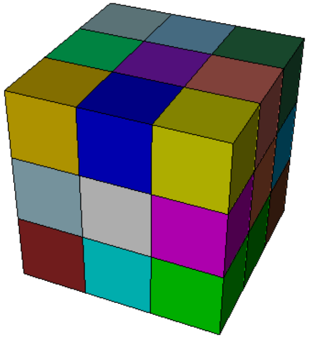

☑

Rubik's cube
3D polycrystals

g

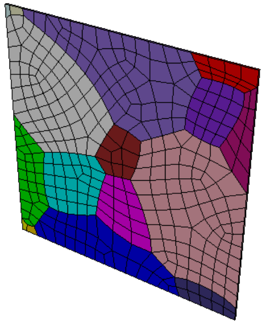

☑

2D polycrystals

many elements per grain

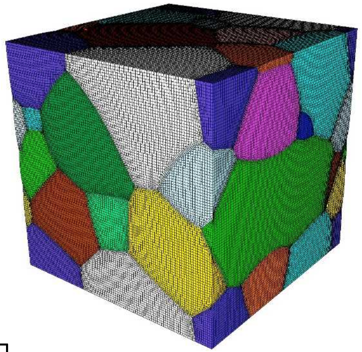

☐

3D polycrystals
~10^2 grains/~10^6 elements

anisotropic hardening

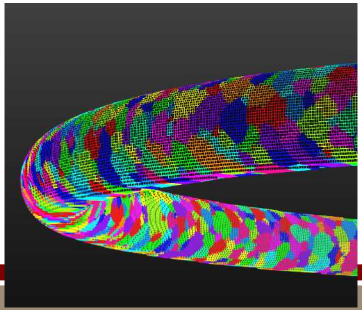

☐

Component scale
~10^6 grains/~10^9 elements
concurrent coupling

Leveraging Conformal Microstructures LDRD

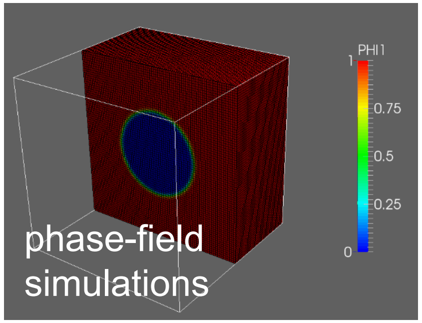

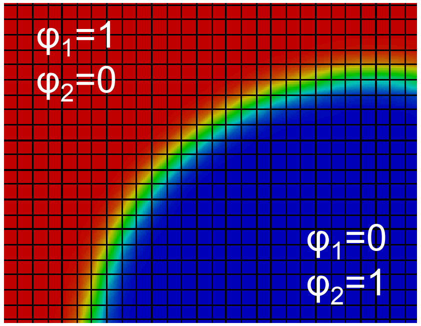

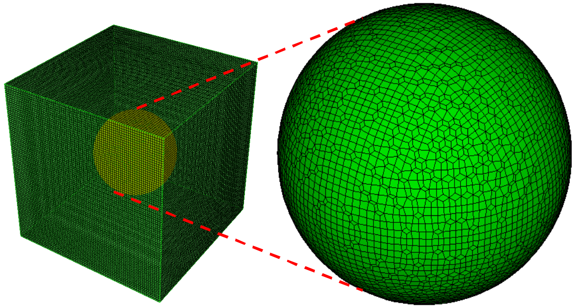

interfacial reconstruction (SCULPT)

Conformal boundaries are critical to our effort.

Employing tools and providing support for the extension to tetrahedral elements.

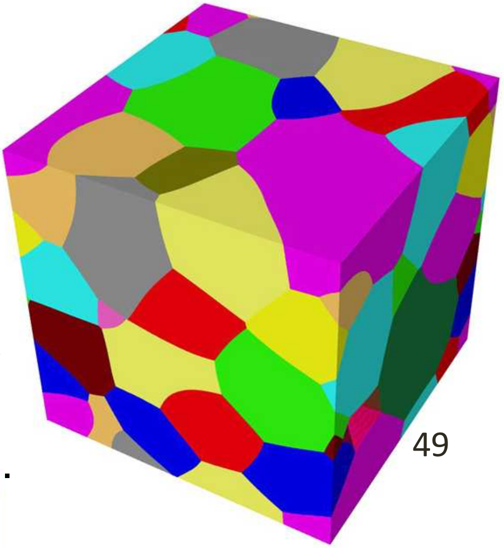

Meso-Continuum Scale Hierarchy

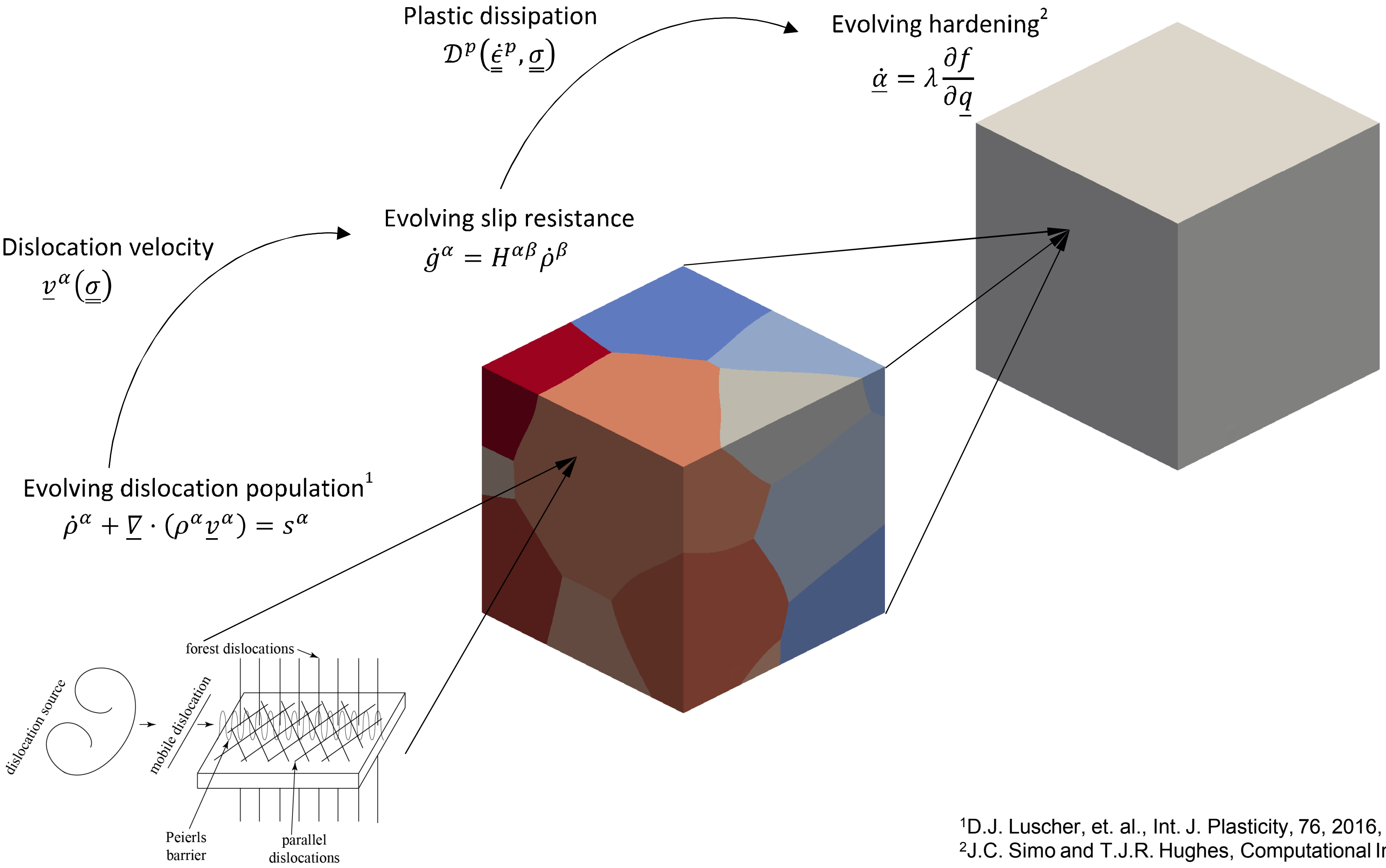

Plastic dissipation

$\mathcal{D}^p\left(\underline{\underline{\dot{\epsilon}}}^p, \underline{\underline{\sigma}}\right)$

Evolving hardening[2]

$\dot{\underline{\alpha}} = \lambda \dfrac{\partial f}{\partial \underline{q}}$

Evolving slip resistance

$\dot{g}^\alpha = H^{\alpha\beta}\dot{\rho}^\beta$

Dislocation velocity

$\underline{v}^\alpha\left(\underline{\underline{\sigma}}\right)$

Evolving dislocation population[1]

$\dot{\rho}^\alpha + \underline{\nabla}\cdot\left(\rho^\alpha \underline{v}^\alpha\right) = s^\alpha$

[1] D.J. Luscher, et. al., Int. J. Plasticity, 76, 2016, 111-129.

[2] J.C. Simo and T.J.R. Hughes, Computational Inelasticity, 1998.

Microstructural equivalency

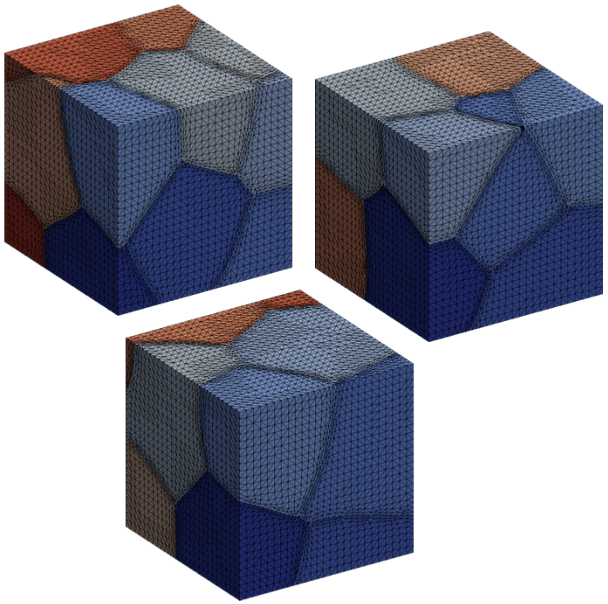

Microstructural realizations from a single set of underlying morphological statistics

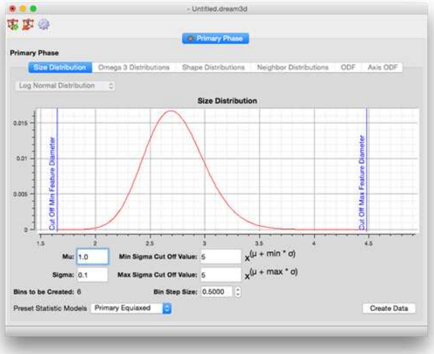

- Untitled.dream3d

Primary Phase

Primary Phase

Size Distribution | Omega 3 Distributions | Shape Distributions | Neighbor Distributions | ODF | Axis ODF

Log Normal Distribution

Mu: 1.0

Sigma: 0.1

Min Sigma Cut Off Value: 5 $x^{(\mu + min * \sigma)}$

Max Sigma Cut Off Value: 5 $x^{(\mu + max * \sigma)}$

Bins to be Created: 6

Bin Step Size: 0.5000

Preset Statistic Models: Primary Equiaxed

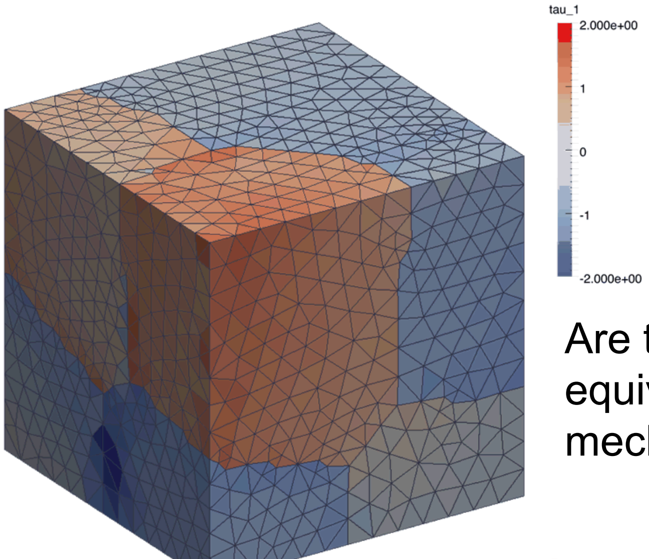

Are the realizations equivalent in terms of mechanical response?

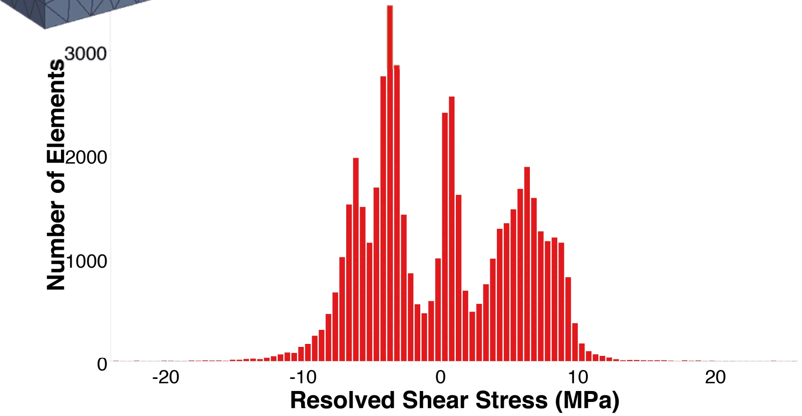

Finite Element Meshing Workflow

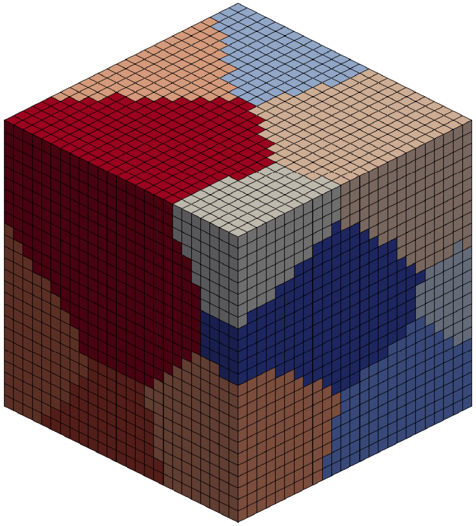

DREAM.3D
Input: microstructure statistics
Output: voxelized microstructure

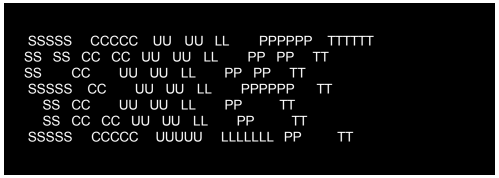

```
 SSSSS   CCCCC   UU   UU  LL      PPPPPP   TTTTTT
SS   SS  CC   CC  UU   UU  LL      PP   PP    TT
SS       CC       UU   UU  LL      PP   PP    TT
 SSSSS   CC       UU   UU  LL      PPPPPP     TT
     SS  CC       UU   UU  LL      PP         TT
     SS  CC   CC  UU   UU  LL      PP         TT
 SSSSS   CCCCC    UUUUU   LLLLLLL  PP         TT
```

SCULPT
Input: voxelized microstructure
Output: finite element mesh (hexahedral)

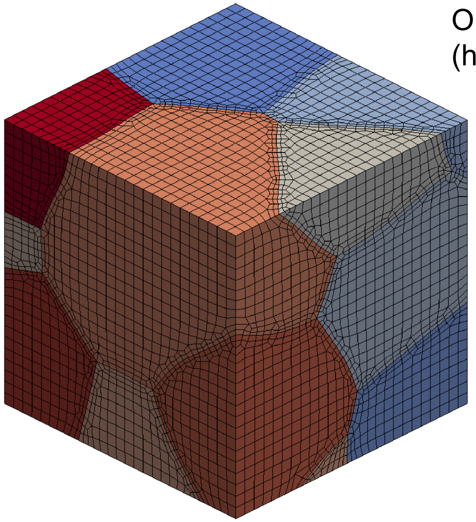

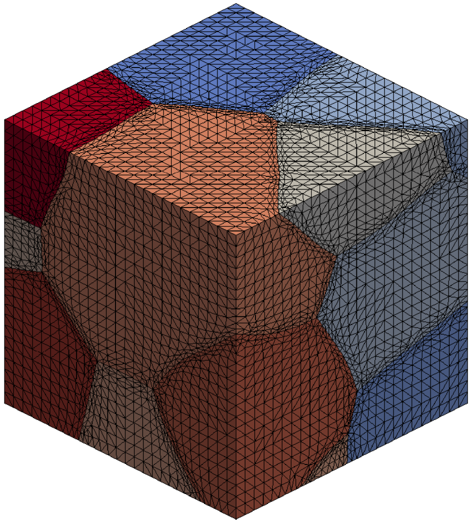

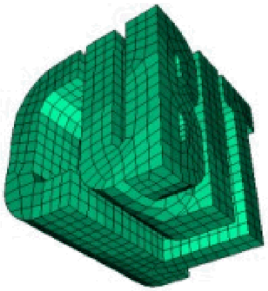

CUBIT
Input: finite element mesh (hexahedral)
Output: finite element mesh (e.g., tetrahedral)

Constitutive equation development

Elasticity

Micro

Second Piola-Kirchhoff stress

$$\underline{\underline{T}}^{*} = \mathbb{L}^{c} : \underline{\underline{E}}^{e}$$

Elasticity tensor

$$\mathbb{L}^{c} = \underline{\underline{R}}^{T} \cdot \underline{\underline{R}}^{T} \cdot \mathbb{L} \cdot \underline{\underline{R}} \cdot \underline{\underline{R}}$$

Elastic Lagrangian strain

$$\underline{\underline{E}}^{e} = \frac{1}{2}\left[(\underline{\underline{F}}^{e})^{T}\underline{\underline{F}}^{e} - \underline{\underline{I}}\right]$$

Macro

Cauchy stress

$$\underline{\underline{\sigma}} = \mathbb{C} : \left(\underline{\underline{\epsilon}} - \underline{\underline{\epsilon}}^{p}\right)$$

Elasticity tensor

$$\mathbb{C} = \lambda \underline{\underline{I}} \otimes \underline{\underline{I}} + 2\mu \mathbb{I}^{sym}$$

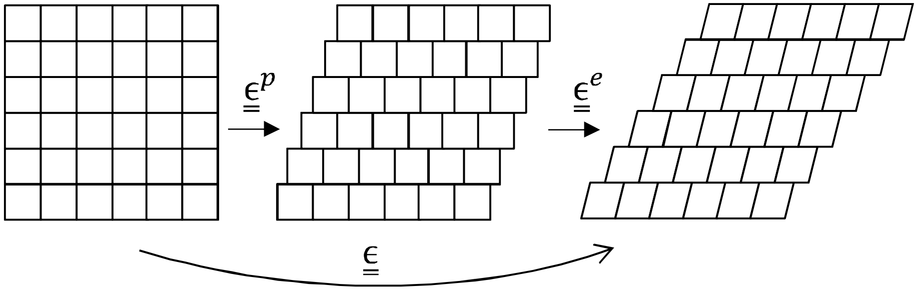

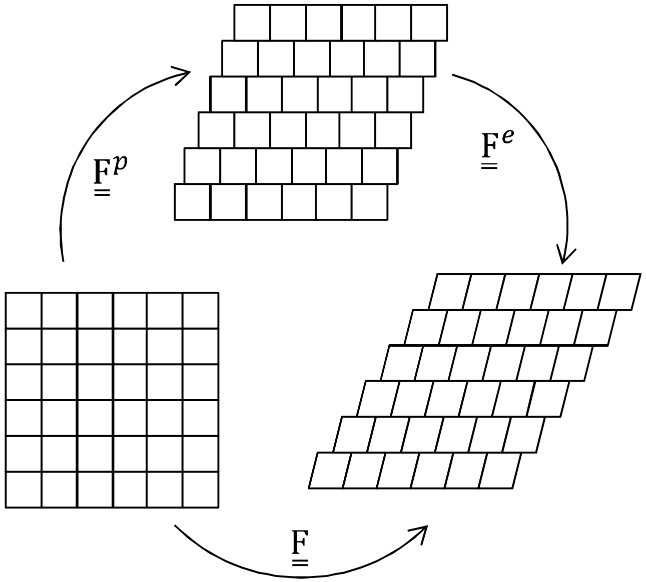

Plasticity

Micro

Plastic deformation gradient

$$\dot{\underline{\underline{F}}}^{p} = \underline{\underline{L}}^{p*} \cdot \underline{\underline{F}}^{p}$$

Plastic velocity gradient

$$\underline{\underline{L}}^{p*} = \sum_{\alpha} \dot{\gamma}^{\alpha} \underline{\underline{P}}_{0}^{\alpha}$$

Flow rule

$$\dot{\gamma}^{\alpha} = \dot{\gamma}_{0} \left| \frac{\underline{\underline{\tau}} : \underline{\underline{P}}_{0}^{\alpha}}{\tau_{0} + g^{\alpha}} \right|^{k} \mathrm{sign}\left(\underline{\underline{\tau}} : \underline{\underline{P}}_{0}^{\alpha}\right)$$

Evolving slip resistance

$$\dot{g}^{\alpha} = H^{\alpha\beta} \dot{\gamma}^{\beta}$$

Plastic dissipation

$$\mathcal{D}^{p} = \sum_{\alpha} \tau^{\alpha}\dot{\gamma}^{\alpha} - \dot{g}^{\alpha} q^{\alpha}$$

Macro

Yield function

$$f\left(\underline{\underline{\sigma}}\right) = \phi\left(\mathbb{I}^{dev} : \underline{\underline{\sigma}}\right) - \sigma_{Y}\left(\bar{\epsilon}^{p}\right)$$

Plastic strain rate

$$\dot{\underline{\underline{\epsilon}}}^{p} = \lambda \frac{\partial f}{\partial \underline{\underline{\sigma}}}$$

Evolving hardening

$$\dot{\alpha} = \lambda \frac{\partial f}{\partial \bar{\epsilon}^{p}}$$

Plastic dissipation

$$\mathcal{D}^{p} = \underline{\underline{\sigma}} : \dot{\underline{\underline{\epsilon}}}^{p} - \dot{\alpha}\bar{\epsilon}^{p}$$

Composite Tet

Combined F-bar Formulation

☐ Isochoric-volumetric split (Hughes 1975, Simo 1975)

$$\boldsymbol{F} = \boldsymbol{F}_{\text{vol}} \cdot \boldsymbol{F}_{\text{iso}}$$

☐ Replacing volumetric split with assumed term

$$\overline{\boldsymbol{F}} = \underset{\underset{\text{Modified det(F)}}{\uparrow}}{\bar{J}^{1/3}} \boldsymbol{F}_{\text{iso}} = \bar{J}^{1/3} \underset{\underset{\text{Original det(F)}}{\uparrow}}{J^{-1/3}} \boldsymbol{F}$$

Relaxing too much, we get instabilities
Relaxing too little, we get the volumetric locking

☐ Combined F-bar approach

$$\widetilde{\boldsymbol{F}} = \alpha \boldsymbol{F} + (1-\alpha)\overline{\boldsymbol{F}}. \longleftarrow$$

Invalid operation

☐ Current Approach via Lie algebra

$$\widetilde{J} = \exp\left(\frac{1-\beta}{\mathrm{V}_{\mathcal{B}^e}} \int_{\mathcal{B}^e} \log J \,\mathrm{dV} + \beta \log J\right).$$

$$\boxed{\widetilde{J}_M = \exp\left(\log \widetilde{J} - 3\left(\frac{1-\beta}{\mathrm{V}_{\mathcal{B}^e}} \int_{\mathcal{B}^e} \alpha_{sk}(\theta - \theta_o) \,\mathrm{dV} + \beta\alpha_{sk}(\theta - \theta_o\,)\right)\right.}$$

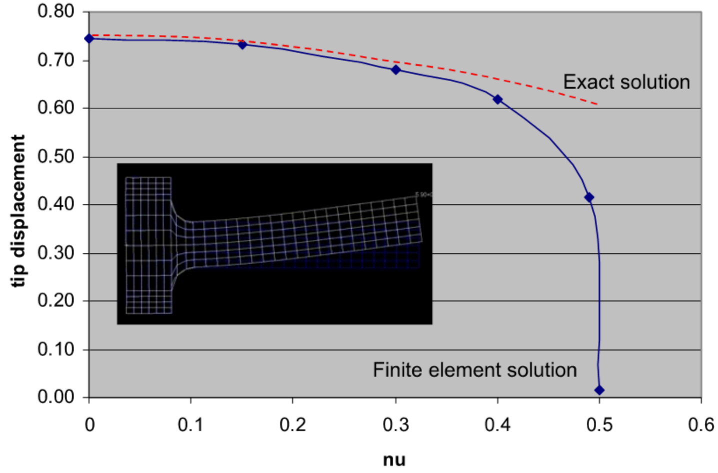

Standard F leads to Volumetric Locking

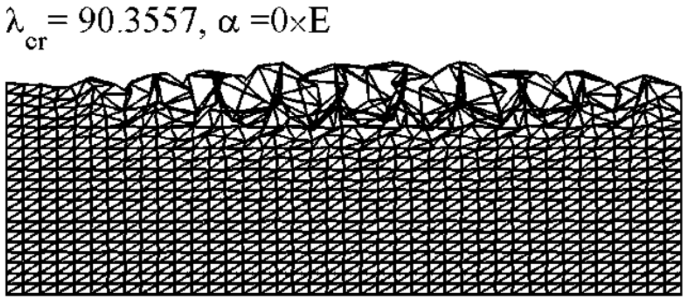

Pure F-bar leads to instability
(Brocardo, Micheloni, Krysl, IJNME, 2009)

See Sun, Ostien, Salinger, International Journal for Numerical and Analytical Methods in Geomechanics, 2013

10-Node Composite Tetrahedral Element

Motivated by prior work of Thoutireddy, et. al., IJNME (2002)

$$\Phi[\boldsymbol{\varphi}, \bar{\boldsymbol{F}}, \bar{\boldsymbol{P}}] := \int_B A(\bar{\boldsymbol{F}})\,\mathrm{d}V + \int_B \bar{\boldsymbol{P}} : (\boldsymbol{F} - \bar{\boldsymbol{F}})\,\mathrm{d}V - \int_B R\boldsymbol{B} \cdot \boldsymbol{\varphi}\,\mathrm{d}V - \int_{\partial_T B} \boldsymbol{T} \cdot \boldsymbol{\varphi}\,\mathrm{d}S$$

$$\bar{\boldsymbol{P}} = \lambda_\alpha \left(\int_\Omega \lambda_\alpha \lambda_\beta \boldsymbol{I}\,\mathrm{d}V \right)^{-1} \int_\Omega \lambda_\beta \boldsymbol{P}\,\mathrm{d}V,$$

$$\bar{\boldsymbol{F}} = \lambda_\alpha \left(\int_\Omega \lambda_\alpha \lambda_\beta \boldsymbol{I}\,\mathrm{d}V \right)^{-1} \int_\Omega \lambda_\beta \boldsymbol{F}\,\mathrm{d}V$$

$$\boldsymbol{R}_a(\boldsymbol{\varphi}) := \int_\Omega \bar{\boldsymbol{P}} \cdot \boldsymbol{\mathcal{B}}_a\,\mathrm{d}V - \int_\Omega R\boldsymbol{B} N_a\,\mathrm{d}V - \int_{\partial_T \Omega} \boldsymbol{T} N_a\,\mathrm{d}S = \boldsymbol{0}$$

$$\boldsymbol{\mathcal{B}}_a(\boldsymbol{X}) := \delta_{ik} \frac{\partial N_a(\boldsymbol{X})}{\partial X_J}\, \boldsymbol{e}_i \otimes \boldsymbol{E}_J \otimes \boldsymbol{e}_k$$

$\boldsymbol{\varphi}$ C^0 piecewise linear

$\bar{\boldsymbol{F}}$ C^{-1} linear over parent element

$\bar{\boldsymbol{P}}$ C^{-1} linear over parent element

12 sub-tets

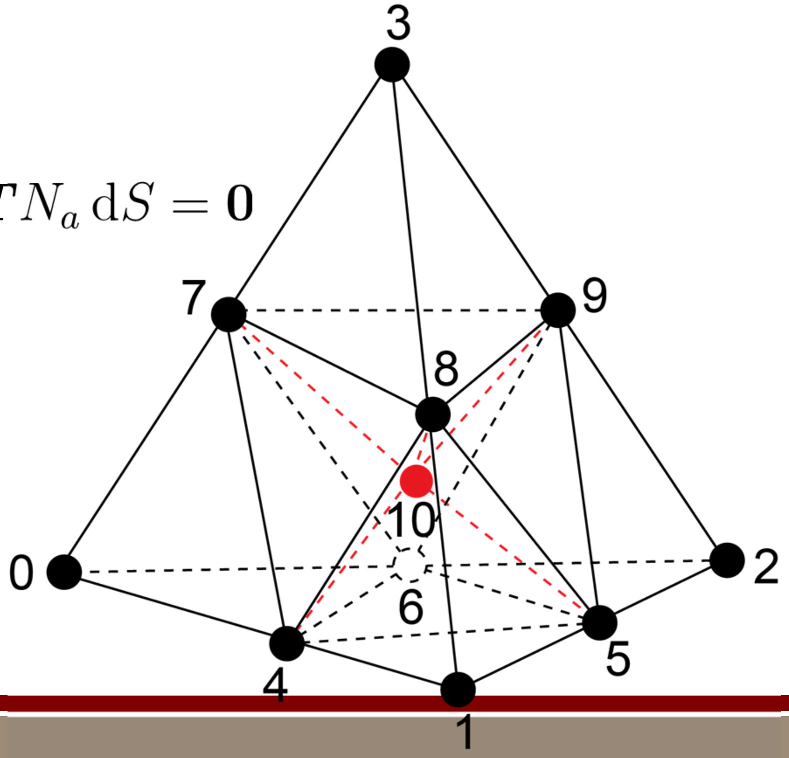

Analytical gradient operator

Develop an exact gradient operator that projects and interpolates sub-tet gradients

$$\bar{\boldsymbol{F}}(\boldsymbol{X}) := \bar{\boldsymbol{\mathcal{B}}}_a(\boldsymbol{X})\boldsymbol{x}_a$$

$$\bar{\boldsymbol{\mathcal{B}}}_a(\boldsymbol{X}) := \lambda_\alpha(\boldsymbol{X})\left[\int_\Omega \delta_{ik}\lambda_\alpha(\boldsymbol{X})\lambda_\beta(\boldsymbol{X})\,\mathrm{d}V\right]^{-1}\int_\Omega \lambda_\beta(\boldsymbol{X})\frac{\partial N_a(\boldsymbol{X})}{\partial X_J}\,\mathrm{d}V\,\boldsymbol{e}_i\otimes\boldsymbol{E}_J\otimes\boldsymbol{e}_k$$

$$\bar{\boldsymbol{\mathcal{B}}}_a(\boldsymbol{\xi}) = \lambda_\alpha(\boldsymbol{\xi})\left[\int_{\Omega_{\boldsymbol{\xi}}} \delta_{ik}\lambda_\alpha(\boldsymbol{\xi})\lambda_\beta(\boldsymbol{\xi})\,\mathrm{d}V_{\boldsymbol{\xi}}\right]^{-1}\int_{\Omega_{\boldsymbol{\xi}}} \lambda_\beta(\boldsymbol{\xi})\frac{\partial N_a(\boldsymbol{\xi})}{\partial\boldsymbol{\xi}}\,\mathrm{d}V_{\boldsymbol{\xi}}\left(\frac{\partial\boldsymbol{\xi}}{\partial X_J}\right)\boldsymbol{e}_i\otimes\boldsymbol{E}_J\otimes\boldsymbol{e}_k$$

$$\bar{\boldsymbol{\mathcal{B}}}_a(\boldsymbol{\xi}) = \bar{\mathcal{L}}_{a;ilk}(\boldsymbol{\xi})\left(\frac{\partial\xi_l}{\partial X_J}\right)\boldsymbol{e}_i\otimes\boldsymbol{E}_J\otimes\boldsymbol{e}_k$$

$$\bar{\boldsymbol{\mathcal{L}}}_a(\boldsymbol{\xi}) = \lambda_\alpha(\boldsymbol{\xi})\delta_{ik}(M_{\alpha\beta})^{-1}\sum_{S=0}^{11}\frac{\partial N_a}{\partial\xi_l}\int_{E_S}\lambda_\beta(\boldsymbol{\xi})\,\mathrm{d}V_{\boldsymbol{\xi}}\,\boldsymbol{e}_i\otimes\boldsymbol{a}_l\otimes\boldsymbol{e}_k$$

$$\bar{\boldsymbol{\mathcal{B}}}_a(\boldsymbol{\xi}) = \bar{\mathcal{L}}_{a;ilk}(\boldsymbol{\xi})\left[\bar{\mathcal{L}}_{b;JlM}(\boldsymbol{\xi})X_{b;M}\right]^{-1}\boldsymbol{e}_i\otimes\boldsymbol{E}_J\otimes\boldsymbol{e}_k$$

$$\bar{B}_{aJ}(\boldsymbol{\xi}) = \bar{L}_{al}(\boldsymbol{\xi})\left[X_{Jb}\bar{L}_{bl}(\boldsymbol{\xi})\right]^{-1}$$

$$\bar{F}_{iJ}(\boldsymbol{\xi}) = x_{ia}\bar{B}_{aJ}(\boldsymbol{\xi})$$

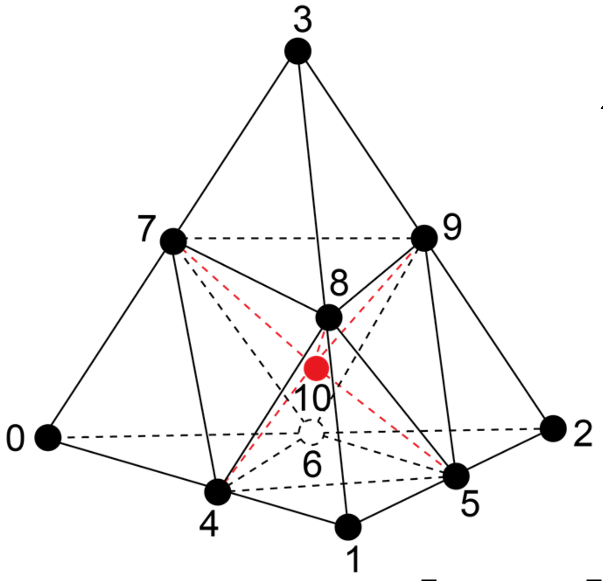

$$\bar{L}_{al}(\boldsymbol{\xi}) \equiv \bar{L}_{10\times 3} = \frac{1}{24}\begin{pmatrix} 9-60\xi_0 & 9-60\xi_0 & 9-60\xi_0 \\ -9+60\xi_1 & 0 & 0 \\ 0 & -9+60\xi_2 & 0 \\ 0 & 0 & -9+60\xi_3 \\ 70(\xi_0-\xi_1) & 2(-4-35\xi_1+5\xi_2+10\xi_3) & 2(-4-35\xi_1+10\xi_2+5\xi_3) \\ 2(-1+5\xi_1+40\xi_2-5\xi_3) & 2(-1+40\xi_1+5\xi_2-5\xi_3) & 10(\xi_0-\xi_3) \\ 2(-4+5\xi_1-35\xi_2+10\xi_3) & 70(\xi_0-\xi_2) & 2(-4+10\xi_1-35\xi_2+5\xi_3) \\ 2(-4+5\xi_1+10\xi_2-35\xi_3) & 2(-4+10\xi_1+5\xi_2-35\xi_3) & 70(\xi_0-\xi_3) \\ 2(-1+5\xi_1-5\xi_2+40\xi_3) & 10(\xi_0-\xi_2) & 2(-1+40\xi_1-5\xi_2+5\xi_3) \\ 10(\xi_0-\xi_1) & 2(-1-5\xi_1+5\xi_2+40\xi_3) & 2(-1-5\xi_1+40\xi_2+5\xi_3) \end{pmatrix}.$$

Evaluate for your integration scheme

Suitable for isochoric motions

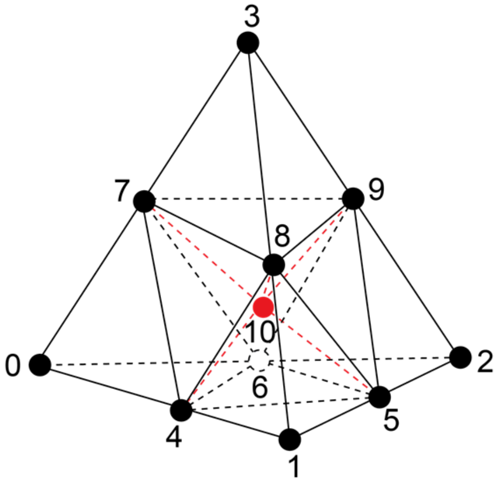

Volume-averaged formulation does not exhibit spurious pressure oscillations.

$$\bar{\boldsymbol{F}}^\star(\boldsymbol{\xi}) := \left(\frac{\bar{J}^\star}{\bar{J}(\boldsymbol{\xi})}\right)^{\frac{1}{3}} \bar{\boldsymbol{F}}(\boldsymbol{\xi})$$

$$\bar{J}^\star := \frac{\int_\Omega \bar{J}\,\mathrm{d}V}{\int_\Omega \mathrm{d}V}$$

$$\bar{p}^\star := \frac{1}{V_\Omega}\int_\Omega \mathrm{tr}\,\frac{\partial A(\boldsymbol{F}^\star)}{\partial \bar{\boldsymbol{b}}^\star}\,\mathrm{d}V$$

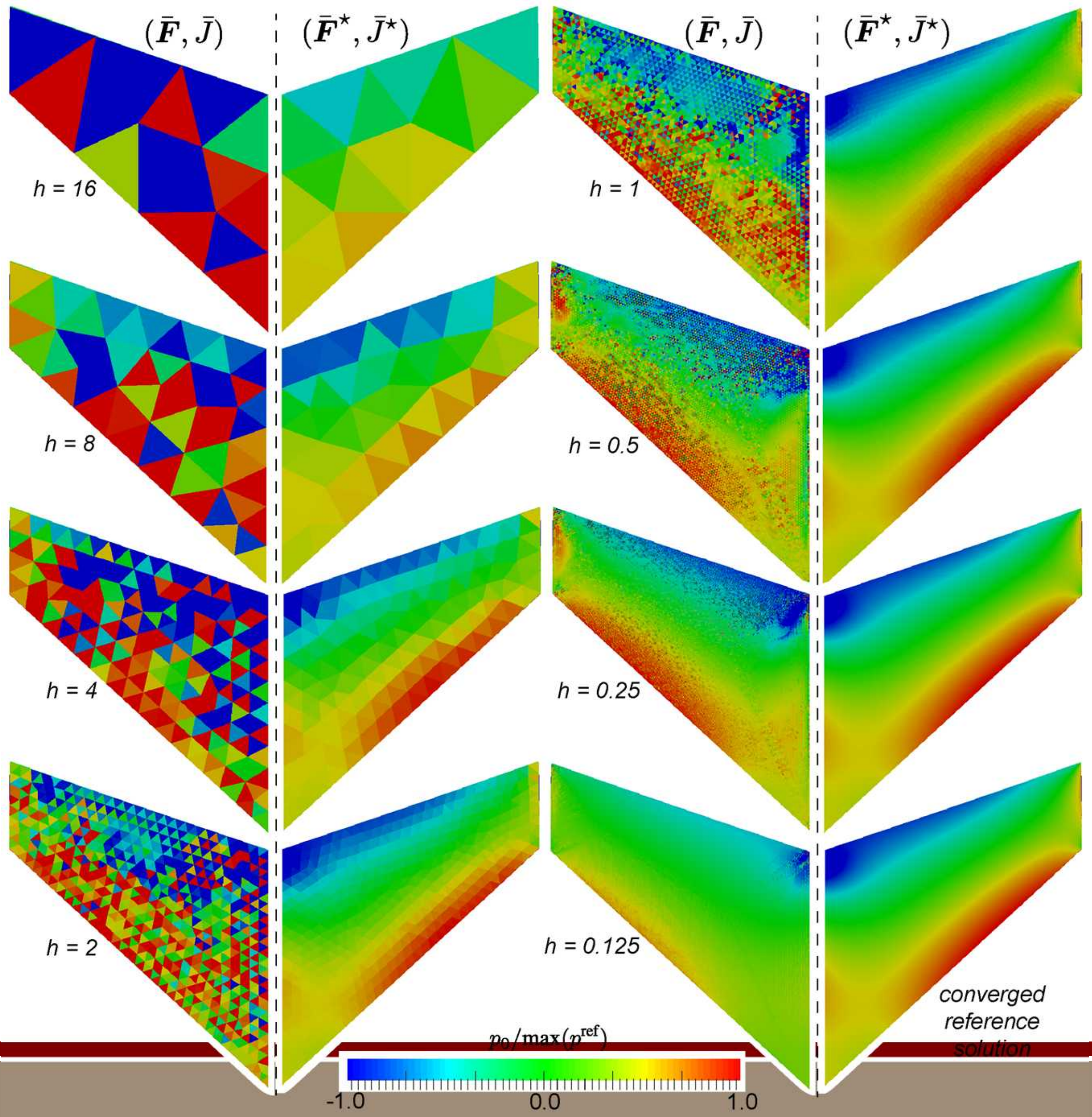

Composite Tet

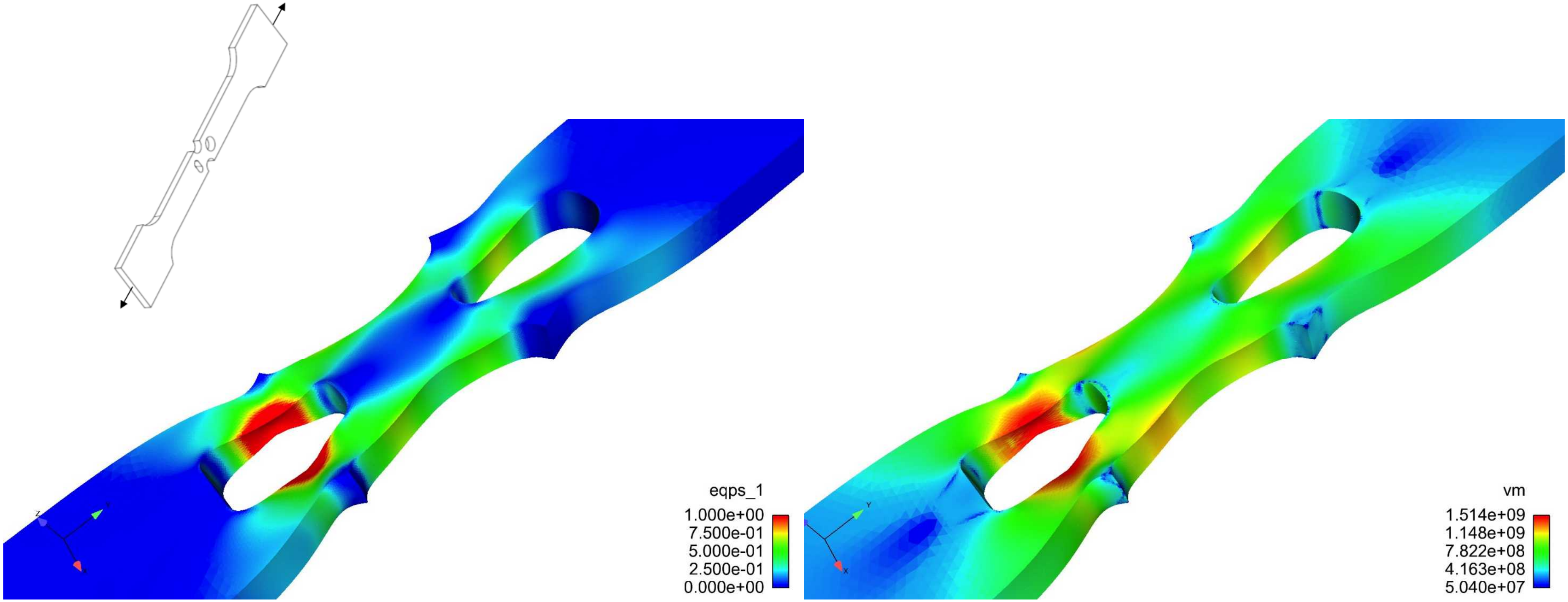

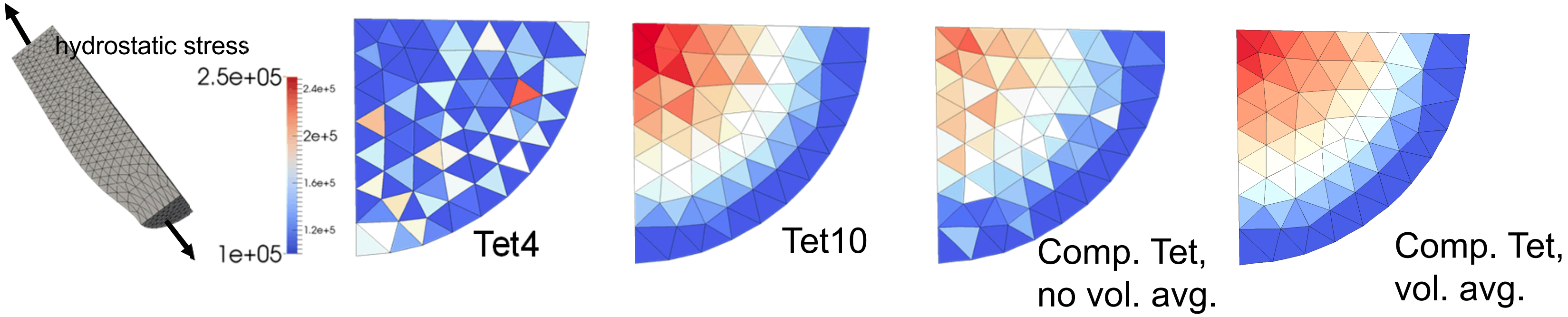

Note: Results from Sierra using Intrepid, same Basis available in Albany

Projecting IP Data to Nodes

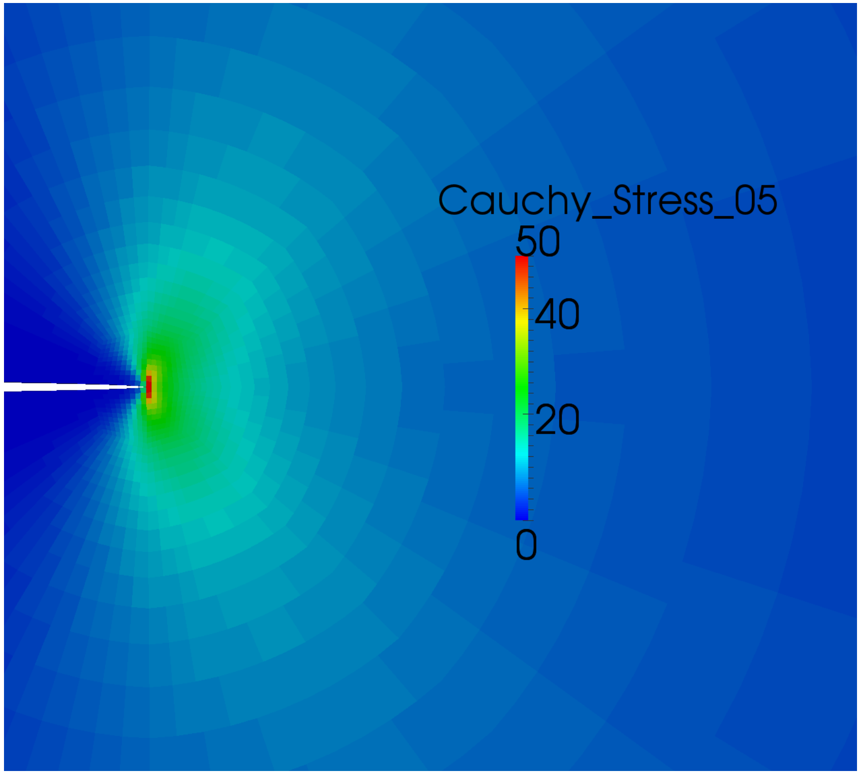

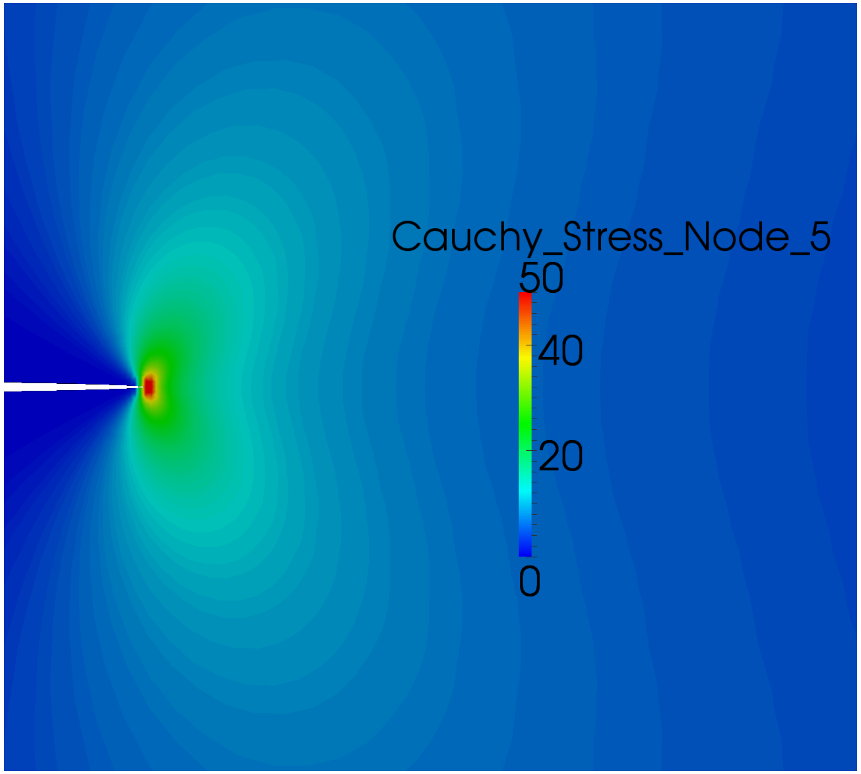

To facilitate the mapping procedure, state variable data known at the integration points need to be projected to the nodes. The following interpolation can then use the standard basis functions.

Currently in Albany, we can approximate a global L2 projection by computing a nodal volume average for integration point quantities.

Exceptional service in the national interest

Remeshing/Mapping

ISVs - Remeshing and (Re)mapping

$$\Phi[\boldsymbol{\varphi}, \bar{\boldsymbol{z}}, \bar{\boldsymbol{y}}] := \int_B W(\boldsymbol{F}, \bar{\boldsymbol{z}})\, dV + \int_B \bar{\boldsymbol{y}} \cdot (\bar{\boldsymbol{z}} - \boldsymbol{z})\, dV - \int_B \rho_0 \boldsymbol{B} \cdot \boldsymbol{\varphi}\, dV - \int_{\partial_T B} \boldsymbol{T} \cdot \boldsymbol{\varphi}\, dS$$

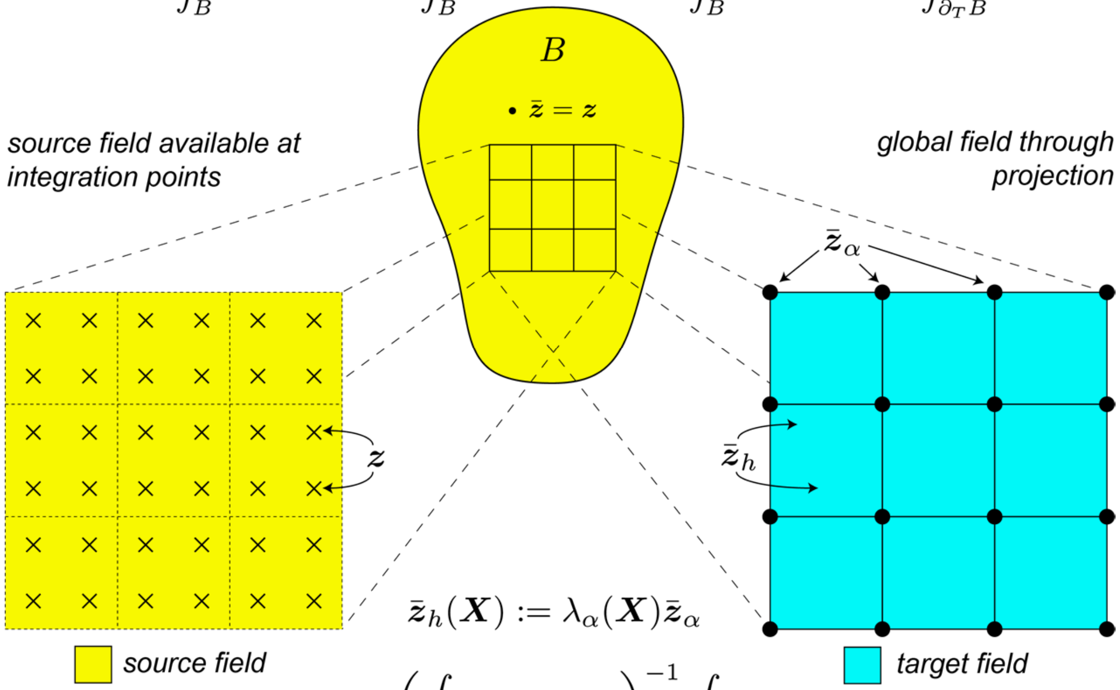

$$\bar{\boldsymbol{z}}_h(\boldsymbol{X}) := \lambda_\alpha(\boldsymbol{X})\bar{\boldsymbol{z}}_\alpha$$

$$\bar{\boldsymbol{z}}_h = \lambda_\alpha \left(\int_B \lambda_\alpha \lambda_\beta \boldsymbol{I}\, dV \right)^{-1} \int_B \lambda_\beta \boldsymbol{z}\, dV$$

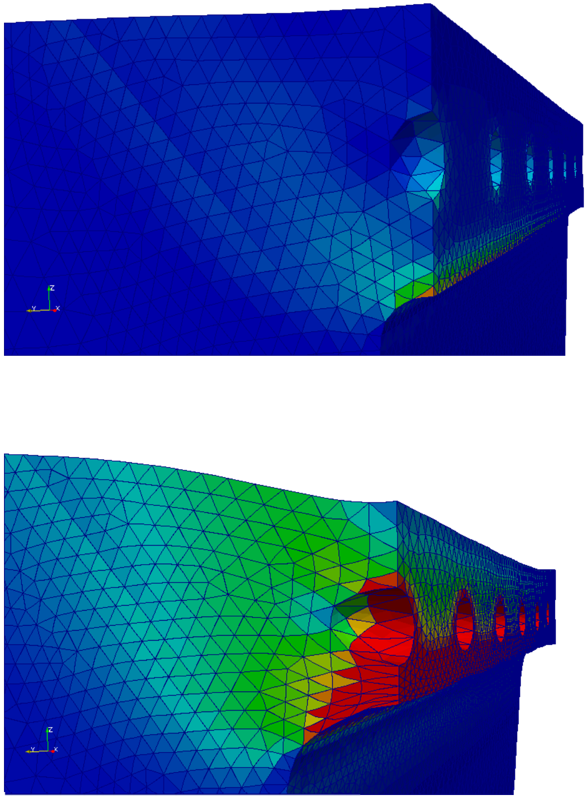

SOURCE FIELD

LOG

LIE ALGEBRA

MAPPING

LIE ALGEBRA

EXP

TARGET FIELD

Mota, Sun, Ostien, Foulk, and Long [2013] *Computational Mechanics*

Objectives for FY13

Using the Theory of Groups, state variable constraints can be maintained during an interpolation step!

- Solution and State remapping

Lie Group G	$\boldsymbol{Z}_1$	$\boldsymbol{Z}_2$	$\boldsymbol{Z}(0)$	$\in G$	$\boldsymbol{Z}(2)$	$\in G$
$\mathbb{R}^+$	0.90	0.10	0.50	yes	-0.70	no
$GL^+(3)$	$\begin{pmatrix} 2 & 0 & 4 \\ 0 & 2 & 0 \\ 0 & 0 & 2 \end{pmatrix}$	$\begin{pmatrix} 2 & 0 & 0 \\ 0 & 2 & 0 \\ 4 & 0 & 2 \end{pmatrix}$	$\begin{pmatrix} 2 & 0 & 2 \\ 0 & 2 & 0 \\ 2 & 0 & 2 \end{pmatrix}$	no	$\begin{pmatrix} 2 & 0 & -2 \\ 0 & 2 & 0 \\ 6 & 0 & 2 \end{pmatrix}$	yes
$SL(3)$	$\begin{pmatrix} 1 & 2 & 0 \\ 0 & 1 & 0 \\ 0 & 0 & 1 \end{pmatrix}$	$\begin{pmatrix} 1 & 0 & 0 \\ 2 & 1 & 0 \\ 0 & 0 & 1 \end{pmatrix}$	$\begin{pmatrix} 1 & 1 & 0 \\ 1 & 1 & 0 \\ 0 & 0 & 1 \end{pmatrix}$	no	$\begin{pmatrix} 1 & -1 & 0 \\ 3 & 1 & 0 \\ 0 & 0 & 1 \end{pmatrix}$	no
$SO(3)$	$\begin{pmatrix} 1 & 0 & 0 \\ 0 & 0 & -1 \\ 0 & 1 & 0 \end{pmatrix}$	$\begin{pmatrix} 0 & 0 & 1 \\ 0 & 1 & 0 \\ -1 & 0 & 0 \end{pmatrix}$	$\begin{pmatrix} 0.50 & 0.00 & 0.50 \\ 0.00 & 0.50 & -0.50 \\ -0.50 & 0.50 & 0.00 \end{pmatrix}$	no	$\begin{pmatrix} -0.50 & 0.00 & 1.50 \\ 0.00 & 1.50 & 0.50 \\ -1.50 & -1.50 & 0.00 \end{pmatrix}$	no

Table 2: Interpolation and extrapolation without Lie algebras. $\boldsymbol{Z}_1 = \boldsymbol{Z}(-1)$ and $\boldsymbol{Z}_2 = \boldsymbol{Z}(1)$ are given data and belong to the corresponding Lie group. $\boldsymbol{Z}(\xi) := N_1(\xi)\boldsymbol{Z}_1 + N_2(\xi)\boldsymbol{Z}_2$. $N_1(\xi) := \frac{1}{2}(1-\xi)$ and $N_2(\xi) := \frac{1}{2}(1+\xi)$.

Lie Group G	$\boldsymbol{Z}_1$	$\boldsymbol{Z}_2$	$\boldsymbol{Z}(0)$	$\in G$	$\boldsymbol{Z}(2)$	$\in G$
$\mathbb{R}^+$	0.90	0.10	0.30	yes	0.03	yes
$GL^+(3)$	$\begin{pmatrix} 2 & 0 & 4 \\ 0 & 2 & 0 \\ 0 & 0 & 2 \end{pmatrix}$	$\begin{pmatrix} 2 & 0 & 0 \\ 0 & 2 & 0 \\ 4 & 0 & 2 \end{pmatrix}$	$\begin{pmatrix} 3.09 & 0.00 & 2.35 \\ 0.00 & 2.00 & 0.00 \\ 2.35 & 0.00 & 3.09 \end{pmatrix}$	yes	$\begin{pmatrix} -0.32 & 0.00 & -1.14 \\ 0.00 & 2.00 & 0.00 \\ 3.42 & 0.00 & -0.32 \end{pmatrix}$	yes
$SL(3)$	$\begin{pmatrix} 1 & 2 & 0 \\ 0 & 1 & 0 \\ 0 & 0 & 1 \end{pmatrix}$	$\begin{pmatrix} 1 & 0 & 0 \\ 2 & 1 & 0 \\ 0 & 0 & 1 \end{pmatrix}$	$\begin{pmatrix} 1.54 & 1.18 & 0.00 \\ 1.18 & 1.54 & 0.00 \\ 0.00 & 0.00 & 1.00 \end{pmatrix}$	yes	$\begin{pmatrix} -0.16 & -0.57 & 0.00 \\ 1.71 & -0.16 & 0.00 \\ 0.00 & 0.00 & 1.00 \end{pmatrix}$	yes
$SO(3)$	$\begin{pmatrix} 1 & 0 & 0 \\ 0 & 0 & -1 \\ 0 & 1 & 0 \end{pmatrix}$	$\begin{pmatrix} 0 & 0 & 1 \\ 0 & 1 & 0 \\ -1 & 0 & 0 \end{pmatrix}$	$\begin{pmatrix} 0.72 & 0.28 & 0.63 \\ 0.28 & 0.72 & -0.63 \\ -0.63 & 0.63 & 0.44 \end{pmatrix}$	yes	$\begin{pmatrix} -0.61 & -0.54 & 0.58 \\ -0.54 & 0.82 & 0.19 \\ -0.58 & -0.19 & -0.79 \end{pmatrix}$	yes

Table 3: Interpolation and extrapolation with Lie algebras. $\boldsymbol{Z}_1 = \boldsymbol{Z}(-1)$ and $\boldsymbol{Z}_2 = \boldsymbol{Z}(1)$ are given data and belong to the corresponding Lie group. $\boldsymbol{Z}(\xi) := \exp \boldsymbol{z}(\xi)$, $\boldsymbol{z}(\xi) := N_1(\xi)\boldsymbol{z}_1 + N_2(\xi)\boldsymbol{z}_2$, $\boldsymbol{z}_1 := \log \boldsymbol{Z}_1$, $\boldsymbol{z}_2 := \log \boldsymbol{Z}_2$. $N_1(\xi) := \frac{1}{2}(1-\xi)$ and $N_2(\xi) := \frac{1}{2}(1+\xi)$.

Adaptivity Example

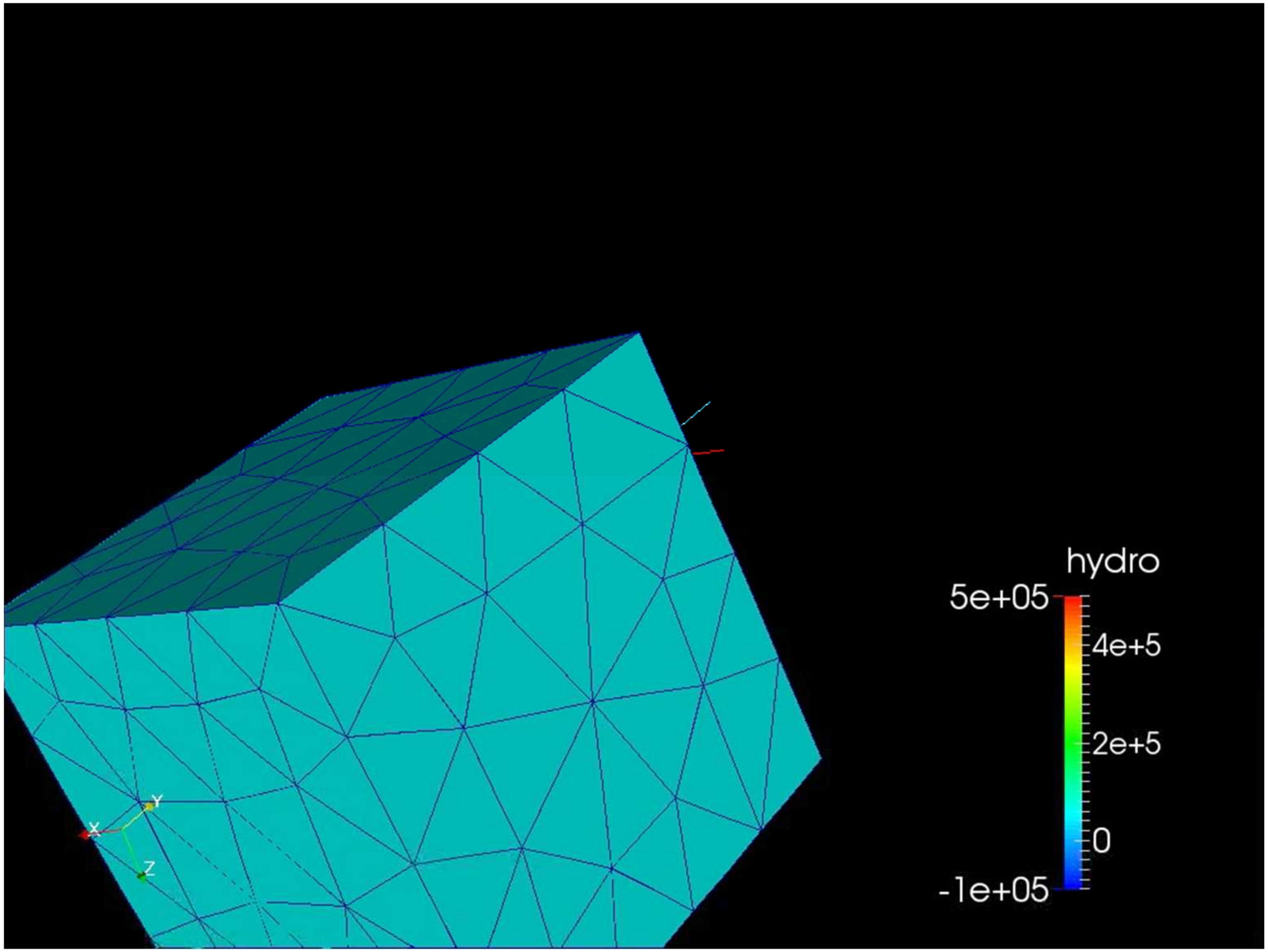

Capturing the evolution of inelasticity

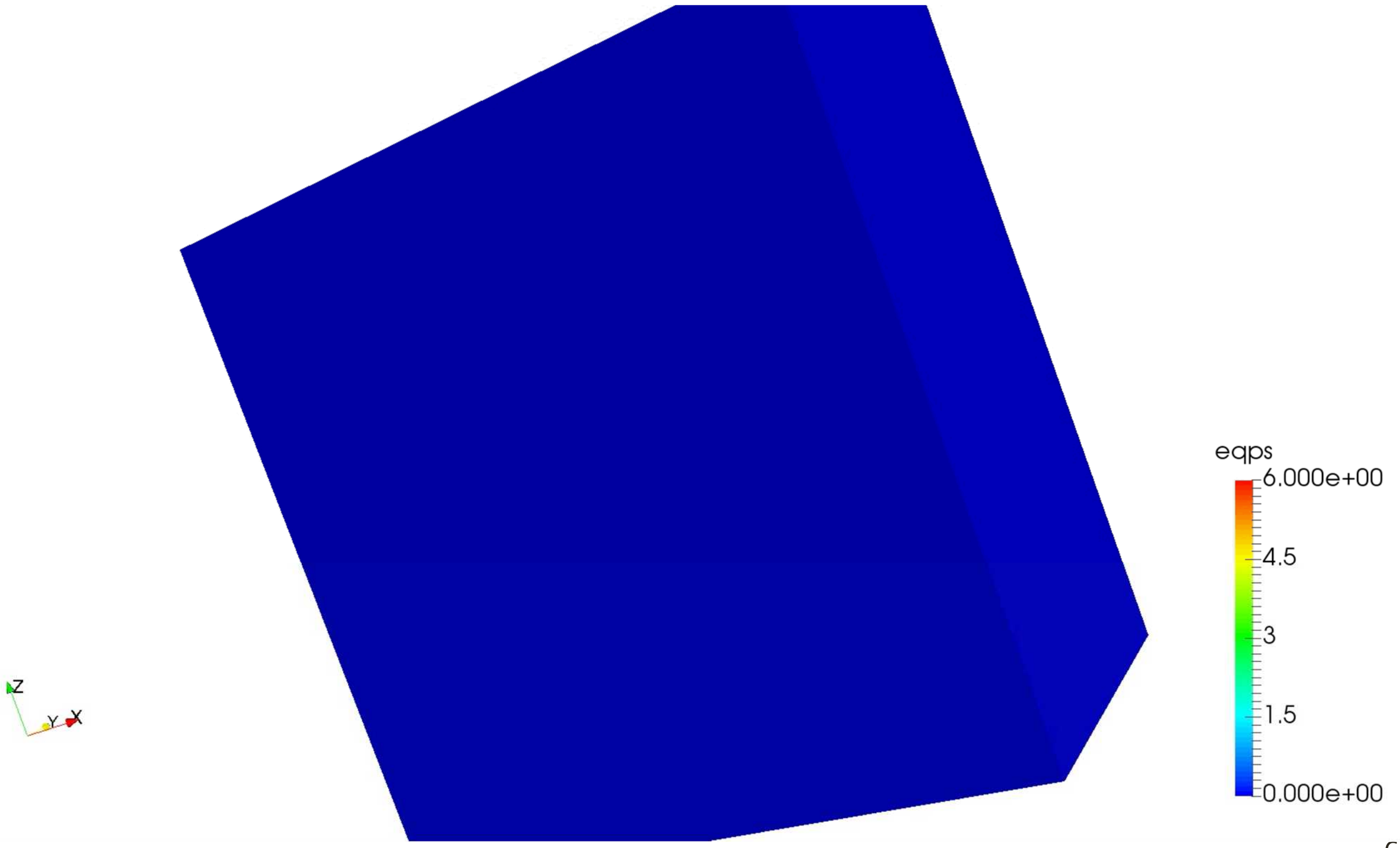

Resolving the deformation with remeshing/mapping

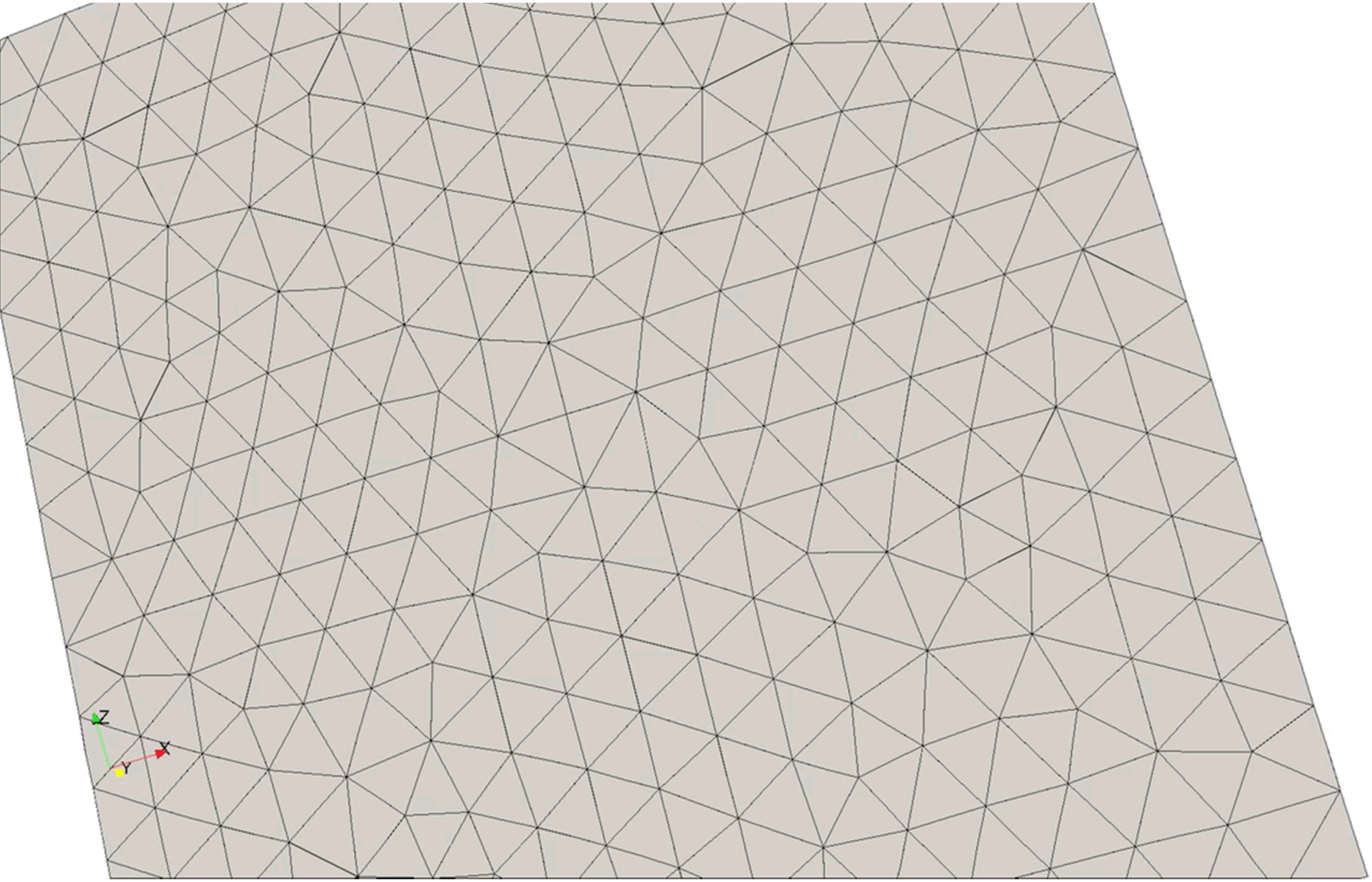

(necking of a square cross-section)

Local processes are requisite for prediction

Remeshing the body 30 times in ~0.25 ε_p increments

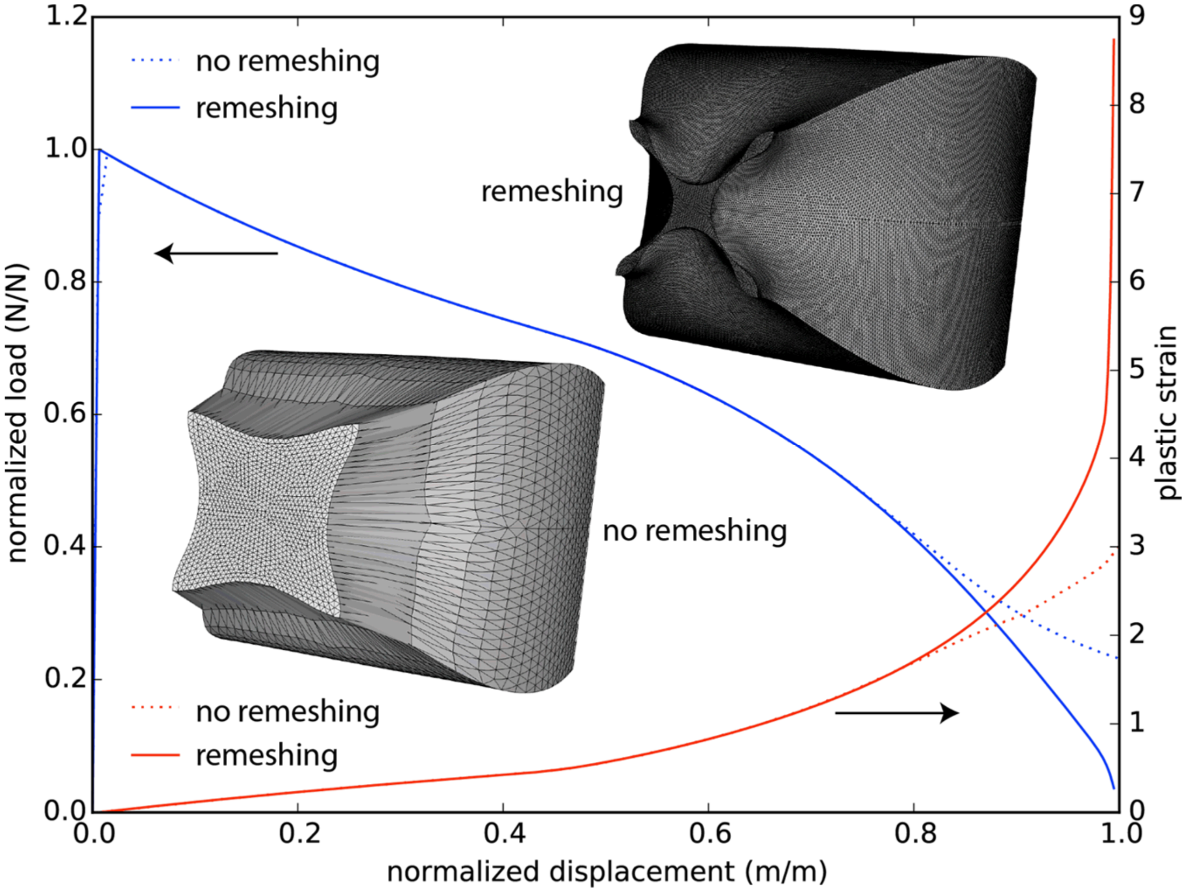

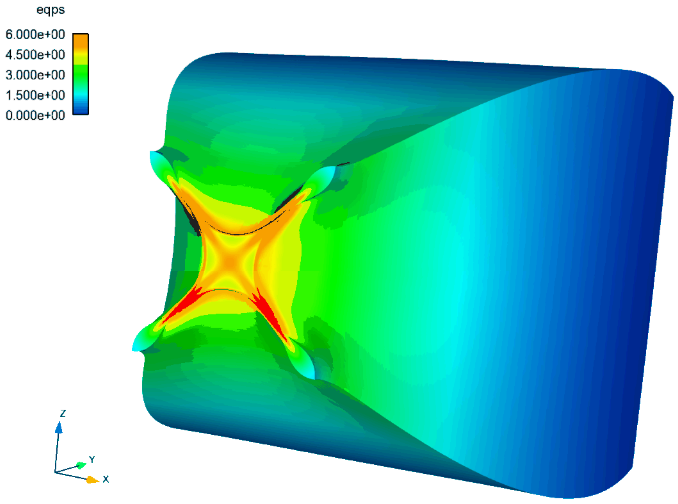

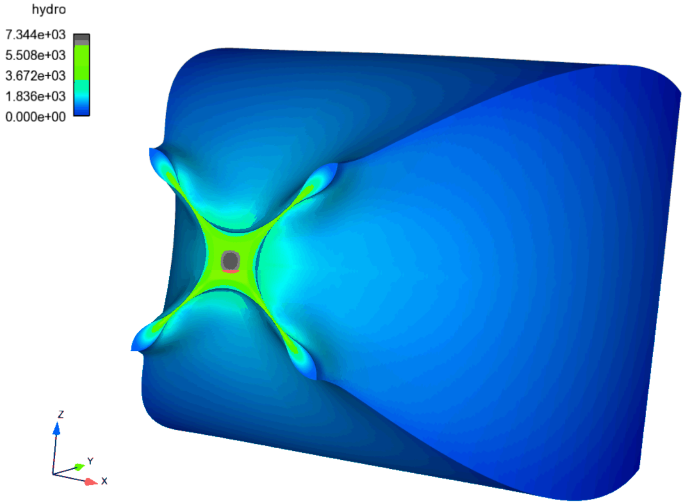

J_2 plasticity w/linear hardening (PH 13-8 H950)

Exceptional service in the national interest

Sandia
National
Laboratories

Regularized damage evolution for ductile fracture using localization elements

J.W. Foulk III, A. Lindblad, J.M. Emery, A. Mota, J.T. Ostien, A.A. Brown, T.J. Vogler

U.S. DEPARTMENT OF ENERGY

NNSA National Nuclear Security Administration

Sandia National Laboratories is a multi-program laboratory managed and operated by Sandia Corporation, a wholly owned subsidiary of Lockheed Martin Corporation, for the U.S. Department of Energy's National Nuclear Security Administration under contract DE-AC04-94AL85000. SAND NO. 2011-XXXXP

Capture sub-grid processes for R(a)

Goal: Capture sub-grid processes through methods that regularize the jump

$$\boldsymbol{F} = \boldsymbol{F}^{\parallel} \boldsymbol{F}^{\perp}$$

$$\boldsymbol{F}^{\parallel} = \boldsymbol{g}_i \otimes \boldsymbol{G}^i$$

$$\boldsymbol{F}^{\perp} = \boldsymbol{I} + \frac{[\![\boldsymbol{\Phi}]\!]}{h} \otimes \boldsymbol{N}$$

$$\boldsymbol{F} = \boldsymbol{F}^{\parallel} + \frac{[\![\boldsymbol{\varphi}]\!]}{h} \otimes \boldsymbol{N}$$

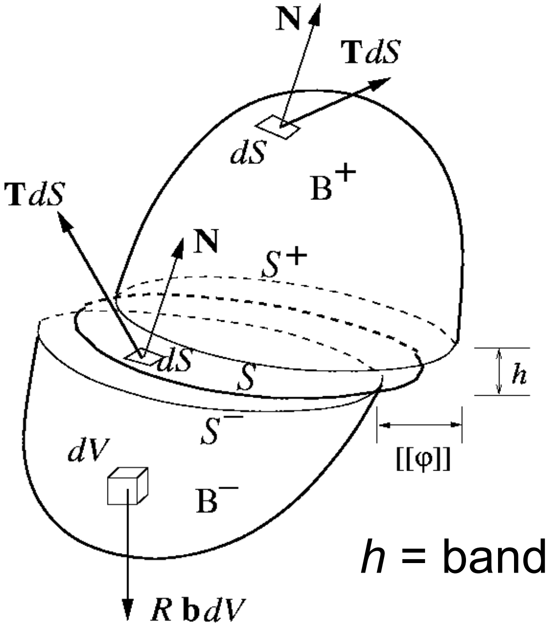

h = band thickness

- Finite-deformation kinematics
- Simulation of strain localization
- No additional constitutive assumptions

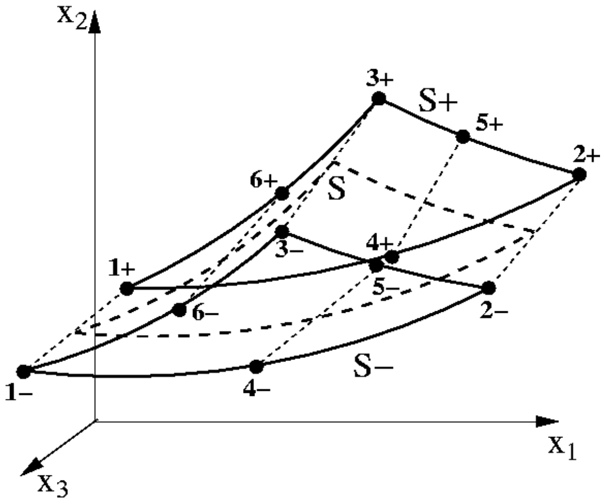

Akin to "cohesive" element

Yang, Mota and Ortiz (IJNME, 2005), Armero and Garikipati (IJSS, 1996)

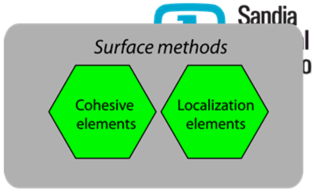

Kinematic assumptions

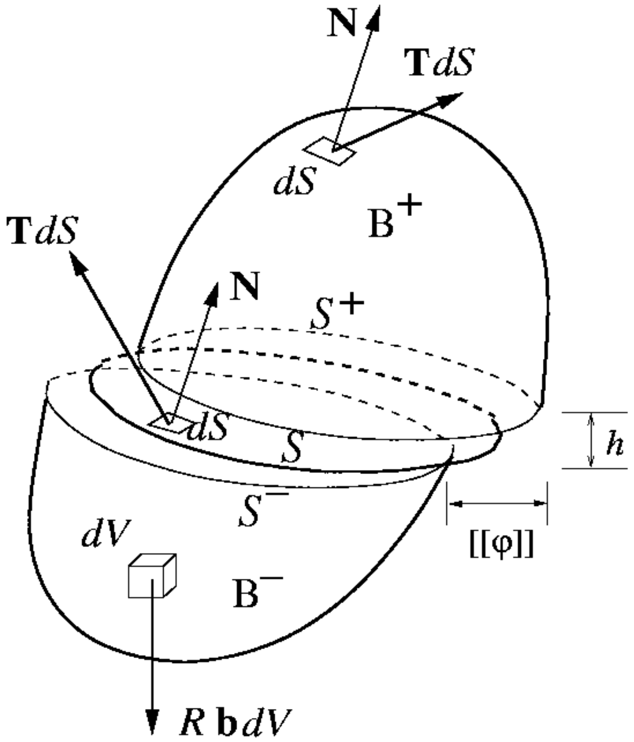

Topical: Plenary talk by Xaiver Oliver

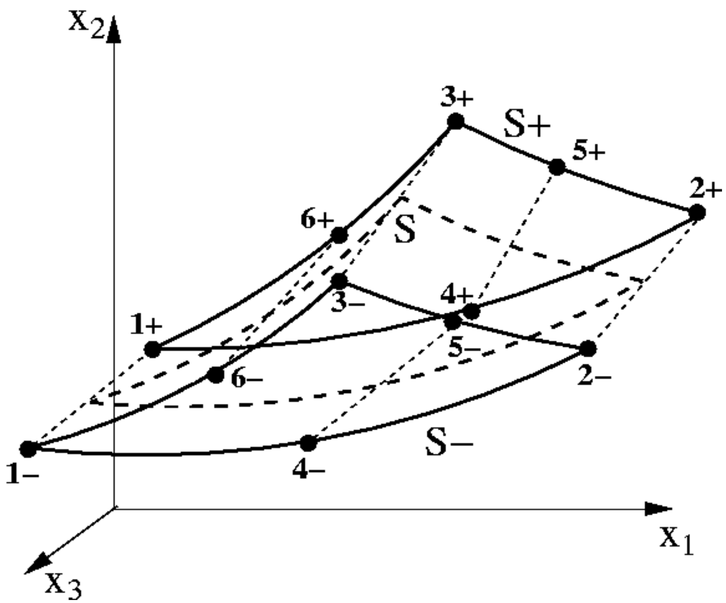

- Finite-deformation kinematics.
- Simulation of strain localization.
- No additional constitutive assumptions

$$\boldsymbol{F}^{\perp} = \boldsymbol{I} + \frac{[\![\varphi]\!]}{h} \otimes \boldsymbol{N} \quad \boldsymbol{F}^{\|} = \boldsymbol{g}_i \otimes \boldsymbol{G}^i$$

$$\boldsymbol{F} = \boldsymbol{F}^{\|} \boldsymbol{F}^{\perp}$$

Yang, Mota and Ortiz, IJNME, 2005

h = band thickness

An intermediate configuration

$$\boldsymbol{F}^{\perp} = \boldsymbol{I} + \frac{\llbracket \boldsymbol{\Phi} \rrbracket}{h} \otimes \boldsymbol{N}$$

$$\boldsymbol{F}^{\|} = \boldsymbol{g}_i \otimes \hat{\boldsymbol{G}}^i$$

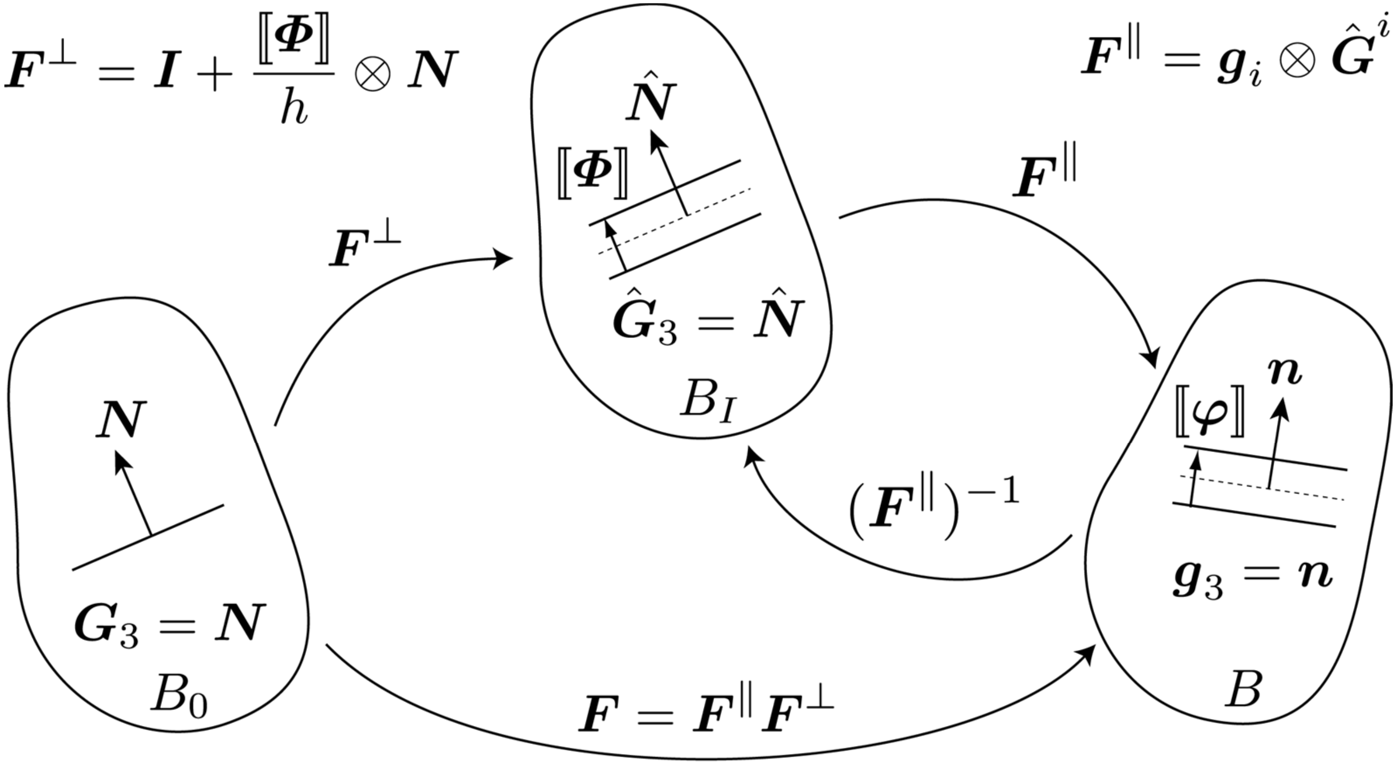

$$\hat{\boldsymbol{G}}_A \parallel \boldsymbol{G}_A \longrightarrow \boldsymbol{F} = \boldsymbol{F}^{\|} + \frac{\llbracket \boldsymbol{\varphi} \rrbracket}{h} \otimes \boldsymbol{N}$$

additive decomposition!

The jump is pushed backwards $\llbracket \boldsymbol{\Phi} \rrbracket = (\boldsymbol{F}^{\|})^{-1} \llbracket \boldsymbol{\varphi} \rrbracket$

Retain definition of membrane def. grad. $\boldsymbol{F}^{\|} = \boldsymbol{g}_i \otimes \boldsymbol{G}^i$

The order is not unique

$$\boldsymbol{F}^{\|} = \hat{\boldsymbol{G}}_A \otimes \boldsymbol{G}^A$$

$$\boldsymbol{F}^{\perp} = \boldsymbol{I} + \frac{[\![\boldsymbol{\varphi}]\!]}{h} \otimes \bar{\boldsymbol{N}}$$

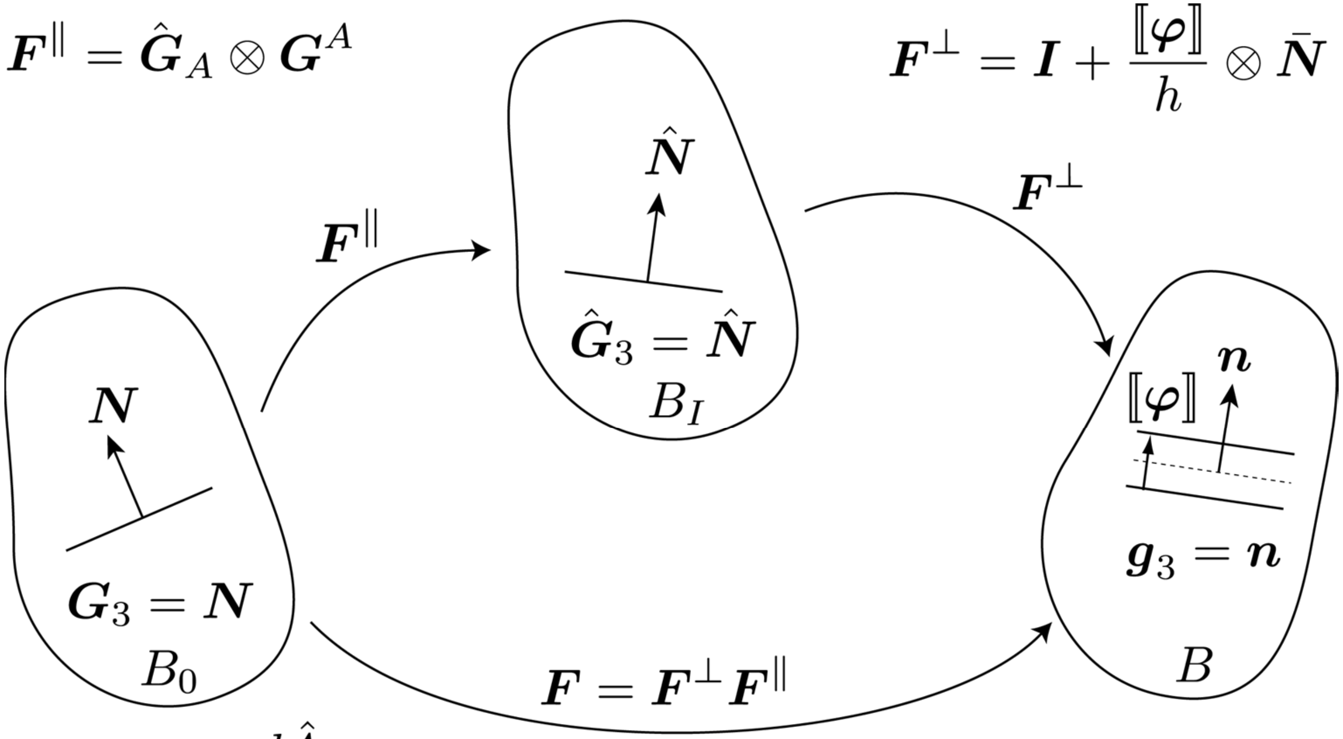

$$\bar{\boldsymbol{N}} = \hat{\boldsymbol{N}} \frac{d\hat{A}}{\hat{J}dA} \qquad \boldsymbol{g}_i \parallel \hat{\boldsymbol{G}}_i \longrightarrow \boldsymbol{F} = \boldsymbol{F}^{\|} + \frac{[\![\boldsymbol{\varphi}]\!]}{h} \otimes \boldsymbol{N}$$

additive decomposition!

The normal used for construction $\bar{\boldsymbol{N}} = (\boldsymbol{F}^{\|})^{-T}\boldsymbol{N}$

Retain definition of membrane def. grad. $\boldsymbol{F}^{\|} = \boldsymbol{g}_i \otimes \boldsymbol{G}^i$

Extending surface to multiphysics

Our work in finite-deformation diffusion has extended elements to multiphysics (LCM)

Fox and Simo (1990), Callari, Armero, Abati (2010)

redefine space

$$\boldsymbol{X} = \boldsymbol{\Phi}(\xi^1, \xi^2, \xi^3) = \bar{\boldsymbol{\Phi}}(\xi^1, \xi^2) + \boldsymbol{N}(\xi^1, \xi^2)\xi^3 \qquad \boldsymbol{G}_i = \boldsymbol{\Phi}_{,i} = \frac{\partial \boldsymbol{X}}{\partial \xi^i}$$

include jump in C

$$C(\boldsymbol{X}) = \bar{C}(\phi[\xi^1, \xi^2]) + \frac{[\![C]\!](\phi[\xi^1, \xi^2)])}{h}\xi^3 \qquad \nabla_{\boldsymbol{X}} C = (\nabla \boldsymbol{\Phi})^{-T} \frac{\partial C}{\partial \xi^i}$$

Given this gradient operator, we can use the same PDE for finite-deformation diffusion

$$D^* \dot{C}_L - \nabla_{\boldsymbol{X}} \cdot d_l \boldsymbol{C}^{-1} \nabla_{\boldsymbol{X}} C_L + \nabla_{\boldsymbol{X}} \cdot \frac{d_l V_H}{RT} \boldsymbol{C}^{-1} \nabla_{\boldsymbol{X}} \tau_h C_L + \theta_T \frac{dN_T}{d\epsilon_p} \dot{\epsilon}_p$$

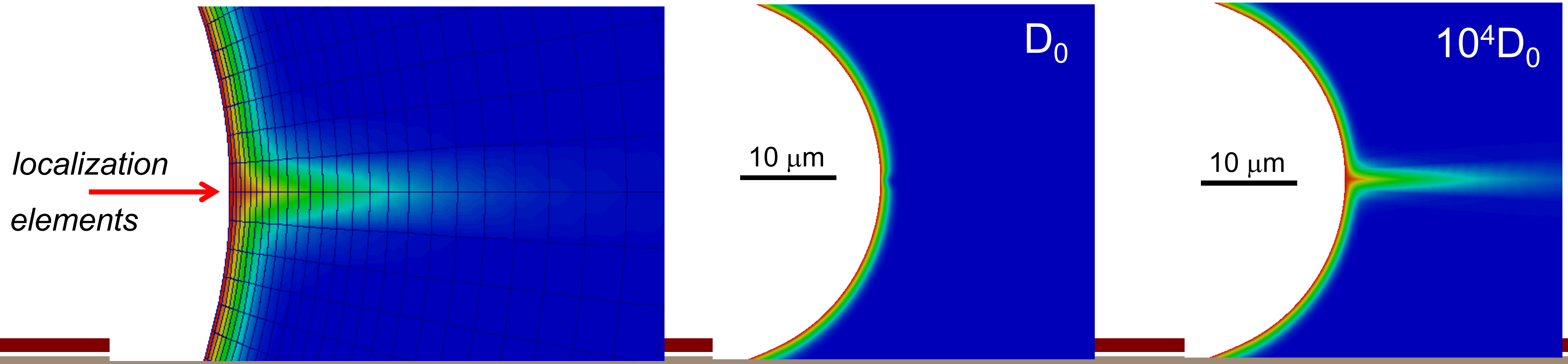

Exceptional service in the national interest

Sandia Fracture Challenge

Initial approach to SFC geometry

- Production codes (Sierra) employed for all calculations
- Simulations employ segregated coupling (Adagio/Aria)
- Implicit solution for long time scales (statics & dynamics)
- Isotropic poro-thermo-viscoplasticity model
- Hexahedral elements (SD, constant pressure)
- Elastic pins are contiguously meshed w/BC on centerline
- Element death was employed when the first integration point reached the coalescence criterion ϕ_{coal} (0.15)
- Learn with local damage and coarse meshes
- Employ techniques for regularizing the solution
  - Variational nonlocal method
  - Localization elements

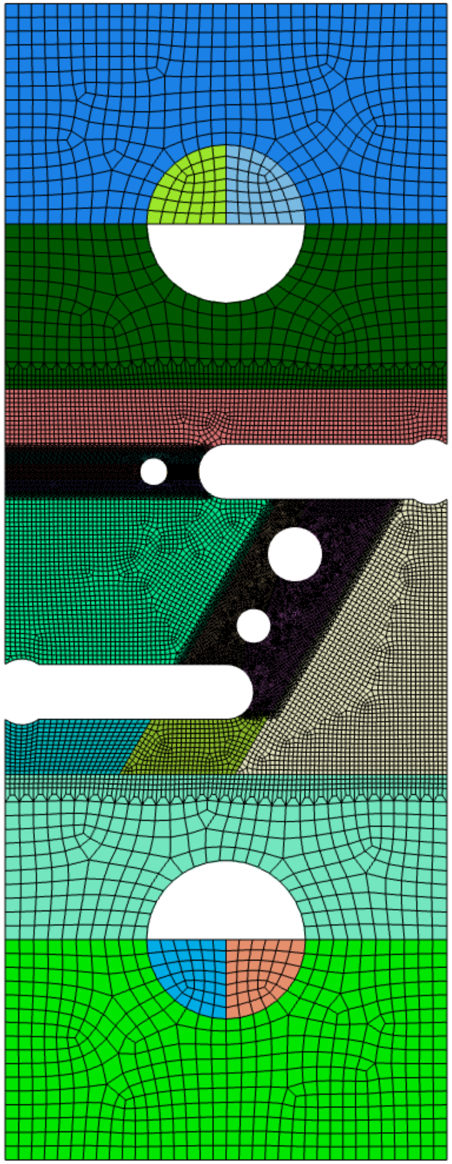

Initial model calibration (tension)

$\beta = 0.8$

$H = 3084 \times 10^6$ (Pa)

$R_d = 13$

$f = 1 \times 10^{-6}$

$n = 26$

$Y_{RT} = 493 \times 10^6$ (Pa)

$\phi_0 = 1 \times 10^{-4}$

$\phi_{coal} = 0.15$

$m = 6$

Thermo-mechanical simulations employed for model calibration

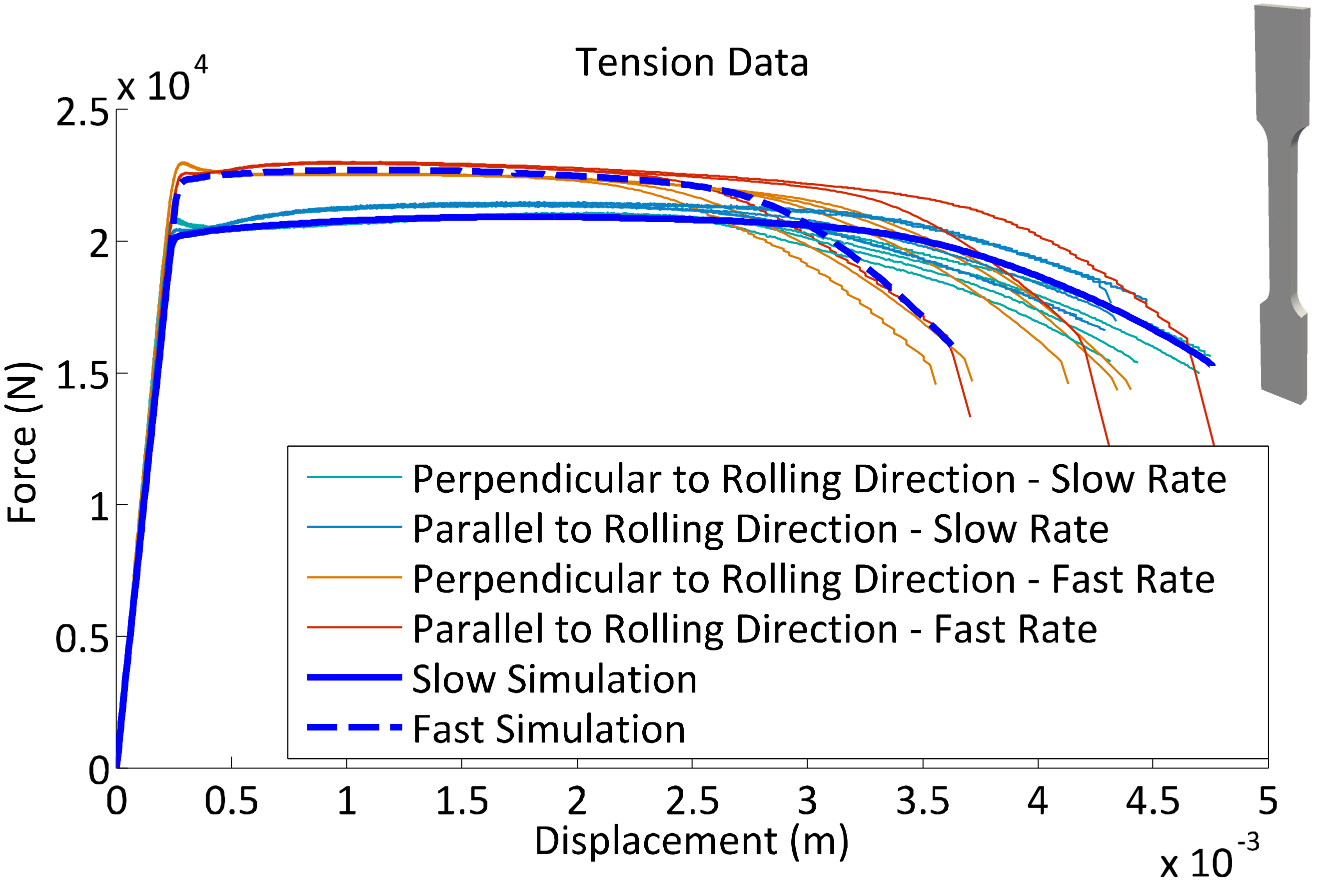

$$\sigma_y = (1-\phi)\left[Y(\theta) + \frac{H}{R_d}\left(1 - e^{-R_d \epsilon_p}\right)\right]\left\{1 + \sinh^{-1}\left[\left(\frac{\dot{\epsilon}_p}{f}\right)^{1/n}\right]\right\}$$

$$\dot{q} = \beta \bar{\boldsymbol{\sigma}} : \boldsymbol{D}^p$$

uncertainty in conversion of plastic work to heat β

$$\dot{\phi} = \sqrt{\frac{3}{2}}\dot{\epsilon}_p \frac{1-(1-\phi)^{m+1}}{(1-\phi)^m} \sinh\left[\frac{2(2m-1)}{2m+1}\frac{\langle \frac{I_1}{3} \rangle}{\sqrt{3J_2}}\right]$$

isotropic damage ϕ taken from Cocks and Ashby (1972)

NOTE: Temperature-dependent thermal conductivity and specific heat also taken from MMPDS-08.

Incorporating shear data

- Calibrated model did not predict the shear behavior
- Anisotropy evident in yield, hardening and damage evolution
- Focused on orientations relevant (// to RD) to the SFC
- Reduced the initial yield Y_{RT} and the recovery R_d
- Incorporated void nucleation through J_3 (n is the evolving void density)

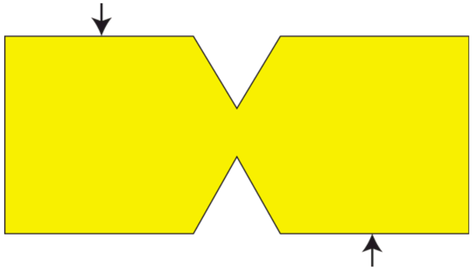

$$\frac{\dot{n}}{n} = N_1 \dot{\epsilon}_p \left(\frac{4}{27} - \frac{J_3^2}{J_2^3} \right)$$

(Horstemeyer, Gokhale, 1999)

$$\frac{\dot{\phi}_n}{\phi} = k_w \dot{\epsilon}_p \left(1 - \frac{27 J_3^2}{4 J_2^3} \right)$$

(Nahshon, Hutchinson, 2008)

$$N_1 = \frac{27}{4} \left(\frac{1}{1-\phi} \right) k_\omega$$

$$Y_{RT}^s = 0.87 Y_{RT}$$

$$R_d^s = 0.92 R_d$$

$$N_1 = 54$$

$$k_\omega \sim 8$$

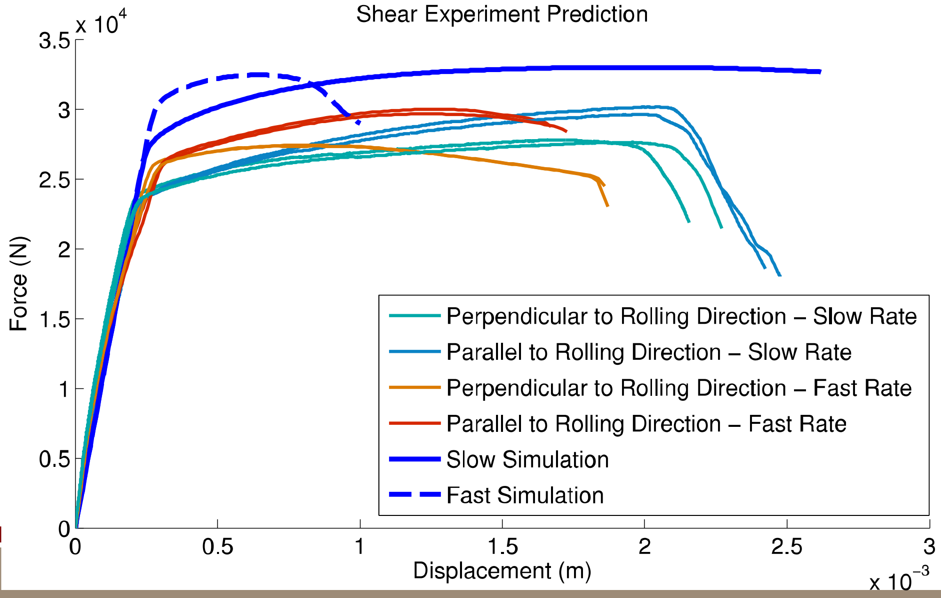

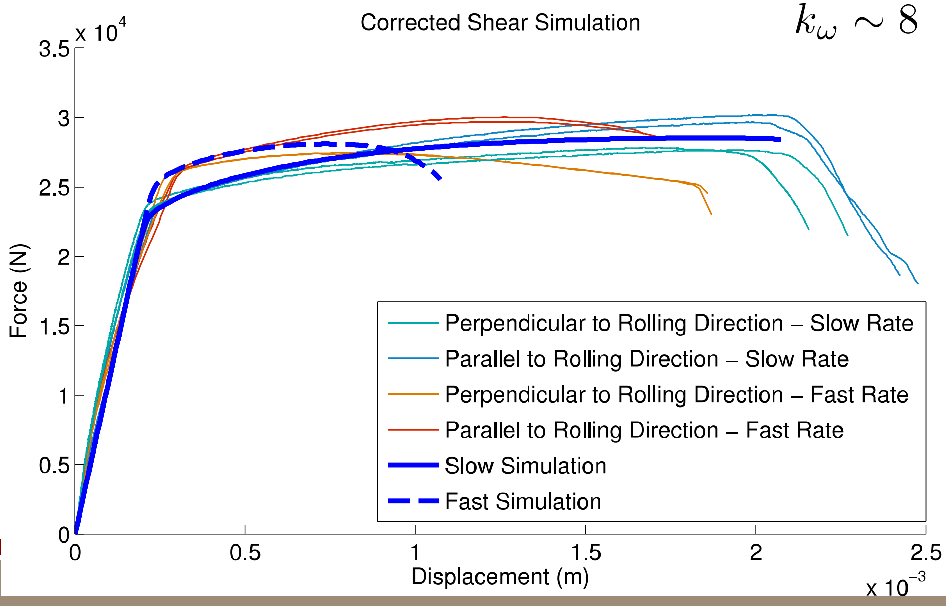

Revised approach to SFC geometry

- Calibrated a Hill, anisotropic yield surface to the shear and tensile data
- Although rate and temperature independent, modest agreement at lower rates
- Anisotropic yield predicted SFC would localize in the lower notch

Idealization. Keep poro-thermo-viscoplasticity. Accept isotropy. Assign different isotropic material parameters to regions being sheared.

Goal. Mimic Hill at lower notch, add physics

$Y^s_{RT} = 0.87 Y_{RT}$

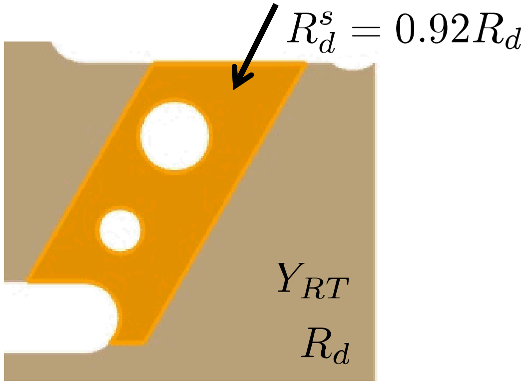

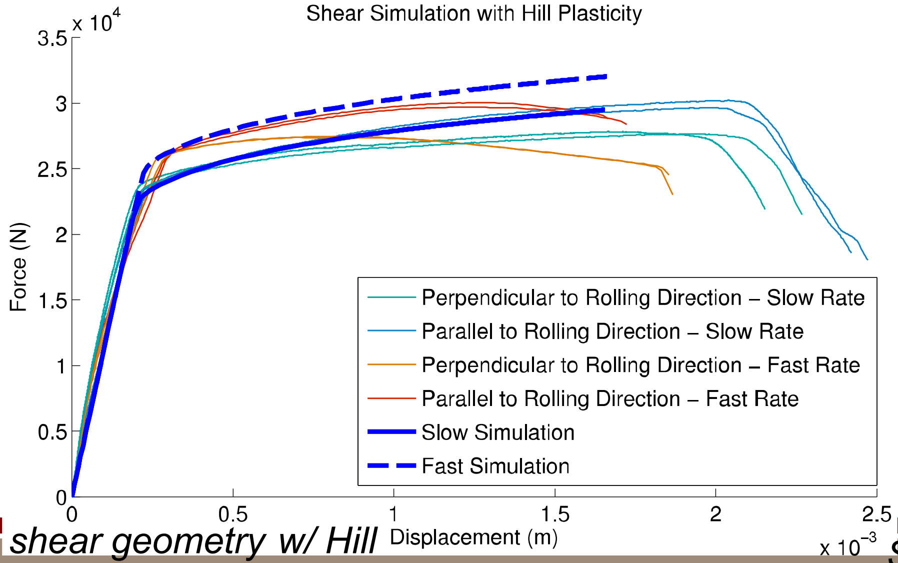

shear geometry w/ Hill

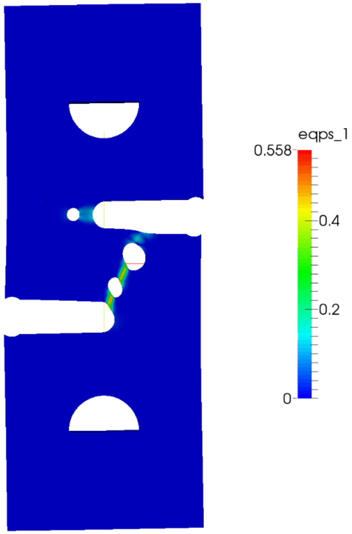

SFC geometry w/Hill

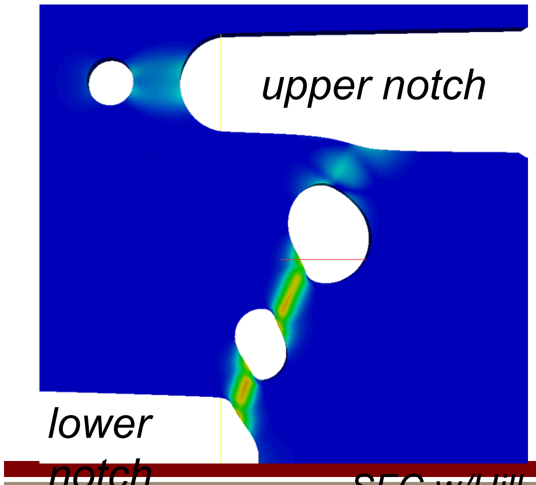

SFC w/Hill

Blind predictions

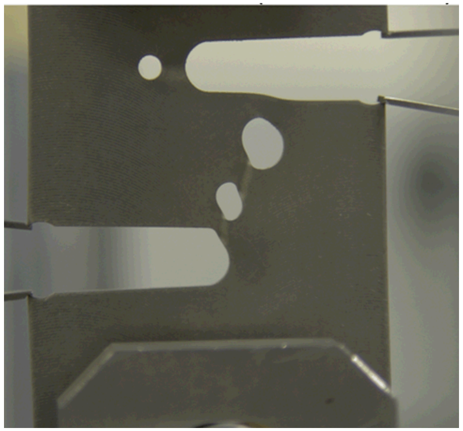

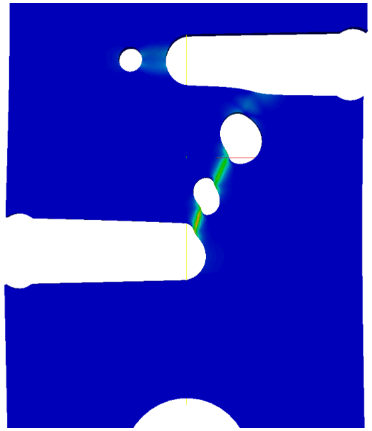

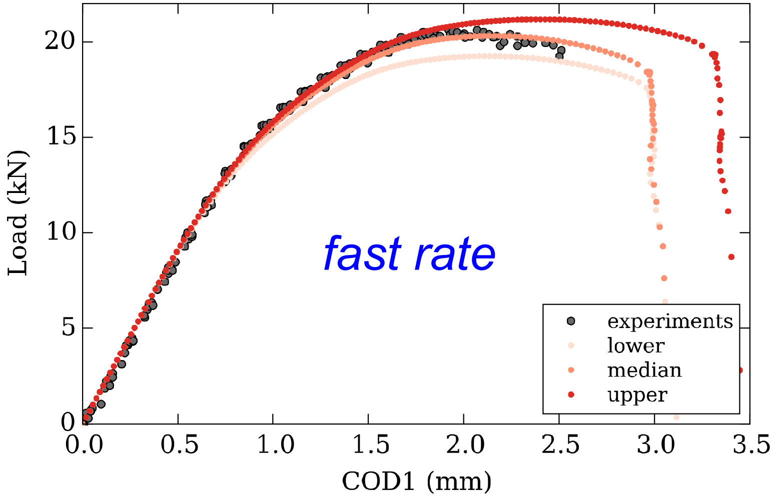

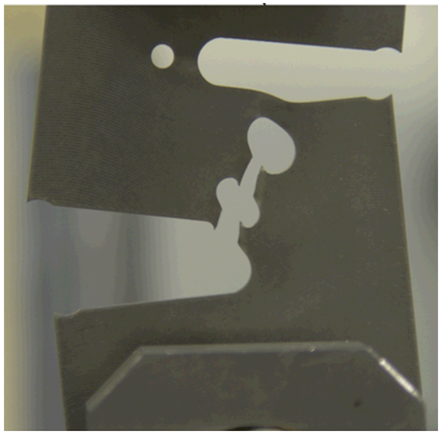

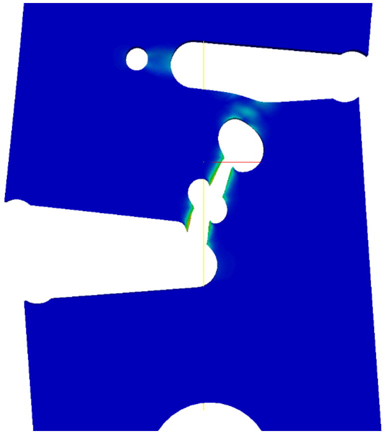

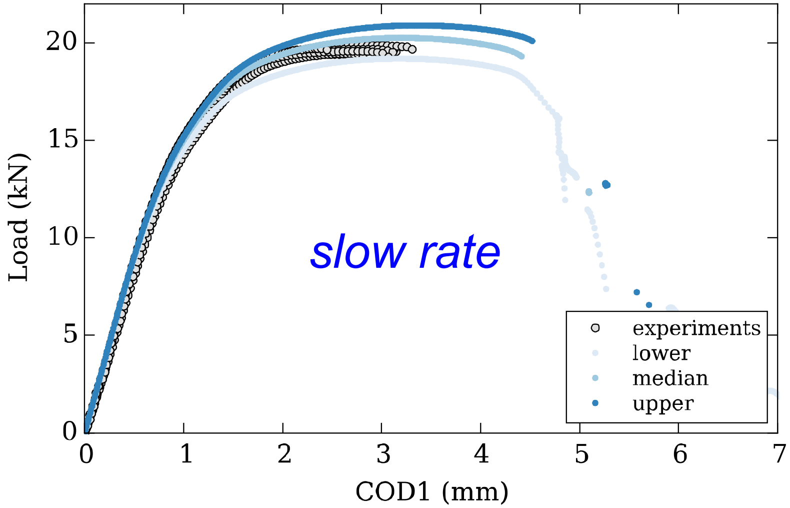

In good company…

- Majority of teams predicted the correct crack path w/error in load-displacement
- Majority of teams over-predicted both the loads and displacements to failure
- We believed that the role of plastic anisotropy would improve our predictions
- Sensitivity studies and new physics were pursued

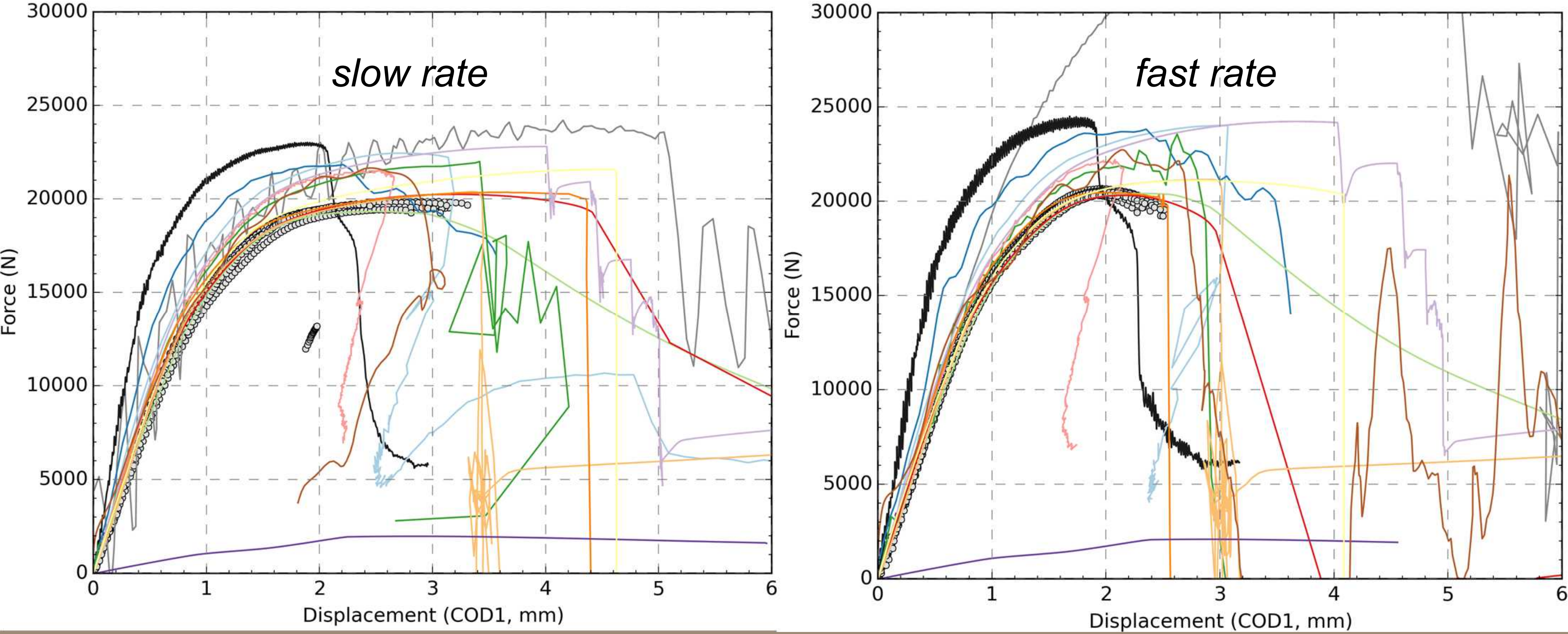

Revisiting anisotropy

- Keep micromechanics (damage)
- Add Hill yield surface
- Aids understanding

$$\dot{\phi} = \sqrt{\frac{3}{2}}\dot{\epsilon}_p \frac{1-(1-\phi)^{m+1}}{(1-\phi)^{m}} \sinh\left[\frac{2(2m-1)}{2m+1}\frac{\langle \frac{I_1}{3}\rangle}{\sqrt{3J_2}}\right]$$

$$\dot{\eta} = \eta\dot{\epsilon}_p N_1\left[\frac{4}{27}-\frac{J_3^2}{J_2^3}\right]$$

$$\begin{aligned} f_Y^2\left(\sigma_{ij}\right) \equiv & F\left(\sigma_{22}-\sigma_{33}\right)^2 + G\left(\sigma_{33}-\sigma_{11}\right)^2 \\ & + H\left(\sigma_{11}-\sigma_{22}\right)^2 + 2L\sigma_{23}^2 \\ & + 2M\sigma_{31}^2 + 2N\sigma_{12}^2 = \bar{\sigma}_c^2\left(\epsilon_p\right) \end{aligned}$$

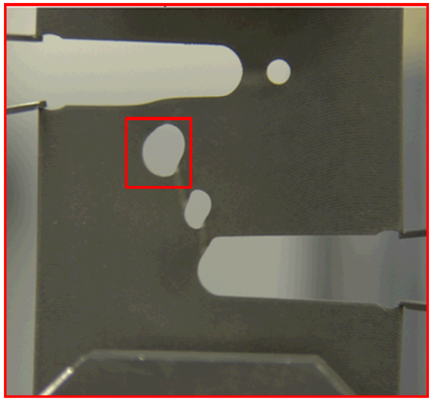

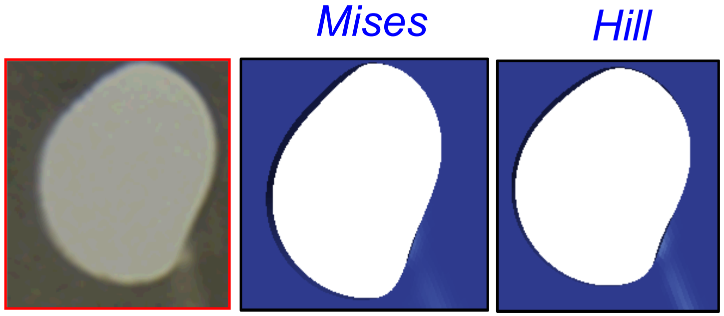

hole elongation reflects anisotropy

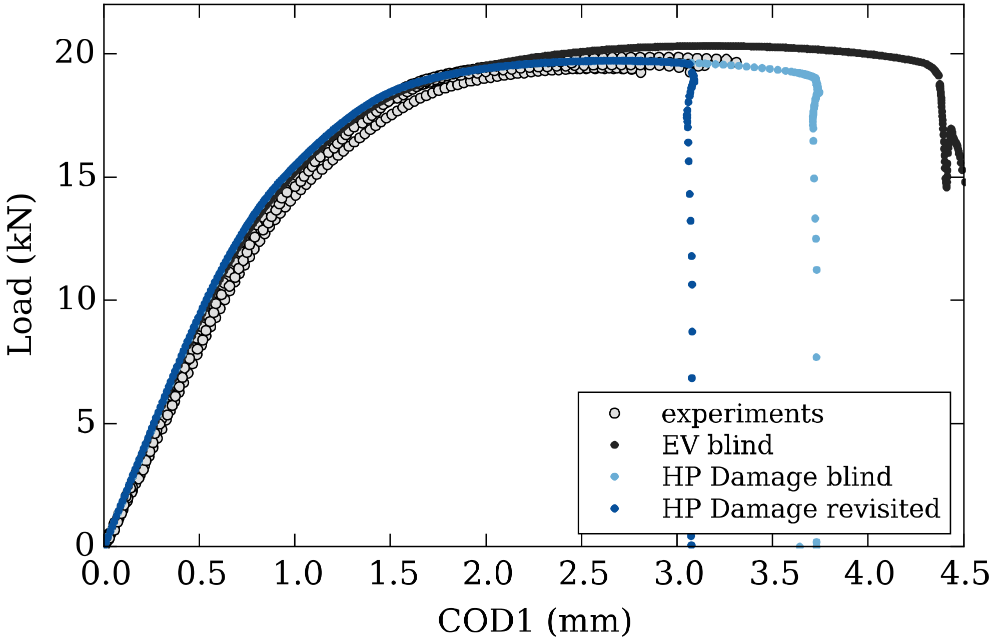

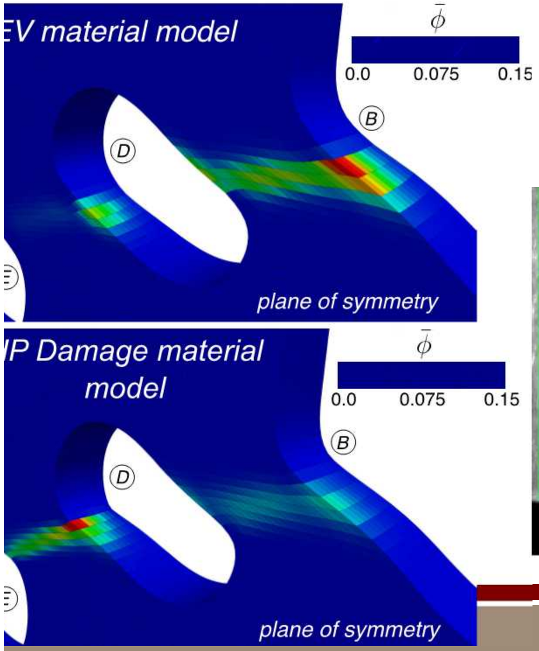

Ravi-Chandar Gross (UT)